TWO TOPICS IN PARTICLE PHYSICS: I. TESTS FOR HELICITY CONSERVATION ...
SILVER, RICHARD NEIL
ProQuest Dissertations and Theses; 1971; ProQuest Dissertations & Theses Global

SILVER, Richard Neil, 1
TWO TOPICS IN PART
FOR HELICITY CONS
SELECTION RULES I
II. INDEPENDENT P

California Institut
Physics, elementary

University Microfilms, A XEROX Compa , Ann Arbor, Michigan

THIS DISSERTATION HAS BEEN MICROFILMED EXACTLY AS RECEIVED

Reproduced with permission of the copyright owner. Further reproduction prohibited without permission.

Two Topics in Particle Physics

I. TESTS FOR HELICITY CONSERVATION AND SPIN-PARITY SELECTION RULES IN DIFFRACTION DISSOCIATION

II. INDEPENDENT PRODUCTION OF PIONS

Thesis by

Richard Neil Silver

In Partial Fulfillment of the Requirements for the

Degree of Doctor of Philosophy

California Institute of Technology

Pasadena, California

1971

(Submitted May 25, 1971)

XUM

Reproduced with permission of the copyright owner. Further reproduction prohibited without permission.

ACKNOWLEDGMENTS

It is a pleasure to thank Professor George Zweig for his supervision, advice, and criticism. I am indebted to Professor David Horn of Tel Aviv University with whom I collaborated on the second half of this thesis. I have benefited greatly from innumerable discussions with the members of the Caltech high energy experimental and theoretical groups. The National Science Foundation and Atomic Energy Commission have provided appreciated financial support. Last but not least I thank my wife, Leda, who made it all worthwhile.

XUM

Reproduced with permission of the copyright owner. Further reproduction prohibited without permission.

ABSTRACT

I. Tests for Helicity Conservation and Spin-Parity Selection Rules in Diffraction Dissociation

A phenomenological discussion of diffraction dissociation is presented in which the development of experimental tests for its conjectured properties is emphasized. Of particular interest is the problem of distinguishing between the behavior of resonances and background. Simple tests for the helicity, spin-parity, and internal quantum number selection rules proposed for resonance production would be possible only if the nonresonant background were absent. These would include an isotropy in azimuthal angle test for helicity conservation and a symmetry under parity inversion test for the Chou-Yang and Carlitz-Frautschi-Zweig rules. The more general and realistic case is that in which nonresonant background is present as well as resonances. It is found that a nonresonant pion exchange mechanism can account for the production characteristics of the broad low mass enhancements seen in present diffraction dissociation data. These include the variation of momentum transfer dependence with invariant mass and the spin-parity of the enhancements. It is unlikely that this background obeys the selection rules expected of resonance production. Nevertheless, the rapid variation in phase and possibly high spins of resonance contributions when interfered with the slow variation in phase and predominantly low spins expected of a pion exchange contribution should make possible tests for resonance production selection rules given adequate statistics.

XUM

Reproduced with permission of the copyright owner. Further reproduction prohibited without permission.

ABSTRACT

II. Independent Production of Pions

We investigate theoretical limitations on the possibility that multiparticle experiments at high energies are dominated by the independent production of uncorrelated pions. A description of pion production in coherent states is developed in order to systematically study the effects of conservation laws. Charge conservation leads to modifications of Poisson distributions for charged particle production in purely hadronic reactions that agree well with experiment. Other systems such as $e^+e^- \rightarrow$ pions are so limited by charge conjugation considerations that production of uncorrelated pions is ruled out. A formalism for the isospin analysis of pions with identical momentum distributions is developed and applied to coherent states. The fixed phase of a coherent state is important for minimizing the increase of $\langle I^2 \rangle$ with $\langle n \rangle$. The minimum that can be achieved with independent uncorrelated pions is a random walk in isospace. In this case the dominant contributions at present multiplicites come from the lowest isospins so that independent and coherent pions can be an approximation to experiment. Finally, the role of two pion correlations is studied. Independent emission of isoscalar pairs of pions solves the isospin problem and gives reasonable distributions of charged pions, but leads to negative correlations between charged and neutral pions that seriously disagree with experiment. Emission of charged isovector pairs of pions would improve the agreement with the observed slightly positive correlations. It is concluded that the effects of the many possible correlations may be difficult to resolve in the present analysis of existing data.

XUM

Reproduced with permission of the copyright owner. Further reproduction prohibited without permission.

TABLE OF CONTENTS

ACKNOWLEDGMENT ii

ABSTRACTS iii

TABLE OF CONTENTS v

PART I - DIFFRACTION DISSOCIATION

I. Introduction 1

II. Angular Distributions and Null Tests 22

A. Definitions 22

B. Two-Particle Decays 24

C. Three-Particle Decays 27

III. The OPE Model 31

A. The Deck Effect 33

B. Variation of Momentum Transfer Dependence with Invariant Mass 36

C. Partial Wave Analysis of Kinematic Enhancements 39

D. What Can OPE Say about Helicities? 42

IV. OPE and Selection Rules 46

V. Summary and Discussion 49

Appendix 1: Angular Distributions 52

References 56

PART II - INDEPENDENT PRODUCTION OF PIONS

I. Introduction 60

II. The Coherent State 76

III. Emission of a Coherent State 81

IV. Distributions of Charged Pions 88

XUM

Reproduced with permission of the copyright owner. Further reproduction prohibited without permission.

V. Parity and Charge Conjugation 95

VI. Isospin Analysis of Identical Pions 97

VII. Implications of Isospin Conservation 102

VIII. Two-Pion Correlations 111

IX. Conclusions 116

References 119

XUM

Reproduced with permission of the copyright owner. Further reproduction prohibited without permission.

PART I

TESTS FOR HELICITY CONSERVATION AND SPIN-PARITY SELECTION RULES IN DIFFRACTION DISSOCIATION

XUM

Reproduced with permission of the copyright owner. Further reproduction prohibited without permission.

I. Introduction

Diffraction is commonly understood in classical optics in terms of Huygen's principle. In the case of light incident upon an opaque object this principle states that the scattering may be calculated by supposing that the object radiates a field which exactly cancels with the incident field directly behind it. Thus, even if the opaque object absorbs all light which strikes its surface (no reflection) it must also elastically scatter part of the incident light. One may calculate that a black sphere of radius R will have an elastic cross section of πR^2. The absorbed energy is presumably dissipated by other modes of radiation. The entire process of absorption and reradiation is inelastic scattering, and one may calculate that the inelastic cross section for scattering on a black sphere will also be πR^2.

This idea may be applicable to the scattering of strongly interacting particles as well. At high energies the cross sections for elastic scattering appear to approach constant values. The inelastic cross sections are typically three to five times the elastic ones. One may achieve this result in a diffractive picture by making the target particles perfectly absorbing but with opacities decreasing with increasing distance from their centers. To calculate elastic scattering one presumably needs some model of how inelastic scattering (absorption) takes place.

There is, however, another class of reactions with constant cross sections at high energies for which no analogue in classical optics exists. Diffraction dissociation is the name applied to all

XUM

Reproduced with permission of the copyright owner. Further reproduction prohibited without permission.

inelastic reactions with asymptotically constant cross sections. One component of diffraction dissociation may be resonance formation reactions of the type $a+b \to a+d$ where d subsequently decays into a multiparticle final state. The other component of diffraction dissociation may be nonresonant formation of multiparticle final states. Diffraction dissociation cross sections are typically less than ten percent of elastic cross sections.

Since diffraction dissociation and elastic scattering share a common asymptotic behavior, they may also share a common dynamical origin. Presumably the study of one may give insight into the other. In Part I of this thesis we present a phenomenological discussion of diffraction dissociation in which the development of experimental tests for its conjectured properties is emphasized.

These tests will be applied to the analysis of data from an experiment on diffraction dissociation to be performed by the Caltech High Energy Users Group at the Stanford Linear Accelerator Center. One difficulty in testing the properties of diffraction dissociation in the past has been the insufficient statistics of previous experiments. One must measure the four momenta of all final particles, which makes use of the bubble chamber the preferred experimental technique. Conventional bubble chamber procedures require one to photograph all expansions of the chamber. Since diffraction dissociation comprises only a small fraction of the total cross section for a given collision, only a small fraction of the photographs will contain events of interest. This can make the observation of large numbers of events prohibitively expensive.

XUM

Reproduced with permission of the copyright owner. Further reproduction prohibited without permission.

In a novel experimental approach the Caltech Users Group will employ electronic counter techniques to determine that an event of interest has occurred, and only then trigger the cameras to photograph the expansion of the chamber. The Caltech experiment will collect up to one hundred times the typical number of events of previous experiments. The particular reactions to be investigated will be 14 GeV/c πp collisions to $\pi^-(\pi N)^+$ and $\pi^-(\pi\pi N)^+$ final states. We will make our discussion of experimental tests sufficiently general that they can be applied to other systems as well.

In order to illustrate some of what is presently known about diffraction dissociation, we discuss some experimental examples. Consider $\pi^+ p \to \pi^+(\pi N)^+$ where $(\pi N)^+$ denotes a pion nucleon system whose net charge is positive. By combining data from various charge states of the $(\pi N)^+$ system, one may isolate the contributions of particular isospins. This is illustrated in Fig. 1 where the contributions of $I = 1/2$ and $I = 3/2$ are given at 8 Gev/c and 16 Gev/c. We see a strong narrow enhancement at 1236 Mev in the $I = 3/2$ system that corresponds to the well-known P_{33} resonance of pion nucleon phase shifts. The $I = 3/2$ contribution falls rapidly with increasing energy. In the $I = 1/2$ system we find a strong broad enhancement at 1400 Mev and a weaker narrow enhancement at 1680 Mev. The cross section for producing the $I = 1/2$ system falls more slowly with increasing energy and appears to approach a constant at high energies. Thus production of the $I = 1/2$ component fits the definition of diffraction dissociation. Like the elastic reactions it involves no change in internal quantum numbers between the initial particles and the final dissociated "particles". All

XUM

Reproduced with permission of the copyright owner. Further reproduction prohibited without permission.

XUM

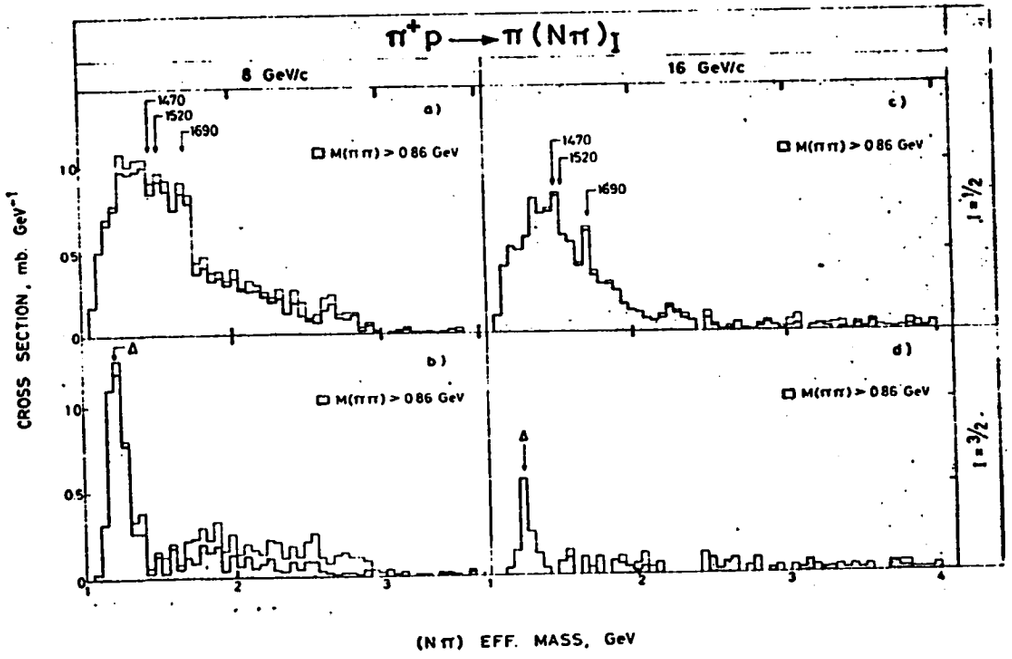

Fig. 1. (Nπ) mass distributions for the I = 1/2 and I = 3/2 states at 8 and 16 Gev/c , respectively. Taken from Ref. 28.

Reproduced with permission of the copyright owner. Further reproduction prohibited without permission.

other diffraction dissociation reactions also have this characteristic, e.g., $\gamma p \to \rho^o p$, $\pi p \to$ "A_1"p where by "A_1" we mean an $I = 1$ predominantly $J^{PG} = 1^{+-}$ 3π enhancement, $Kp \to$ "Q"p where by "Q" we mean an $S = \pm 1$ predominantly $J^P = 1^+$ $K\pi\pi$ enhancement, etc.

We learn from the above examples that one interesting feature of diffraction dissociation is the existence of selection rules. The established selection rules are that there are no changes of I, I_z, C, S, or B between initial and final particles. Other, at present unverified, selection rules for resonance production via diffraction dissociation have been suggested by various authors. Morrison has conjectured on an empirical basis that $\Delta P = (-1)^{\Delta J}$ where ΔP and ΔJ are respectively the change in parity and spin between the initial and final particles. Chou and Yang have suggested that if the product of the parities of the incoming and outgoing particles is odd, then the cross section for forward scattering is zero. The internal quantum number selection rules have been extended by Carlitz, Frautschi, and Zweig who suggest that in diffraction dissociation the $SU(6)$ character is preserved. There may also be selection rules that restrict the change in spin direction between initial and final particles. The type of spin or helicity selection rule has a special relation to the mechanism responsible for diffraction dissociation, which will be discussed further below. Naturally, one of the prime objects of the Caltech experiment is to test these rules.

To gain insight into the reactions with constant cross sections, it is useful to discuss the description of diffraction in scattering matrix theory. The conservation of probability implies that the

XUM

Reproduced with permission of the copyright owner. Further reproduction prohibited without permission.

scattering matrix is unitary

$$\sum_n (ab|S^\dagger|n)(n|S|cd) = \delta_{ac}\,\delta_{bd} \tag{1}$$

i.e., the probability that something happens is one. This means that the amplitude for $a + b \to c + d$ satisfies schematically

$$\mathrm{Im}(ab|T|cd) = \sum_n (ab|T^\dagger|n)(n|T|cd) \tag{2}$$

where $S = 1 + iT$. For elastic scattering $(a,b) = (c,d)$, equation (2) says that large inelastic amplitudes may generate via unitarity the imaginary part of the elastic amplitude.

We would like to show that via unitarity one may calculate properties of elastic scattering observed experimentally. For forward scattering $t = (q_c - q_a)^2 = 0$ unitarity relates the imaginary part of the elastic amplitude to the total cross section according to the "optical theorem"

$$\mathrm{Im}\, T_{el}\Big|_{t=0} = 4k^2\, \sigma_{tot} \tag{3}$$

where k is the center of mass momentum and σ_{tot} is the total cross section. If we assume that the elastic amplitude is imaginary (perfect absorption) and that for $t \neq 0$ $T_{el} \propto e^{at}$ (Gaussian distribution of opacities), then

$$\frac{d\sigma_{el}}{dt} = \frac{\sigma_{tot}^2}{16\pi}\, e^{2at}$$

This implies that $2a = \sigma_{tot}^2/16\pi\, \sigma_{el}$. To the extent that these assumptions are true, a plot of $X(t) \equiv d\sigma/dt \Big/ d\sigma/dt\Big|_{t=0}$ versus

XUM

Reproduced with permission of the copyright owner. Further reproduction prohibited without permission.

$\rho = \frac{\sigma_{tot}^2}{4\pi\,\sigma_{el}}(-t)$ should exhibit the universal behavior $X(t) = e^{-\rho/4}$. This is plotted in Fig. 2 for $\pi^{\pm}p$, $K^{\pm}p$, pp and $\bar{p}p$ reactions. The contribution to the lowest partial wave is

$$1 - \eta_{\ell=0} = \frac{1}{2}\int \mathrm{Im}\, T_{el}\, d\cos\theta \cong 4\sigma_{el}/\sigma_{tot} \qquad (5)$$

which is bounded by $0 \leq \eta_o \leq 1$ due again to unitarity (an object cannot be more than completely opaque at its center). As a consequence $\sigma_{el}/\sigma_{tot} \leq .25$. Experimentally at high energies $x = \sigma_{el}/\sigma_{tot}$ is .17, .19, .23, and .21 for $\pi^{\pm}p$, $K^{\pm}p$, pp, and $\bar{p}p$ respectively. Finally, for most reactions x is approximately independent of s even for moderate energies. One may express the elastic differential cross section in terms of x and σ_{inel}.

$$\frac{d\sigma_{el}}{dt} = \frac{\sigma_{inel}^2}{16\pi(1-x)^2}\exp\left(\frac{(1-x)}{16\pi x}\sigma_{inel}t\right) \qquad (6)$$

The correlation of the behavior of the inelastic cross sections with the rate of fall with increasing -t is verified experimentally.

Some intuition into why one expects selection rules may be gained by applying our S-matrix approach to diffraction dissociation. Equation (2) is, of course, valid for any reaction of the type $a + b \to c + d$. If one assumes that the phases of the various inelastic amplitudes which contribute to the sum are essentially unrelated to one another, then the maximum coherence of this sum should occur when a and b have the same quantum numbers as c and d respectively. Thus, the reactions which survive in the limit of high

XUM

Reproduced with permission of the copyright owner. Further reproduction prohibited without permission.

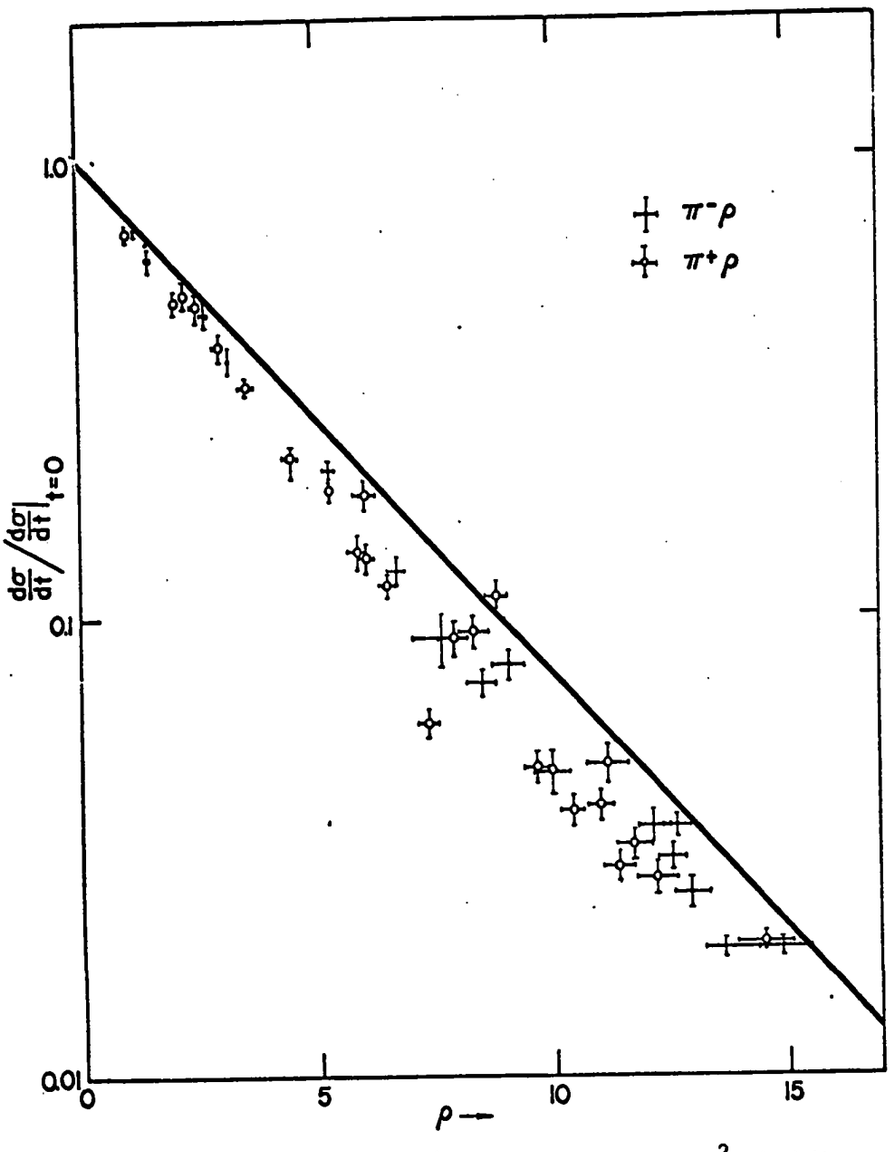

Fig. 2a. Plot of $X(t) = d\sigma/dt \Big/ d\sigma/dt\Big|_{t=0}$ versus $\rho = \sigma_{tot}^2(-t)/4\pi\sigma_{el}$ for $\pi^{\pm}p$ elastic scattering. The solid curve is $X(t) = e^{-\rho/4}$.

XUM

Reproduced with permission of the copyright owner. Further reproduction prohibited without permission.

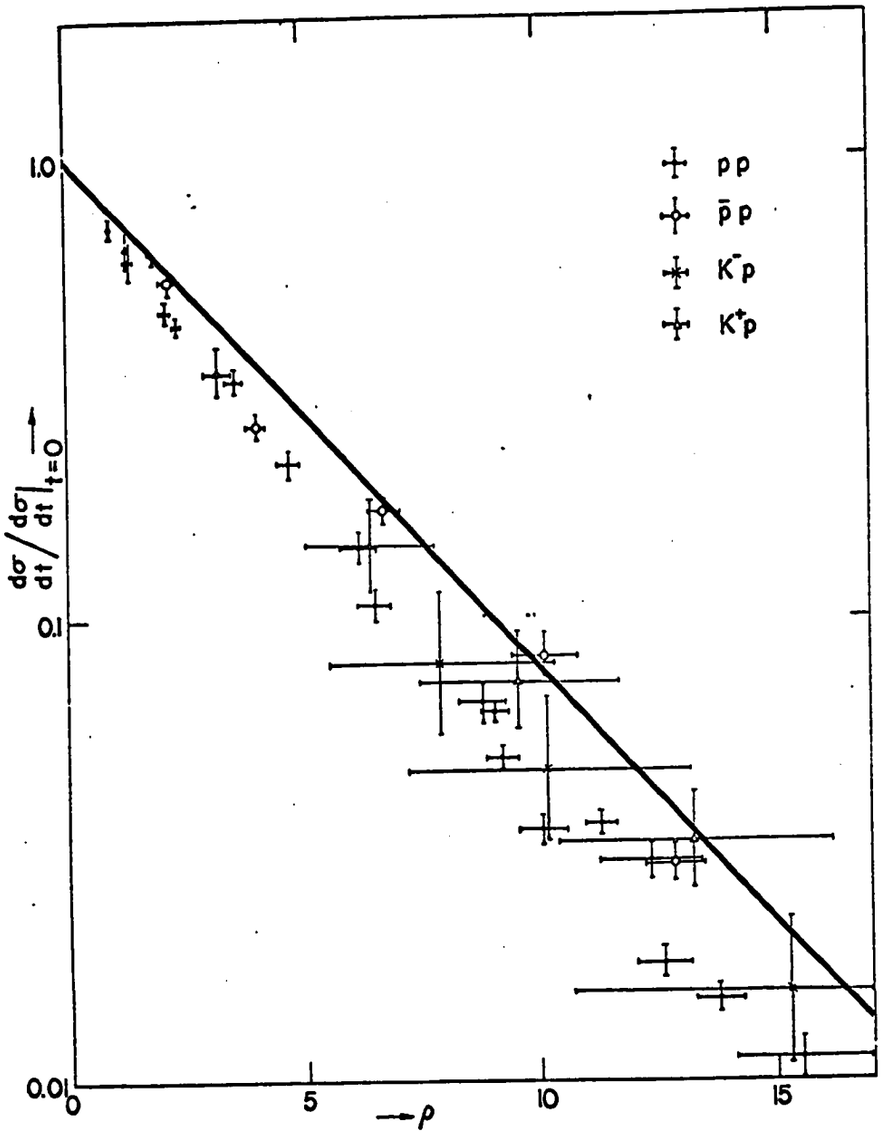

Fig. 2b. Same as 2a for pp, $\bar{p}p$, $K^{\pm}p$ elastic scattering.

XUM

Reproduced with permission of the copyright owner. Further reproduction prohibited without permission.

energies should obey the selection rule that there is no internal quantum number change between initial and final particles, as we have for elastic scattering and have observed empirically for diffraction dissociation. One must remark, however, that this random phase approximation is not strictly justifiable, since one believes that the various amplitudes in (2) are related to one another by the dynamics which govern all of the strong interactions.

One may naively argue that the diffraction model suggests that there be no change in spin between initial and final particles, but this could not be a relativistically invariant statement. A spin selection rule that can be true relativistically is that there be no change in "helicity" between initial and final particles. Helicity is defined as the component of spin along the direction of motion of a particle. The utility of states of definite helicity is that they are invariant under Lorentz boosts that bring a particle to rest. For the reaction $a + b \to c + d$, which one calls the s channel reaction, the "s-channel helicities" are equal to the spin along (against) $\vec{p}_a = -\vec{p}_b$ for particle $a(b)$ and the spin along (against) $\vec{p}_c = -\vec{p}_d$ for particle $c(d)$ in the s-channel center of mass. Another set of base states for the description of spin which is often discussed is where one quantizes along the direction of the incident particles a and b in the s-channel center of mass. We refer to these as states of definite "s-channel spin". Note that in the limit of high energies and fixed t the s-channel helicity and s-channel spin become identical.

XUM

Reproduced with permission of the copyright owner. Further reproduction prohibited without permission.

Since in diffraction the wave elastically scattered by the absorber should cancel with the incident wave, it should have the same spin orientation as the incident wave. Hence, if a diffraction mechanism is responsible at high energies for elastic scattering and the resonance production component of diffraction dissociation, then one would expect as a selection rule that either the s-channel helicities or s-channel spins are conserved between initial and final particles.

There is, however, another model for the reactions with asymptotically constant cross sections which would suggest a different spin selection rule and for which there is considerable theoretical motivation. It is worthwhile to review the experimental situation that suggests it to us. It is an empirical fact that for most strong interaction reactions of the type $a + b \to c + d$ above incident lab energies of, say, 5 Gev/c the sizes and energy dependences of the cross sections are correlated with the exchanged quantum numbers, i.e., with the quantum numbers of the reaction $a + \bar{c} \to \bar{b} + d$ which we refer to as the "t-channel".

The elastic cross sections are largest and appear to approach constant values of from 4 to 10 mb at high energies. They are followed by the meson exchange cross sections which fall slowly with increasing energy, then by the baryon exchange ones which fall more rapidly with energy, and finally by those termed exotic exchange, down at 1 μb or less, that correspond to the exchange of quantum numbers possessed by no observed resonance. The energy dependence of the cross section for production of the $I = 3/2$ component in our example $\pi^+ p \to \pi^+ (\pi N)^+$ falls neatly into this hierarchy at the position of meson

XUM

Reproduced with permission of the copyright owner. Further reproduction prohibited without permission.

exchange.

One of the most important developments in the past ten years of particle physics has been the qualitative understanding of this ordering of cross sections in terms of "regge or regge-like" theories. Intuition gained from the study of non-relativistic potential scattering led to the proposal that the energy dependences of cross sections are connected to the particle spectrum. The resonances in the t-channel are found to lie along straight lines called "trajectories" in a plot of spin versus mass squared. A property of quantum electrodynamics assumed to be true as well of strong interactions is "crossing symmetry" which says that the amplitude which describes scattering in one channel may be analytically continued to give the scattering amplitude in another channel. Regge or regge-like theories parameterize the amplitude in terms of the t-channel resonances and then analytically continue to describe the s-channel reaction at high energies. The value of the spin extrapolated to zero mass squared, called the "intercept" $\bar{\alpha} = J(m^2 = 0)$ governs approximately the energy dependence of the s-channel reaction $a + b \to c + d$ according to

$$\left.\frac{d\sigma}{dt}\right|_{t=0} \propto s^{2\bar{\alpha} - 2} \qquad (7)$$

where the incident lab energy is proportional to s at high energies. The intercepts $\bar{\alpha}$ for meson trajectories range from 0.5 to 0 and for baryon trajectories from 0 to -1. If exotic mesons exist they are presumably of high mass, since they have not been seen as yet experimentally. As a consequence the intercepts for exotic trajectories should be even more negative, and hence the exotic exchange cross

XUM

Reproduced with permission of the copyright owner. Further reproduction prohibited without permission.

sections should fall the most rapidly with energy.

Elastic scattering and diffraction dissociation represent anomalies in the regge picture. Their intercept, obtained by fitting to (7) at high energies, is $\bar{\alpha} \sim 1$ which does not correspond to any observed trajectories. Nor has the degree to which these processes resemble the meson and baryon exchange reactions been established. Nevertheless, they are described in regge language by saying that they proceed via "Pomeron" exchange. The Pomeron is assigned the quantum numbers of the vacuum to ensure its exchange in elastic scattering and diffraction dissociation.

A logical extension of this approach is that the Pomeron carry no information about spin either. If a regge mechanism is responsible at high energies for elastic scattering and the resonance component of diffraction dissociation, then one would expect as a selection rule that the "t-channel helicities" are conserved. For the reaction $a + \bar{c} \to \bar{b} + d$, the t-channel helicities are equal to the spin along (against) $\vec{p}_a = -\vec{p}_c$ for particle $a(\bar{c})$ and the spin along (against) $\vec{p}_{\bar{b}} = -\vec{p}_d$ for particle $\bar{b}(d)$ in the t-channel center of mass. When an amplitude for t-channel scattering from and into states of definite t-channel helicities is analytically continued to describe the s-channel reaction, the resulting amplitude is in general a linear combination of the amplitudes for scattering from and into states of definite s-channel helicities. Hence, in general conservation of t-channel helicities is not equivalent to the conservation of s-channel helicities.

XUM

Reproduced with permission of the copyright owner. Further reproduction prohibited without permission.

In summary, apart from the question of possible particles on a Pomeron trajectory, the primary difference between regge and diffractive viewpoints is that the former suggests that high energy scattering looks simple when expressed in terms of t-channel variables while the latter suggests that s-channel variables are preferable.

At the time of writing, s-channel helicity conservation has been observed experimentally in $\pi N \to \pi N$ and $\gamma p \to \rho^o p$, while t-channel helicity conservation has been seen in $\pi N \to "A_1" N$ and $KN \to "Q" N$. One way to resolve this rather confused experimental situation is to observe that in the latter two reactions the nonresonant component of diffraction dissociation may be dominating the cross sections. In order to justify this interpretation one needs a model for the nonresonant component that can explain the properties of these reactions. Deck, Drell, and Hiida have suggested that a simple multipheral model involving pion exchange can give the observed enhancements in the 3π and $K\pi\pi$ masses. In Part I of this thesis we shall show that the pion exchange model accounts for most of the other properties of the broad low mass enhancements observed in diffraction dissociation.

Pion exchange, like all regge exchanges, is calculated by parameterizing the amplitude in terms of the pion and its recurrences in the t-channel and then analytically continuing to describe the s-channel reaction. The intercept for the pion trajectory is $\alpha = -.02$. The value of the intercept implies that an amplitude dominated by pion exchange is predominantly real. One may derive this by appeal to

XUM

Reproduced with permission of the copyright owner. Further reproduction prohibited without permission.

the relativistic extension of dispersion theory, which is worthwhile discussing briefly.

In the case of optics, one may express the real part of the amplitude for forward scattering by light of a fixed frequency ω as an integral over the cross section for absorption by atoms of light of all frequencies. Via the optical theorem this cross section is proportional to the imaginary part of the forward scattering amplitude. One derives this "dispersion relation" by establishing that the forward scattering amplitude is analytic in the upper half of the ω plane, a mathematical property based on the physical limitation of "causality" which states that electromagnetic signals cannot travel with a speed greater than that of light.

The belief that the strong interactions also obey causality lead one to expect that similar dispersion relations may be written for the strong interaction amplitudes, except that in the extension of this idea to a relativistic theory one acquires a contribution to the integral from the "u-channel" $\bar{c} + b \to \bar{a} + d$. An amplitude may be expressed as a function of t and ν , where for positive values ν is proportional to the incident lab energy in the s-channel and for negative values ν is proportional to the incident lab energy in the u-channel. The dispersion relation is then schematically

$$T(\nu,t) = -\frac{1}{\pi}\int_{-\infty}^{0} \frac{\text{Im } T(\nu',t)d\nu'}{\nu' - \nu} + \frac{1}{\pi}\int_{0}^{\infty} \frac{\text{Im } T(\nu',t)d\nu}{\nu' - \nu} \qquad (8)$$

where $\text{Im } T(\nu,0)$ is related to the total cross sections in the s and u channels via the optical theorem.

XUM

Reproduced with permission of the copyright owner. Further reproduction prohibited without permission.

Let us consider the case of the power law behavior which characterizes regge theories $\text{Im } T(\nu,t) = \beta(t)\, \nu^{\alpha(t)}$. An amplitude is said to be even or odd under crossing from s to u channels depending on whether τ in $T(-\nu,t) = \tau T(\nu,t)$ is +1 or -1. Then, one may derive from (8)

$$T(\nu,t) = \frac{\beta(t)(\tau + e^{+i\pi\alpha(t)})\, \nu^{\alpha(t)}}{\sin \pi\alpha(t)} \tag{9}$$

Using $\tau = +$ and $\bar{\alpha} \simeq 0$ for the pion trajectory, one derives that pion exchange is indeed predominantly real at least in the forward direction. This will be useful in establishing tests for resonance production selection rules. One may also note that the pion pole at $\alpha(t = .02) = \alpha(m_\pi^2) = 0$ is very near the forward scattering of the s-channel where $t = 0$. This means that an amplitude dominated by pion exchange will fall rapidly with increasing $-t$. It is primarily this aspect of pion exchange, which is true of both the data and all theoretical models, that will be sufficient to establish in Part I that pion exchange can account for the properties of the low mass enhancements observed in diffraction dissociation.

(Elastic scattering and diffraction dissociation are dominated by $\alpha(0) = \bar{\alpha} = 1$ which (9) says would be a purely imaginary contribution if it appears only in amplitudes which are even under crossing. The optical theorem tells us that evenness under crossing may be checked experimentally by observing whether s and u channel total cross sections become equal at asymptotic energies. At incident lab energies around 40 Gev/c, $\sigma_T(\pi^+ p) \simeq 25$ mb while $\sigma_T(\pi^- p) \simeq 23.5$ mb,

XUM

Reproduced with permission of the copyright owner. Further reproduction prohibited without permission.

$\sigma_T(K^+p) \simeq 17$ mb while $\sigma_T(K^-p) \simeq 20.5$ mb, $\sigma_T(pp) \simeq 39.0$ mb while $\sigma_T(\bar{p}p) \simeq 45.0$ mb. That s and u channel total cross sections do indeed approach one another as the energy increases appears to be the trend of the present data, except for the recent but unverified small discrepancies reported from Surphukov.)

While exchanges arise from resonances in the t-channel, a scattering amplitude may also receive contributions from resonances in the s-channel. In the partial wave expansion of a two-body amplitude

$$T(s,t) = \sum_{\ell=0}^{\infty} (2\ell+1)\, f_\ell(s)\, P_\ell(\cos\theta) \tag{10}$$

a resonance contribution may be approximated by a Breit-Wigner

$$\text{Im } f_\ell = \frac{(\Gamma + \Gamma_t)/4 \;\; \Gamma_t/2}{(\sqrt{s}-M)^2 - \Gamma_t^2/4} \qquad \text{Re } f_\ell = -\frac{(\Gamma+\Gamma_t)/4 \;\; (\sqrt{s}-M)}{(\sqrt{s}-M)^2 - \Gamma_t^2/4} \tag{11}$$

where M is the mass of the resonance, Γ_t its total width, and Γ its partial width. The imaginary part peaks at the position of the resonance and falls as $(\sqrt{s} - M)^{-2}$ away from the resonance mass, whereas the real part changes sign at the resonance mass and falls only as $(\sqrt{s} - M)^{-1}$ far from the resonance. In Part I of this thesis we shall argue that the contrast between the rapid variation in phase of a resonance and the relative constancy of the pion exchange phase should prove valuable in testing selection rules for resonance production.

One of the more significant developments of the past few years in hadron physics has been the suggestion that the direct channel

XUM

Reproduced with permission of the copyright owner. Further reproduction prohibited without permission.

resonances are related to the nondiffractive regge exchanges (intercept $\bar{\alpha} < 1$). The term "duality" designates the assumption that amplitudes exist with the properties: 1) at least at low energies, their imaginary parts can be approximated by direct channel resonance contributions; 2) at least at high energies, regge exchange also describes their imaginary parts; and 3) a region of energies and angles exists over which both these approximations may be simultaneously employed. Obviously, since resonant contributions are bumpy, while a regge exchange gives a smooth energy dependence, these two descriptions can be equivalent only in some average sense. This hypothesis has been used to derive a number of experimentally valid constraints on the regge intercepts.

Because diffraction can occur in reactions where s-channel resonances have not been observed, duality cannot be true for elastic scattering amplitudes. However, it has been conjectured that, even for elastic scattering, amplitudes with diffractive contributions removed can be constructed in which the average of the resonance contributions to the imaginary parts equals the regge exchange contributions. When combined with the optical theorem this conjecture explains a correlation observed among total cross sections. This observation is that in reactions such as K^+p and pp where no strong s-channel resonances have been observed, the σ_{tot} fall at most slowly with energy and approach their asymptotic values at low energies, while in reactions such as $\bar{p}p$, πp, and K^-p where there are many s-channel resonances the σ_{tot} fall rapidly in energy and approach their asymptotic values only at high energies. In regge

XUM

Reproduced with permission of the copyright owner. Further reproduction prohibited without permission.

language, one would say that the various exchanges with $\bar{\alpha} < 1$ are cancelling against one another in the imaginary parts of elastic amplitudes when s-channel resonances are absent, while they contribute substantially when s-channel resonances are present.

In view of our separation of the contributions to diffraction dissociation into resonance production and pion exchange components, the important question is whether duality can be true for the real parts of scattering amplitudes. The objection is that the empirical correlation we have noted for the imaginary parts of elastic amplitudes is not observed for the real parts, e.g., K^+p and pp elastic amplitudes have large real parts whose average energy dependence is governed by $\bar{\alpha} < 1$ even though s-channel resonances are absent. Hence one must in general expect that s-channel resonances and the real parts of regge exchanges are distinct components of scattering amplitudes. Equation (8) tells us that these real parts may be generated by the existence of resonances in the u-channel K^-p and $\bar{p}p$ reactions. Another way to state this is to note that the contribution of a resonance is localized to a small energy region only in the imaginary part, while resonances in other channels can make significant contributions to the real parts.

In this thesis diffraction dissociation is discussed phenomenologically with emphasis upon the development of tests for the helicity, spin-parity, and internal quantum number selection rules proposed for resonance production. It is argued that the alternative selection rules are distinguishable by their characteristic angular distributions for the decay products of produced resonances. Indeed,

XUM

Reproduced with permission of the copyright owner. Further reproduction prohibited without permission.

if the nonresonant background were absent, then simple tests for selection rules could be performed without having to isolate the individual resonance contributions. In general, one must expect background as well as resonances. It is established that a simple pion exchange model, such as Deck, Drell, and Hiida[1] have suggested to explain the "A_1" and "N*(1400)" enhancements, can account for most of the production characteristics of the broad low mass enhancements observed in present diffraction dissociation data. These include the variation of momentum transfer dependence with invariant mass and the spin-parity of the enhancements. It is likely that this pion exchange background does not obey the selection rules expected of resonance production. Therefore, the question of tests for resonance production selection rules in the presence of significant pion exchange background is addressed.

For the sake of convenience, let us summarize here the selection rules we wish to test. For a reaction $a + b \to c + d$ helicity conservation is defined by

$$\langle \lambda_c \lambda_d | T(s,t) | \lambda_a \lambda_b \rangle = \delta_{\lambda_c \lambda_a} \delta_{\lambda_d \lambda_b} \langle \lambda_a \lambda_b | T(s,t) | \lambda_a \lambda_b \rangle \qquad (12)$$

There are three types of helicity conservation that could be expected: 1) t-channel helicity conservation based on concepts of a t-channel origin for the asymptotic behavior (Pomeron exchange); 2) s-channel spin conservation; and 3) s-channel helicity conservation[2,3] based on concepts of an s-channel origin for the asymptotic behavior analogous to the diffraction of classical optics. Morrison[4] has conjectured $\Delta P = (-1)^{\Delta J}$, although there is no current theoretical

XUM

Reproduced with permission of the copyright owner. Further reproduction prohibited without permission.

justification for this rule except when the initial dissociating particle is spinless. Chou and Yang[5] (CY) have suggested that if the product of the parities is odd in a quasi-two-body reaction with an asymptotically constant cross section, then $d\sigma/dt = 0$ at $t = 0$. Carlitz, Frautschi, and Zweig[6] (CFZ) have suggested that in diffraction dissociation the SU(6) character is preserved between initial and final particles.

In Section II we derive the general angular distributions for the description of diffraction dissociation and we propose a set of null tests for selection rules which would be valid if the nonresonant background were absent. In Section III we demonstrate that the pion exchange model can account for much of the currently available diffraction dissociation data. In view of this success, in Section IV we propose new tests for resonance production selection rules. Section V includes a summary and some concluding remarks concerning the interpretation of present experiments.

XUM

Reproduced with permission of the copyright owner. Further reproduction prohibited without permission.

II. Angular Distribution and Null Tests

A. Definitions

Our purpose in this section is to derive the general angular distributions for reactions of the type

$$a + b \to c + d \to c + \alpha + \beta \tag{13}$$

where d denotes intermediate states of varying spin and parity, and to observe the manner in which these distributions simplify due to the various selection rules[7]. Inasmuch as we are interested in measuring the properties of the state d, the most convenient Lorentz frame in which to view this reaction is that in which d is at rest. One must therefore understand how the various sets of helicity and spin base states appear in this frame (Fig. 3)[7].

The momenta in $a+b \to c+d$ define a plane in the s-channel center of mass. Thus, the normal to this plane which we choose to call the $\hat{y}$-axis is invariant under the Lorentz transformation that brings d to rest. In the s-channel center of mass the s-channel helicity of d is the spin along $\vec{p}_d = -\vec{p}_c$. Clearly under a Lorentz boost that brings d to rest, the s-channel helicity of d remains the spin against the direction of $\vec{p}_c$. This choice of $\hat{z}$-axis when d is at rest defines the "helicity frame". In the t-channel center of mass the t-channel helicity of d is the spin along $\vec{p}_d = -\vec{p}_{\bar{b}}$. Clearly under a Lorentz boost that brings d to rest, the t-channel helicity of d remains the spin against the direction of $\vec{p}_{\bar{b}}$. Under crossing from the t to the s-channel $\vec{p}_{\bar{b}} \to -\vec{p}_b$. Hence, in the s-channel, the t-channel helicity for particle d in its rest frame is the spin along the direction of $\vec{p}_b$. This choice of z-axis when d is at rest defines the "Gottfried-Jackson" frame[8]. The helicity and Gottfried-Jackson

XUM

Reproduced with permission of the copyright owner. Further reproduction prohibited without permission.

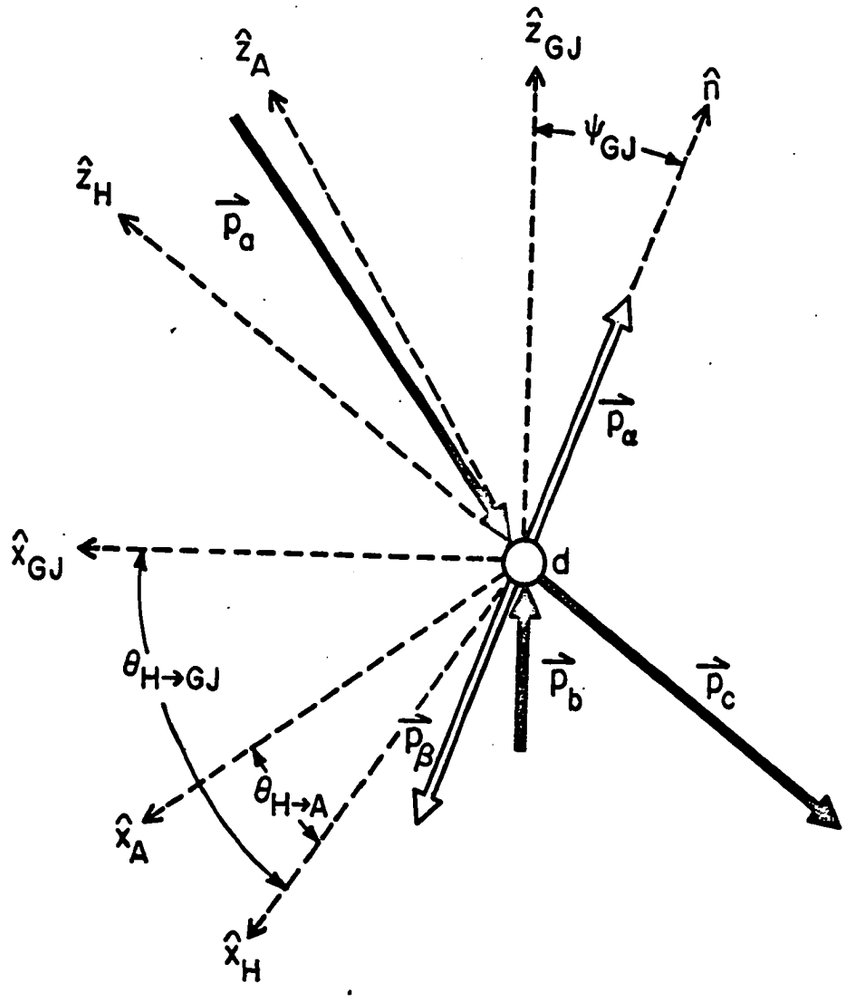

Fig. 3. The reaction $a+b \to c+d \to c+\alpha+\beta$ in the d rest frame The vectors $\vec{p}_a$, $\vec{p}_b$, $\vec{p}_c$ are in the plane of the paper while $\vec{p}_\alpha = -\vec{p}_\beta$ may be out of the plane. The $\hat{y}$-axis is perpendicular to the page. $\hat{z}_H$, $\hat{z}_A$, $\hat{z}_{GJ}$ denote the $\hat{z}$-axis in the helicity, Adair, and Gottfried-Jackson frames respectively. These frames are related by rotations about the $\hat{y}$-axis as denoted by angles $\Theta_{H\to GJ}$ and $\Theta_{H\to A}$. ψ_{GJ} is the polar angle of the decay direction $\hat{n}$ in the GJ frame.

XUM

Reproduced with permission of the copyright owner. Further reproduction prohibited without permission.

frames are related by rotation about the $\hat{y}$-axis by the "crossing angle" $\theta_{H\to GJ}$. Clearly, the angle between the helicity frame and that for quantization of s-channel spin is the s-channel center of mass scattering angle θ. This third choice of $\hat{z}$-axis when d is at rest is called the "Adair" frame [9].

The choice of $\hat{z}$-axis for discribing the angular distribution is therefore to be chosen according to the type of helicity conservation selection rule one wishes to test. Test for t-channel helicity conservation in the Gottfried-Jackson frame, test for s-channel spin conservation in the Adair frame, and test for s-channel helicity conservation in the helicity frame. To move from one frame to another, one rotates about the $\hat{y}$-axis by:

$$\cos\theta_{H\to GJ} = \frac{[(s+d^2-c^2)(t+d^2-b^2)-2d^2(a^2-c^2+d^2-b^2)]}{[s-(c-d)^2]^{1/2}[s-(c+d)^2]^{1/2}[t-(b-d)^2]^{1/2}[t-(b+d)^2]^{1/2}}$$

$$\cos\theta_{H\to A} = \cos\theta \qquad (14)$$

Note that for forward scattering, $\theta = 0$, all frames are equivalent and, except for reactions where double helicity flip is possible, helicity conservation is a consequence of angular momentum conservation. For a given choice of z-axis, $\hat{x} = \hat{y} \times \hat{z}$. The decay angles ψ and ϕ are then defined as the polar and azimuthal angles of the vector $\hat{n}$, which in the case of two-particle decays denotes the direction of one of the decay particles in the d rest frame.

B. Two-Particle Decays

We divide the scattering amplitude into two factors, one for the production of an intermediate state d of spin and parity J^P

XUM

Reproduced with permission of the copyright owner. Further reproduction prohibited without permission.

and the other for its subsequent decay into α and β

$$\langle \psi\phi\ \lambda_\alpha\lambda_\beta\lambda_c|S(s,t)|\ \lambda_a\lambda_b\rangle$$

$$= \sum_{J,P,\lambda_J} \langle \psi\phi\ \lambda_\alpha\lambda_\beta\ |G|J^P\lambda_J\rangle \langle J^P\lambda_J\lambda_c|T(s,t)|\lambda_b\lambda_a\rangle \qquad (15)$$

where[10]

$$\langle \psi\phi\ \lambda_\alpha\lambda_\beta|G|J^P\lambda_J\rangle = e^{i(\lambda_J - (\lambda_\alpha - \lambda_\beta))\phi}\ d^J_{\lambda_J,\lambda_\alpha-\lambda_\beta}(\psi)\ g^{JP}_{\lambda_\alpha\lambda_\beta} \qquad (16)$$

and

$$g^{JP}_{-\lambda_\alpha-\lambda_\beta} = P_\alpha P_\beta P(-1)^{s_\alpha+s_\beta-J}\ g^{JP}_{\lambda_\alpha\lambda_\beta} \qquad (17)$$

where $g^{JP}_{\lambda_\alpha\lambda_\beta}$ is the reduced matrix element for the decay of a state of spin-parity J^P into α and β with helicities λ_α and λ_β. Experiments with unpolarized targets in which the final helicities are not measured can then be described by the general angular distribution

$$W(\psi,\phi) = \sum_{\ell=0}^{\infty} \sum_{m=-\ell}^{\ell} A_{\ell m}\ Y^m_\ell(\psi,\phi) \qquad (18)$$

where

$$A_{\ell m} = \sum_{\lambda_\beta,\lambda_\beta} \sum_{J,P,\lambda_J} \sum_{J',P',\lambda'_J} \frac{1}{4}(-1)^{-\lambda_\alpha+\lambda_\beta} C(J,J',\ell;\lambda_J,-\lambda'_J)$$

$$\times C(J,J',\ell;\lambda_\alpha-\lambda_\beta,-\lambda_\alpha+\lambda_\beta)\sqrt{\frac{4\pi}{2\ell+1}}\ (1+PP'(-1)^\ell)((-1)^{\lambda'_J}\ \delta_{\lambda_J-\lambda'_J,m} +$$

XUM

Reproduced with permission of the copyright owner. Further reproduction prohibited without permission.

$$+ (-1)^{\lambda_J} \delta_{-\lambda_J+\lambda'_J,m}) \; g^{JP}_{\lambda_\alpha \lambda_\beta} \; g^{*J'P'}_{\lambda_\alpha \lambda_\beta} \sum_{\lambda_b>0} \sum_{\lambda_a,\lambda_c} \langle J^P \lambda_J, \lambda_c | T | \lambda_b, \lambda_a \rangle$$

$$\times \langle J'^{P'} \lambda'_J, \lambda_c | T | \lambda_b, \lambda_a \rangle^* \qquad (19)$$

The $C(J,J'',\ell;\lambda_J,\lambda'_J)$ are Clebsch-Gordan coefficients. (A more thorough derivation of this angular distribution is given in Appendix 1).

In this section we are interested in the simplifications that result in (18) from helicity conservation and other selection rules in the presence of many interfering resonances of varying spin and parity. These predicted simplifications will provide experimental tests of the selection rules. In the first part of this discussion we will ignore the problem of a possible nonresonant contribution to the reaction $a + b \to c + \alpha + \beta$.

Helicity conservation (equation (12)) predicts that the $A_{\ell m}$ are zero for $m > 0$ in (14). Thus, the angular distribution (18) is characterized by the absence of an azimuthal dependence. Isotropy in ϕ is a simple test for consistency with helicity conservation. It can be applied without having to isolate the contributions of spin and parity[11]. It is a necessary but not sufficient test, since ϕ independence without helicity conservation could conceivably be achieved if: 1) the density matrices for production of all resonances are diagonal; and 2) the interference terms between contributions of differing spin and parity contribute no ϕ dependence.

The angular distributions (18) may be used to test the validity

XUM

Reproduced with permission of the copyright owner. Further reproduction prohibited without permission.

of the spin-parity and CFZ rules by observing the patterns of interference between contributions of differing J and P in the various moments of the distribution. At $\theta = 0$ or for $\theta \neq 0$ in the case of helicity conservation simpler expressions achieved by invoking Eq. (12) in Eq. (19) may be used. The important feature to notice in Eq. (19) is that because of the factor $(1 + PP'(-1)^{\ell})$, the coefficients of the odd ℓ spherical harmonics involve only terms mixed in parity. If $a = c$ in reaction (2), the CY rule requires d to have the same parity as b. If we restrict our considerations to low mass N*'s where all the established resonances are classified in SU(6) as members of either a $\underset{\sim}{56}$, $L = 0$ or $\underset{\sim}{70}$, $L = 1$ [13], then the CFZ rule forbids production of odd parity N*'s. Thus, in certain cases the CY and CFZ rules predict that the $A_{\ell m}$ are zero for ℓ odd. Equivalently, they predict that in certain reactions the decay angular distributions will be symmetric under parity inversion $\psi \to \pi - \psi$, $\phi \to \pi + \phi$. Again, this simple test may be performed without having to isolate the individual resonance contributions.

Both of these null tests are of course valid only to the extent that the nonresonant background is absent.

C. Three-Particle Decays

In the case of three-particle decays where the reaction is

$$a + b \to c + d \to c + \alpha + \beta + \gamma \qquad (20)$$

there are two ways one may analyze the data. The first is to identify two of the three decay products as forming a resonance and study the angular distribution as a quasi-two-body decay according to the

XUM

Reproduced with permission of the copyright owner. Further reproduction prohibited without permission.

prescription of the preceding section. The difficulty with this approach is that such identifications are often difficult to make and in any case can never be precise. Therefore it is useful to know what information can be learned without having to attempt this identification. Our second approach is to follow the suggestion of Berman and Jacob and study the angular distribution of the normal to the three-particle decay plane. We will show that the tests of the preceding section will continue to be applicable.

We briefly summarize the formalism of Berman and Jacob. A three-particle state is written

$$|q_\alpha\lambda_\alpha;q_\beta\lambda_\beta;q_\gamma\lambda_\gamma> \tag{21}$$

In the d rest frame the three momenta form a triangle in a plane, whose normal we take to be the $\hat{n}$ of Fig. 3. The orientation of this plane is specified by three Euler angles: ψ and ϕ are the polar and azimuthal angles of the normal with respect to a $\hat{z}$-axis chosen according to the type of helicity conservation we wish to test as in the preceding section; and γ corresponds to the rotation of the plane about the normal. In terms of these angles the state may be rewritten as

$$|\omega_\alpha\lambda_\alpha,\omega_\beta\lambda_\beta,\omega_\gamma\lambda_\gamma,\psi,\phi,\gamma> \tag{22}$$

A state of definite angular momentum is specified in this case by three quantum numbers: J the spin, m the eigenvalue along the $\hat{z}$-axis, and M the eigenvalue along the normal.

XUM

Reproduced with permission of the copyright owner. Further reproduction prohibited without permission.

Then, in analogy to the preceding section, we divide the scattering amplitude into two factors, one for the production of a resonance d of spin and parity J^P and the other for its subsequent decay into α, β, and γ.

$$\langle \psi\phi\gamma;\lambda_\alpha,\lambda_\beta,\lambda_\gamma,\lambda_c \,|S(s,t)|\,\lambda_a\lambda_b\rangle$$

$$= \sum_{J,P,\lambda_J} \langle \psi,\phi,\gamma;\omega_\alpha\lambda_\alpha,\omega_\beta\lambda_\beta,\omega_\gamma\lambda_\gamma|G|J^P\lambda_J\rangle\langle J^P\lambda_J\lambda_c|T(s,t)|\lambda_b\lambda_a\rangle \tag{23}$$

where

$$\langle \psi\phi\gamma;\omega_\alpha\lambda_\alpha,\omega_\beta\lambda_\beta,\omega_\gamma\lambda_\gamma \,|G|J^P,\lambda_J\rangle = \sum_{M=-J}^{J} e^{i\lambda_J\phi}\, d^J_{\lambda_J M}(\psi) e^{iM\gamma}$$

$$\times\ G_M^{JP}(\omega_\alpha\lambda_\alpha,\omega_\beta\lambda_\beta,\omega_\gamma\lambda_\gamma) \tag{24}$$

For constraints analogous to (17) due to parity conservation and identical particles, we refer the reader to Berman and Jacob's paper. Again for experiments with unpolarized targets in which we do not measure the final helicities, the angular distribution, after integrating over γ and the dalitz plot variables, is given by

$$W(\psi,\phi) = \sum A_{\ell m} Y_\ell^m(\psi,\phi) \tag{25}$$

where

$$A_{\ell m} = 2\pi \sum_{\lambda_\alpha,\lambda_\beta,\lambda_\gamma} \sum_{J,P,\lambda_J} \sum_{J',P',\lambda_J'} \sum_{M=-J}^{J} \sum_{M'=-J'}^{J'} (-1)^{-M} C(J,J',\ell;\lambda_J,-\lambda_J')$$

$$\times\ C(J,J',\ell;M,-M)\delta_{MM'}\sqrt{4\pi/2\ell+1}\,(1+PP'(-1)^\ell)((-1)^{\lambda_J'}\delta_{\lambda_J-\lambda_J',m} +$$

XUM

Reproduced with permission of the copyright owner. Further reproduction prohibited without permission.

$$+ (-1)^{\lambda_J} \delta_{-\lambda_J+\lambda'_J,m}) \; G_M^{JP}(\lambda_\alpha,\lambda_\beta,\lambda_\gamma) \; G_{M'}^{J'P'*}(\lambda_\alpha,\lambda_\beta,\lambda_\gamma)$$

$$\times \sum_{\lambda_b>0} \sum_{\lambda_a,\lambda_c} < J^P \lambda_J,\lambda_c|T|\lambda_b,\lambda_a><J'^{P'}\lambda'_J,\lambda_c|T|\lambda_b,\lambda_a>^* \qquad (26)$$

Note the similarities between this and equation (19). We see immediately that for the angular distribution of the normal to the three-particle decay plane helicity conservation predicts $A_{\ell m} = 0$ for $m > 0$, and the CFZ and CY rules in certain reactions predict $A_{\ell m} = 0$ for ℓ odd. So again we have that helicity conservation predicts isotropy in ϕ, and the CFZ and CY rules predict invariance under $\psi \to \pi - \psi$, $\phi \to \phi + \pi$ in certain reactions. Again, these tests are only true to the extent that nonresonant background is absent.

XUM

Reproduced with permission of the copyright owner. Further reproduction prohibited without permission.

III. The OPE Model

Our purpose in this section is to establish a model for the nonresonant component of diffraction dissociation. We shall exploit the suggestion by Drell and Deck[1] that a simple pion exchange model could give enhancements in mass distributions similar to those observed for genuine resonances. Essentially, their proposal corresponds to the diagram of Fig. 4 wherein the incoming b dissociates into α and β and α scatters elastically off particle $a = c$. In general α is taken to be a pion, but the importance of the α mass being small will be an essential result of our discussion. We shall show that this model can account for most of the properties of the broad low mass enhancements observed in diffraction dissociation.

We shall first summarize the kinematic expressions we will need for our analysis. If we denote $q_a = (p_a, \omega_a)$, etc., then we may choose the five independent kinematic invariants to be:

$$s = (q_a + q_b)^2 \qquad s_{c\alpha} = (q_c + q_\alpha)^2 \qquad s_{\alpha\beta} = (q_\alpha + q_\beta)^2 = d^2$$

$$t = (q_c - q_a)^2 \qquad t_{\beta b} = (q_\beta - q_b)^2 \tag{27}$$

In the d rest frame

$$p_\alpha^2 = p_\beta^2 = \frac{1}{4s_{\alpha\beta}}[(s_{\alpha\beta} - \alpha^2 - \beta^2)^2 - 4\alpha^2\beta^2]$$

$$p_b^2 = \frac{1}{4s_{\alpha\beta}}[(s_{\alpha\beta} + b^2 - t)^2 - 4b^2 s_{\alpha\beta}]$$

$$p_c^2 = \frac{1}{4s_{\alpha\beta}}[(s - c^2 - s_{\alpha\beta})^2 - 4c^2 s_{\alpha\beta}]$$

XUM

Reproduced with permission of the copyright owner. Further reproduction prohibited without permission.

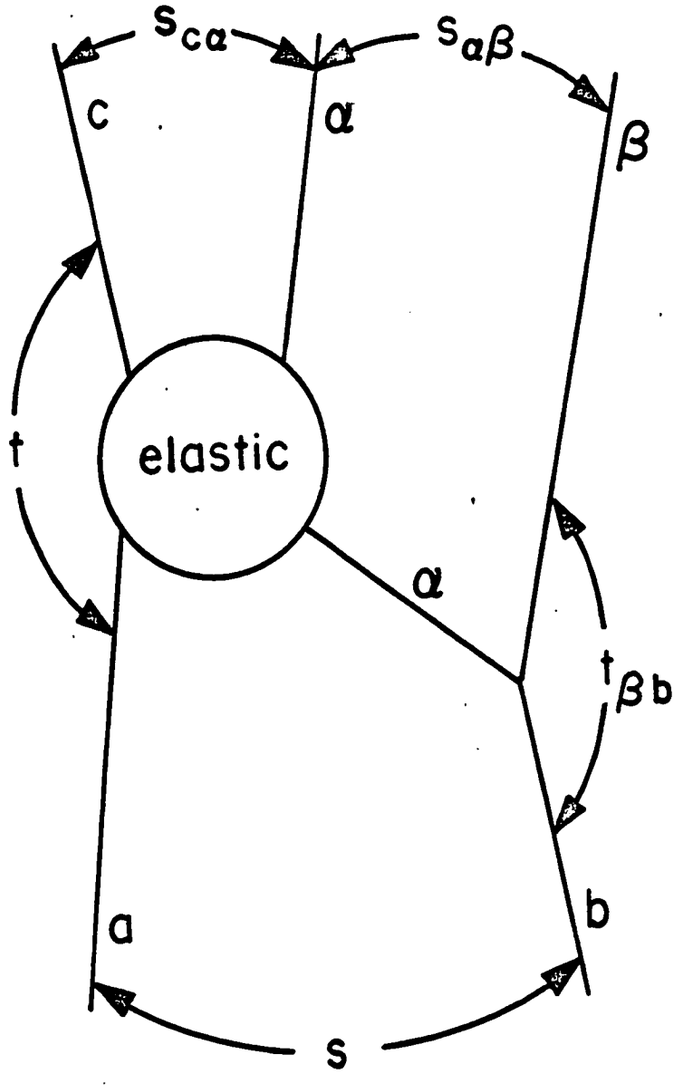

Fig. 4. The Feynman diagram for the pion exchange contribution to diffraction dissociation. The s, t, $s_{c\alpha}$, $s_{\alpha\beta}$, $t_{\beta b}$ denote the five independent kinematic invariants. The particle α is a pion.

XUM

Reproduced with permission of the copyright owner. Further reproduction prohibited without permission.

$$p_a^2 = \frac{1}{4s_{\alpha\beta}}\left[(s+t-c^2-b^2)^2 - 4s_{\alpha\beta}a^2\right] \tag{28}$$

Thus, in the Gottfried-Jackson coordinate system

$$t_{\beta b} = \beta^2 + b^2 - 2\omega_\beta\omega_b - 2p_\beta p_b\cos\psi \tag{29}$$

$$s_{c\alpha} = c^2+\alpha^2+ 2\omega_c\omega_\alpha + 2p_c p_\alpha[\cos\psi\cos\chi - \sin\psi\sin\chi\cos\phi]$$

where χ is $\theta_{H\to GJ}$ given in equation (14). Then, the differential cross section for reaction (13) is given by

$$\frac{d^4\sigma}{ds_{\alpha\beta}dt} = \frac{1}{(4\omega_a\omega_b F_I)^2}\frac{1}{(2\pi)^4}\frac{p_\alpha}{8\sqrt{s_{\alpha\beta}}}\int W(\psi,\phi)d\cos\psi\, d\phi \tag{30}$$

where

$$(4\omega_a\omega_b F_I)^2 = s^2+a^4+b^4 - 2sa^2-2sb^2-2a^2b^2 \tag{31}$$

A. The Deck Effect

At the time of writing, there is no universally accepted or successful model for pion exchange. The relative or even absolute validity of evasion, conspiracy, or absorption models is not settled, and it is not our purpose here to compare them. These models disagree on questions of energy dependence and helicity couplings which for our purposes are irrelevant. They and the data all agree that pion exchange is characterized by a very rapid variation with momentum transfer in the range between 0 and m_π^2, and this is all the physics of pion exchange necessary to explain the properties discussed here.

We write the contribution to the scattering amplitude[13] for reaction (13) that corresponds to the diagram of Fig. 4 as

XUM

Reproduced with permission of the copyright owner. Further reproduction prohibited without permission.

$$< \psi\phi\lambda_\beta\lambda_c|S(s,t)|\lambda_a\lambda_b > = < \bar{\lambda}_c|A(s_{c\alpha},t)|\bar{\lambda}_a > \frac{1}{t_{\beta b}-\alpha^2} V_{\lambda_\beta\lambda_b}(t_{\beta b}) \quad (32)$$

where $< \bar{\lambda}_c|A(s_{c\alpha},t)|\bar{\lambda}_a>$ is the off mass shell αa elastic scattering amplitude[14], $1/t_{\beta b}-\alpha^2$ the α propagator, and $V_{\lambda_\beta\lambda_b}(t_{\beta b})$ is a helicity coupling form factor at the α-β-b vertex which, with the above points in mind, we will set equal to one until part D of this discussion. At high $s_{c\alpha}$ elastic scattering is dominated by diffraction so we may set

$$< \bar{\lambda}_c|A(s_{c\alpha},t)|\bar{\lambda}_a > \propto is_{c\alpha} e^{\frac{Bt}{2}} g_{\bar{\lambda}_c\bar{\lambda}_a} \quad (33)$$

Again, questions of helicity couplings are irrelevant and we will set $g_{\bar{\lambda}_c\bar{\lambda}_a}$ equal to one in what follows. We then find at high s that

$$\frac{d^4\sigma}{ds_{\alpha\beta}dt} \propto \frac{p_\alpha e^{Bt}}{s^2\, 8\sqrt{s_{\alpha\beta}}} \int \frac{s^2[\omega_\alpha+p_\alpha(\cos\psi\cos\chi - \sin\psi\sin\chi\cos\phi)]^2}{s_{\alpha\beta}(t_{\beta b}-\alpha^2)^2} d\cos\psi\, d\phi \quad (34)$$

In the forward direction $t = 0$ we have $\chi \to 0$ and

$$\lim_{t=0} t_{\beta b} - \alpha^2 \to \frac{(s_{\alpha\beta}-b^2)}{\sqrt{s_{\alpha\beta}}}[\omega_\alpha+p_\alpha\cos\psi] \quad (35)$$

which yields

$$\left.\frac{d^2\sigma}{ds_{\alpha\beta}dt}\right|_{t=0} \propto \frac{p_\alpha}{\sqrt{s_{\alpha\beta}}} \frac{1}{(s_{\alpha\beta}-b^2)^2} \quad (36)$$

This function is plotted in Fig. 5a. Thus, the OPE exchange results in a low mass enhancement which qualitatively fits the observed $N^*(1400)$where $b = \beta = N$, $A_1(1070)$ where $b = \pi$ and $\beta = \rho$, $K^*(1320)$.

XUM

Reproduced with permission of the copyright owner. Further reproduction prohibited without permission.

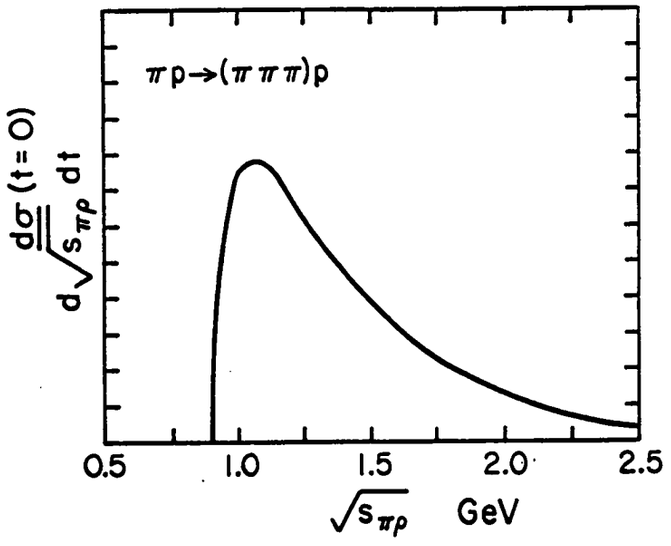

Fig. 5a. The differential cross section of the simple OPE model. The vertical scale is arbitrary.

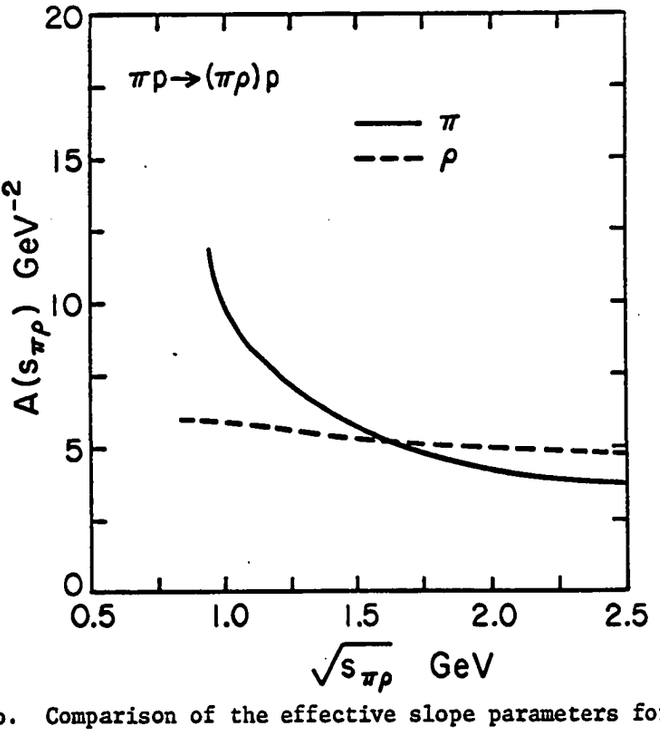

Fig. 5b. Comparison of the effective slope parameters for pion exchange and ρ exchange.

Reproduced with permission of the copyright owner. Further reproduction prohibited without permission.

where $b = K$ and $\beta = K^*(890)$, and $L(1790)$ where $b = K$ and $\beta = K^*(1420)$. Furthermore, at sufficiently high s where the approximation (33) is valid, the cross section (36) is independent of s and therefore fits the definition of diffraction dissociation.

Note that (36) does not depend on α^2 [13]. Thus, at this stage the importance of the pion mass being small is only in justifying the approximation (33) by arguing that the pion pole is very near the physical scattering region $t_{\beta b} < 0$.

B. Variation of Momentum Transfer Dependence with Invariant Mass

Empirically it is found that as a function of t [15], the differential cross section for the production of the above enhancements can be approximated by

$$\frac{d^2\sigma}{ds_{\alpha\beta}dt} = \left.\frac{d^2\sigma}{ds_{\alpha\beta}dt}\right|_{t=0} e^{A(s_{\alpha\beta})t} \tag{37}$$

where $A(s_{\alpha\beta})$ is large $\sim$ 15-20 Gev^{-2} for small $s_{\alpha\beta}$ near threshold and drops to much smaller values for large $s_{\alpha\beta}$. A plot of $A(s_{\alpha\beta})$ for the A_1 at 8 Gev/c is given in Fig. 6b.

In order to give a simple argument for why the OPE model reproduces this behavior, we will consider two limits of $s_{\alpha\beta}$. First, in the limit of small $s_{\alpha\beta}$ near threshold

$$\lim_{s_{\alpha\beta}\to(\alpha+\beta)^2} s_{c\alpha} = c^2+\alpha^2+2\alpha\omega_c \quad \text{independent of } t \tag{38}$$

$$\lim_{s_{\alpha\beta}\to(\alpha+\beta)^2} t_{\beta b} = \beta^2+b^2 - \frac{2\beta(s_{\alpha\beta}+b^2)}{2\sqrt{s_{\alpha\beta}}} + \frac{\beta t}{\sqrt{s_{\alpha\beta}}}$$

XUM

Reproduced with permission of the copyright owner. Further reproduction prohibited without permission.

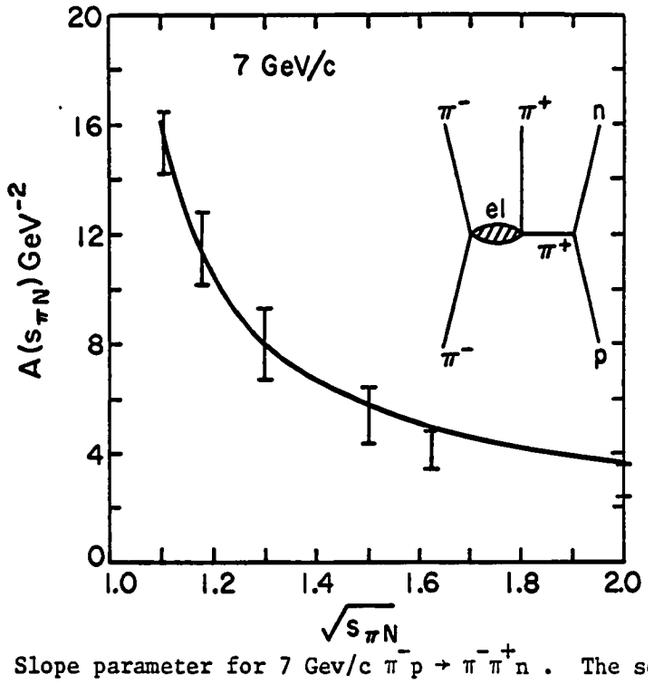

Fig. 6a. Slope parameter for 7 Gev/c $\pi^- p \to \pi^- \pi^+ n$. The solid line is the effective slope parameter predicted by OPE model(inset)

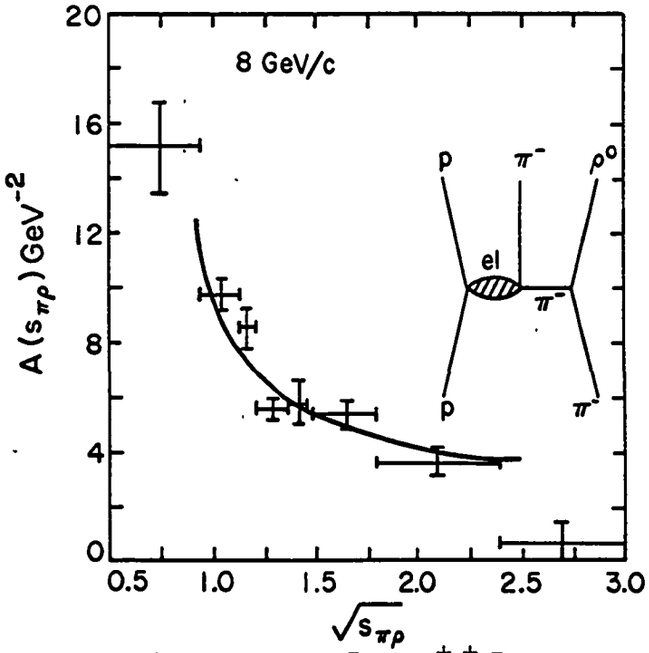

Fig. 6b. Same as 6a for 8 Gev/c $\pi^- p \to (\pi^+\pi^+\pi^-)p$

XUM

Reproduced with permission of the copyright owner. Further reproduction prohibited without permission.

For the A_1 in this limit $t_{\beta b} = -.10 + .84t$. Thus, if in equation (32) α is small on the order of the pion mass, the differential cross section for small $s_{\alpha\beta}$ falls rapidly with increasing negative t. If α were large as for the exchange of a ρ-meson, the t dependence would be much less pronounced. In the limit of large $s_{\alpha\beta}$ we have as in equation (35) $\chi \to 0$ and

$$\lim_{s_{\alpha\beta} \text{ large}} t_{\beta b} - \alpha^2 \to \frac{(s_{\alpha\beta} - b^2)}{\sqrt{s_{\alpha\beta}}} [\omega_\alpha + p_\alpha \cos \psi]$$

independent of t. Thus

$$\lim_{\substack{s_{\alpha\beta} \text{ large} \\ \text{fixed } t}} \frac{d^2\sigma}{ds_{\alpha\beta} dt} \propto e^{Bt} \frac{p_\alpha}{\sqrt{s_{\alpha\beta}}} \frac{1}{(s_{\alpha\beta} - b^2)^2} \tag{40}$$

$A(s_{\alpha\beta})$ asymptotically approaches the slope of the αa elastic scattering for large $s_{\alpha\beta}$. The effective $A(s_{\alpha\beta})$ at $t=-.1$ predicted by this model are compared with the 7 Gev/c data for $\pi^- p \to \pi^- (\pi^+ n)$ in Fig. 6a and the 8 Gev/c $\pi^- p \to (\pi^- \rho) p$ in Fig. 6b. We have adjusted the B's to achieve the best fit to the data, but this freedom changes only the position and not the shape of these curves. In Fig. 5b we demonstrate that such a variation in the slope $A(s_{\alpha\beta})$ with invariant mass is indicative of pion exchange dominance by comparing the predicted slopes for $\alpha = \pi$ and $\alpha = \rho$.

Note that the best fit to the $\pi^- p \to (\pi^- \rho) p$ data at 8 Gev/c is achieved with $B \sim 4$ Gev^{-2}. At first sight this may seem disturbing since for $\pi^- p$ elastic scattering at high energies $B \sim 9$ Gev^{-2}. However, it should be noted that the dynamical restriction to small

XUM

Reproduced with permission of the copyright owner. Further reproduction prohibited without permission.

$t_{\beta b}$ which characterizes pion exchange also restricts $s_{c\alpha}$ to be small even though s may be large. In Fig. 7 we exhibit the bounds on $s_{\pi N}$ in $\pi p \to \pi\pi\pi p$ for various momentum transfers. At 8 Gev/c $s_{\pi N}$ is predominantly restricted to the resonance region of $\pi^- p$ elastic scattering where $B \sim 4\text{-}7$ Gev^{-2}. These general considerations are confirmed by the 25 Gev/c [16] data where $B \sim 9$ gives the best fit to $A(s_{\alpha\beta})$.

The restriction to nonasymptotic $s_{c\alpha}$ at present energies is probably also correlated with the observed fall of nearly a factor of two between 5 and 25 Gev/c in the production cross section for the "A_1".

Although the approximation (33) is less accurate when $s_{c\alpha}$ is small, the argument presented above for the variation in momentum transfer dependence with invariant mass remains valid since, as we have seen, $s_{c\alpha}$ is independent of t in the two limits of $s_{\alpha\beta}$ small and $s_{\alpha\beta}$ large[17]. Generally we expect $A(s_{\alpha\beta})$ to depend strongly on $s_{\alpha\beta}$ in any process where the dynamics can be described by a multiperipheral diagram such as Fig. 4 and the amplitude falls rapidly with $t_{\beta b}$. Indeed, in $K^- p \to K^*(890)p \to (K\pi)^- p$ the absence of a contribution from such a diagram is correlated with $A(s_{K\pi})$ being roughly constant [15].

C. Partial Wave Analysis of Kinematic Enhancements

Because of its sharp peripherality, one pion exchange contributes strongly to high partial waves in pion photoproduction. It may therefore seem at first sight contradictory that kinematic enhancements from pion exchange could be confused with low spin resonances. In this section we examine more closely the partial wave analysis of the Deck

XUM

Reproduced with permission of the copyright owner. Further reproduction prohibited without permission.

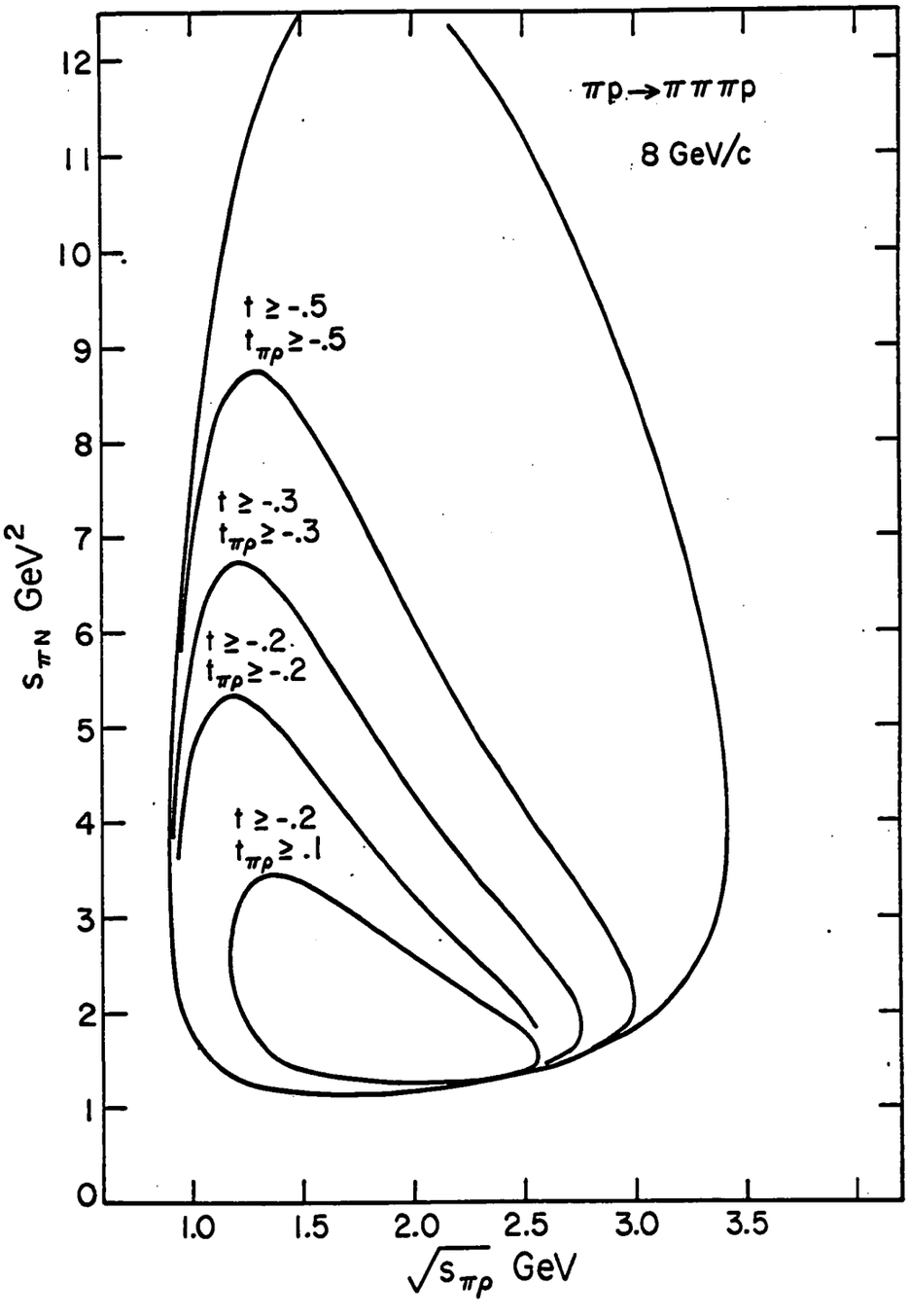

Fig. 7. Bounds on the subenergies as a function of momentum transfer for 8 Gev/c $\pi^- p \rightarrow (\pi\rho)^- p$. The outermost curve is the bound for unrestricted momentum transfer. The inner curves are the bounds for the momentum transfer restricted as indicated.

XUM

Reproduced with permission of the copyright owner. Further reproduction prohibited without permission.

effect[18,19].

From (15),(16) we have

$$<\psi\,\phi\lambda_\alpha\lambda_\beta\lambda_c|S|\lambda_a\,\lambda_b> = \sum_{J,P,\lambda_J} e^{i(\lambda_J-(\lambda_\alpha-\lambda_\beta))\phi}\, d^J_{\lambda_J\lambda_\alpha-\lambda_\beta}(\psi)\; g^{JP}_{\lambda_\alpha\lambda_\beta}$$

$$\times\; <J^P\lambda_J\lambda_c|T(s,t)|\lambda_a\lambda_b> \qquad (41)$$

The more rapidly $(\psi,\phi\,\lambda_\alpha\lambda_\beta\lambda_c|S|\,\lambda_a\,\lambda_b>$ varies with ψ and ϕ, the higher the J's to which it contributes strongly. Were the amplitude to consist of a pion propagator alone

$$1/(t_{\beta b}-\alpha^2) = 1/(\beta^2+b^2-\alpha^2-2\omega_\beta\omega_b-2p_\beta p_b\cos\psi)$$

we would indeed have important contributions to high partial waves as in pion photoproduction. However, an equally important contribution comes from the αa elastic scattering so that in the extremely high s limit

$$<\psi\phi\lambda_\alpha\lambda_\beta\lambda_c|S|\lambda_a\lambda_b> \propto s_{c\alpha}/(t_{\beta b}-\alpha^2) \qquad (42)$$

As noted in the previous sections, in the limits of t near zero or $s_{\alpha\beta}$ large

$$t_{\beta b} \to \frac{(s_{\alpha\beta}-b^2)}{\sqrt{s_{\alpha\beta}}}\,[\omega_\alpha+p_\alpha\cos\psi]$$

$$s_{c\alpha} \to \frac{s}{\sqrt{s_{\alpha\beta}}}\,[\omega_\alpha+p_\alpha\cos\psi]$$

so that their ratio (42) is independent of ψ. Away from these limits this cancellation is still approximately true. Therefore, apart from helicity coupling factors, <u>the Deck effect is most important in the lowest partial wave</u>, i.e., the A_1 enhancement is

XUM

Reproduced with permission of the copyright owner. Further reproduction prohibited without permission.

predominantly 1^+, and N*(1400) enhancement predominantly $J = 1/2$. In Fig. 8 we present a spin-parity analysis of this model for the A_1 using the most obvious $\rho\pi\pi$ coupling[20].

D. What Can OPE Say about Helicities?

Up to this point we have based our discussion on the noncontroversial aspect of pion exchange; the rapid variation with momentum transfer in the range between 0 and m_π^2. In this section we discuss something of more questionable validity, but which we nevertheless believe to be an interesting point: the elementary OPE model is equivalent to approximate t-channel helicity conservation and gives g_1/g_o approximately one for the A_1.

In the elementary OPE model for the A_1 where $\beta = \rho$ and $b = \pi$, we have

$$\langle \psi \phi \lambda_\rho \lambda_c | S | \lambda_a \rangle \propto e^*(\lambda_\rho) \cdot q_b \tag{43}$$

Written in the Gottfried-Jackson frame

$$e^*(0) \cdot q_b = \frac{\omega_\rho p_b \cos\psi}{\rho} - \frac{p_\rho \omega_b}{\rho} \tag{44}$$

$$e^*(+1) \cdot q_b = \frac{1}{\sqrt{2}} p_b \sin\psi \, e^{+i\phi} \qquad e^*(-1) \cdot q_b = \frac{1}{\sqrt{2}} p_b \sin\psi \, e^{-i\phi}$$

To the extent that the ratio (42) is independent of ψ and ϕ, comparison with (41) shows that we do indeed have t-channel helicity conservation and

$$g_1/g_o \cong \rho/\omega_\rho = .93 \quad \text{at} \quad \sqrt{s_{\pi\rho}} = 1.070 \text{ Bev} \tag{45}$$

XUM

Reproduced with permission of the copyright owner. Further reproduction prohibited without permission.

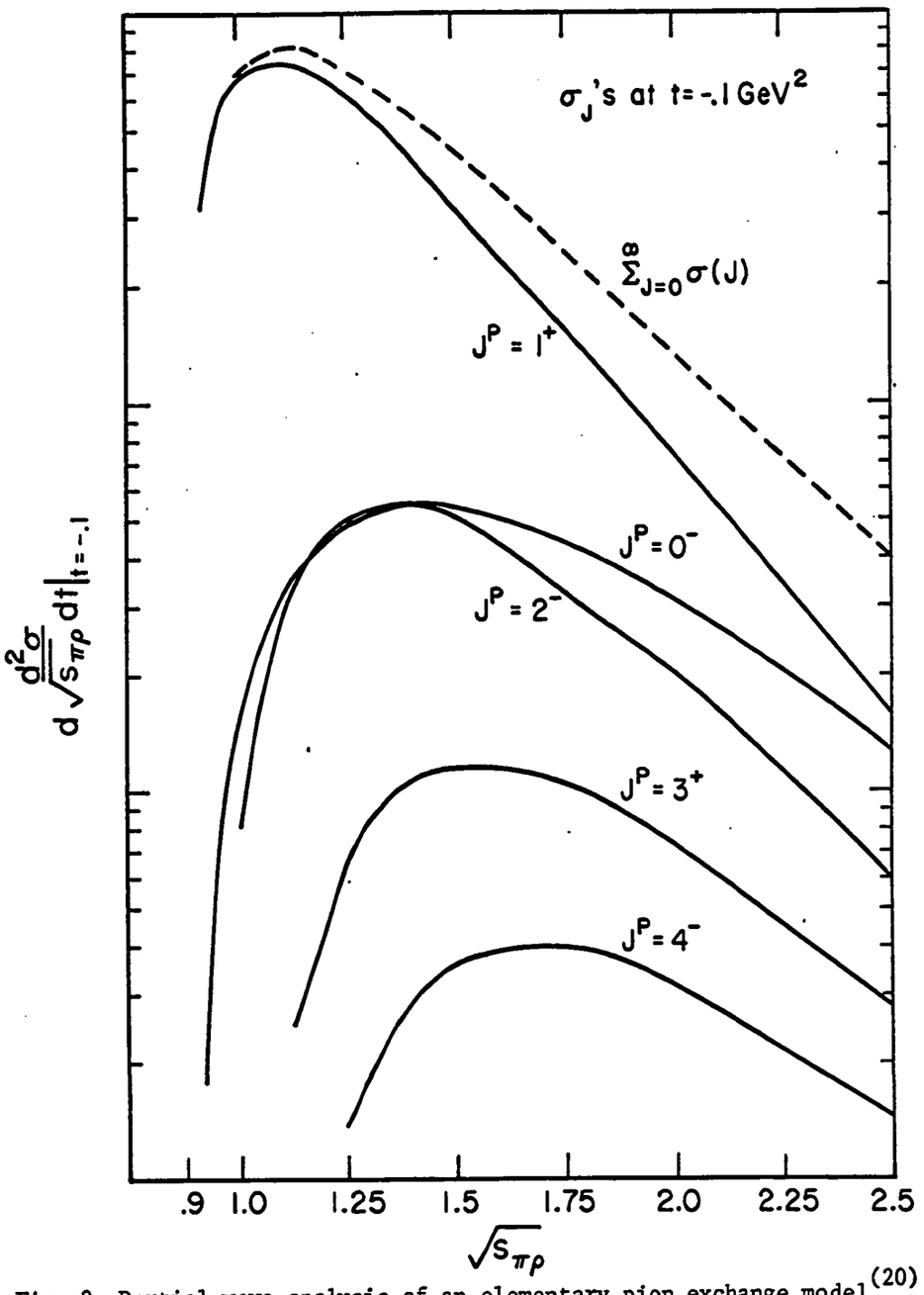

Fig. 8. Partial wave analysis of an elementary pion exchange model[20] displayed as the differential cross sections for production of a given spin and parity at t=-.1 . The vertical scale is arbitrary. Solid curves are the contributions of individual spin and parity. The dashed curve is their sum.

XUM

Reproduced with permission of the copyright owner. Further reproduction prohibited without permission.

This is to be compared with the experiment on the A_1 and Q enhancements by the ABBCCHLV collaboration[21] who find t-channel helicity conservation, with the data of Crennell et al[22] who find $g_1/g_o = (0.89^{+0.07}_{-0.00})e^{-i(1.0\pm0.6)}$, and less successfully with the data of Ballam et al[23] who find $|g_1/g_o| = 0.48 \pm 0.13$.

A similar procedure for the N*(1400) in which one sets

$$<\psi\ \phi\ \lambda_\beta\lambda_c|S|\lambda_b\lambda_a> \ \propto\ \bar{u}_\beta(\lambda_\beta)\gamma_5 u_b(\lambda_b) \tag{46}$$

yields in the Gottfried-Jackson frame

$$\begin{aligned}
\bar{u}_\beta(+1/2)\gamma_5 u_b(+1/2) &= \left(\frac{p_b}{\omega_b+b} - \frac{p_\beta}{\omega_\beta+\beta}\right)\cos\psi/2 \\
\bar{u}_\beta(-1/2)\gamma_5 u_b(+1/2) &= -\left(\frac{p_b}{\omega_b+b} + \frac{p_\beta}{\omega_\beta+\beta}\right)\sin\psi/2\ e^{-i\phi}
\end{aligned} \tag{47}$$

again in approximate agreement with t-channel helicity conservation. Now, however, in order to satisfy (17) the OPE must contribute strongly to both parities in apparent violation of the Morrison, Chou-Yang and CFZ rules[24].

We will not discuss here the manner in which these results of elementary OPE are modified by evasion, conspiracy, absorption or any other version of pion exchange. We only point out that the simplest model in which one sets the couplings (44) and (46) equal to the $V_{\lambda_\beta\lambda_b}(t_{\beta b})$ of equation (32) is clearly wrong. Such a model introduces spurious factors of $t_{\beta b}$ into $W(\psi,\phi)$ that destroy the narrowness of the Deck enhancement and rapid variation of $A(s_{\alpha\beta})$ and so does not fit the data. Indeed, in Fig. 3 of Rushbrook's analysis[19] in which

XUM

Reproduced with permission of the copyright owner. Further reproduction prohibited without permission.

such a model is employed, one fails to find the characteristic Deck shape.

Although the elementary pion exchange model may not be correct for helicity couplings, the understanding of the other features of the data, achieved by the noncontroversial property that pion exchange entails a rapid variation with momentum transfer, we believe sufficient justification to consider pion exchange as primarily responsible for the nonresonant component of diffraction dissociation. It appears unlikely that a pion exchange background would have the same helicity couplings or obey the same selection rules that are expected of resonance production.

XUM

Reproduced with permission of the copyright owner. Further reproduction prohibited without permission.

IV. OPE and Selection Rules

One is left with the question of the role played by one-pion exchange in diffraction dissociation and its relation to resonance production. Certainly the successes of OPE do not exclude the presence of genuine resonances. Indeed, the best fit to ρ^o photoproduction is achieved by Söding's model[25] of a Breit-Wigner interfering with a weaker Deck background. Nor can the N*(1680) and other enhancements be explained as kinematic effects. Difficulties lie in establishing the validity of selection rules, for at least the elementary OPE models do not obey any of the proposed spin-parity selection rules nor do they obey the s-channel helicity conservation that has been observed in πN elastic scattering and ρ^o photoproduction[2,3].

One possibility[26] is that the OPE contribution is equivalent to resonance production in a "duality" sense. If the production of accepted resonances obeys selection rules, the dual interpretation would require the OPE contribution to obey the same selection rules and, therefore, the naive models must be wrong. However, one may expect such local duality applies only to imaginary parts of scattering amplitudes whereas pion exchange, at least in the forward direction, is predominantly real.

The other possibility is that the OPE contribution, or at least its real part, should be considered as a nonresonant background. The problem then is to determine whether the accepted resonances obey selection rules in the presence of a background that may not. In the case of resonance dominance we had a series of "null tests" for helicity conservation and spin-parity selection rules because many of the $A_{\ell m}$

XUM

Reproduced with permission of the copyright owner. Further reproduction prohibited without permission.

in (18) and (25) were predicted to be zero. If resonance production continues to obey selection rules, these $A_{\ell m}$'s would now consist only of OPE-resonance interference terms and OPE-OPE terms. The $A_{\ell m}$'s not predicted zero in the null tests would have resonance-resonance terms as well.

This means that, although the null tests are invalid in the presence of an OPE background, there remains a qualitative test for helicity conservation and spin-parity selection rules in resonance production. We make the reasonable assumption that the OPE contribution is predominantly real and varies smoothly as a function of the mass of the dissociated system, while the resonance contributions have phases and magnitudes which vary approximately like Breit-Wigners as a function of mass. The OPE-resonance interference terms which contribute to the $A_{\ell m}$ in the form

$$A_{\ell m} \propto \mathrm{Re}\, a^{OPE} a^{*res}$$

should then oscillate qualitatively like the real part of a Breit-Wigner and actually pass through zero at the resonance mass. On the other hand, the resonance-resonance terms should have no such simple behavior and may even peak at the resonance mass. Thus, <u>if resonance production obeys selection rules the $A_{\ell m}$ predicted zero in the null tests should in the presence of OPE have the simple behavior of a sequence of Breit-Wigner real parts, apart from OPE-OPE terms.</u>

We would like to emphasize that <u>the OPE-resonance interference terms should prove useful in isolating the contributions of individual resonances</u>, particularly in testing Morrison's rule for which no

XUM

Reproduced with permission of the copyright owner. Further reproduction prohibited without permission.

simple test has been proposed in this paper. Note that in (19) and (26) a given term contributes to the various $A_{\ell m}$ in proportion to well-defined Clebsch-Gordan coefficients. Such an observation is particularly valuable if the nonresonant background is confined primarily to the lowest partial waves. For example, if in $\pi N \to \pi\pi N$ the background is confined to $J = 1/2$ and resonance production obeys helicity conservation, the $A_{\ell m}$ for $m \geq 2$ would be zero. Further, the $5/2^+$-background interference term would appear in A_{2m} and A_{3m} while the $3/2^-$-background interference term would appear only in A_{1m} and A_{2m}. We stress, however, that we expect such simple background distributions to be only approximately true of pion exchange[18,19,20]. If the nonresonant background contributes strongly to several partial waves, such comparisons would be more difficult but still informative.

XUM

Reproduced with permission of the copyright owner. Further reproduction prohibited without permission.

V. Summary and Discussion

We have found that if resonance production were to dominate diffraction dissociation, then: (1) helicity conservation is characterized by an isotropic ϕ-dependence; (2) the Carlitz-Frautschi-Zweig and Chou-Yang rules predict symmetrical angular distributions under $\psi \to \pi - \psi$, $\phi \to \pi + \phi$ in certain reactions (e.g., $\pi N \to \pi\pi N$ and $\pi N \to \pi\pi\Delta$) . Thus, there would be a series of "null tests" with the $A_{\ell m}$ for $m > 0$ in Eqs. (18) and (25) predicted to be zero by helicity conservation, and the $A_{\ell m}$ for ℓ odd predicted to be zero by the Chou-Yang and Carlitz, Frautschi, Zweig rules in certain reactions. In general, nonresonant background should be expected as well as resonances. A simple pion exchange model appears to account for the properties of the low mass enhancements observed in diffraction dissociation[27] including (1) the shape and position of the enhancements (the Deck effect); (2) the variation of momentum transfer dependence with invariant mass; (3) the low spin of the enhancements; and, in certain models, (4) the observed g_1/g_o for the "A_1" and t-channel helicity conservation. Thus, one-pion exchange, if not "dual" to resonance production, may be expected to constitute the nonresonant background. It most likely does not obey the selection rules resonances may obey and, therefore, would destroy the simple null tests. If resonance production continues to obey selection rules, the $A_{\ell m}$ predicted zero in the null tests now would consist of OPE-resonance interference terms as well as OPE-OPE terms. This offers the possibility of a qualitative test for selection rules in resonance production. The OPE-resonance interference terms should also prove useful in isolating the contributions of individual resonances.

XUM

Reproduced with permission of the copyright owner. Further reproduction prohibited without permission.

In any event, it should by now be obvious that analyzing data in terms of the moments of the angular distribution in the various frames is the most informative way of presenting the results of experiments on diffraction dissociation when many interfering contributions are present. We urge that present and future experiments be analyzed in this manner. In view of the need for good resolution to obtain information from the moments, there is a necessity for high statistics experiments to determine the properties of diffraction dissociation.

It is worth mentioning that in choosing experiments in which to test selection rules for N* production $\pi^+ p$ reactions are to be preferred to $\pi^- p$ reactions. The reason is that at finite energies there may be significant contributions from nondiffractive exchanges. In reactions such as $\pi^+ p \to \pi^+ (\pi N)^+$ where there is a definite isospin in the s-channel, one may isolate the $I = 1/2 (\pi N)^+$ system from the $I = 3/2$ [28]. Hence, some of the nondiffractive contamination may be removed.

Two remarks are in order concerning the interpretation of present experiments. The first is that the apparent disagreement between experiments which show s-channel helicity conservation for some reactions and those which show t-channel helicity conservation for others may be removed by the likelihood that the resonance production component of diffraction dissociation dominates the former class of reactions while the nonresonant component dominates the latter class. The procedures of Section IV applied to higher statistics experiments will help to determine whether this is indeed the case.

XUM

Reproduced with permission of the copyright owner. Further reproduction prohibited without permission.

The second remark is that, in view of the likelihood that a nonresonant mechanism dominates $\pi p \to (3\pi)p$, it is questionable to take the experimentally measured values of g_1/g_o for the diffractively produced "A_1" as evidence against symmetry schemes such as $SU(6)_W$ which predict $g_1/g_o = \infty$ for the $I=1\ 1^{++}$ meson of the quark model. One should measure the properties of the A_1, and other low spin resonances which can be produced diffractively from stable particles, in reactions other than diffraction dissociation where the identification of resonances is less ambiguous.

XUM

Reproduced with permission of the copyright owner. Further reproduction prohibited without permission.

Appendix 1: Angular Distributions

In the case of experiments with unpolarized targets where the final helicities are not measured, the general angular distribution for two-particle decays is given by

$$W(\psi,\phi) = \sum_{\lambda_\alpha,\lambda_\beta,\lambda_a,\lambda_b,\lambda_c} |\langle\psi\phi\lambda_\alpha\lambda_\beta\lambda_c|S(s,t)|\lambda_a\lambda_b\rangle|^2$$

$$= \sum_{\lambda_\alpha\lambda_\beta} \sum_{J,P,\lambda_J} \sum_{J',P',\lambda'_J} e^{i(\lambda_J-\lambda'_J)\phi} d^J_{\lambda_J,\lambda_\alpha-\lambda_\beta}(\psi) d^{J'}_{\lambda'_J,\lambda_\alpha-\lambda_\beta}(\psi)$$

$$\times g^{JP}_{\lambda_\alpha\lambda_\beta} g^{*J'P'}_{\lambda_\alpha\lambda_\beta} \sum_{\lambda_a,\lambda_b,\lambda_c} \langle J^P\lambda_J\lambda_c|T(s,t)|\lambda_a,\lambda_b\rangle$$

$$\times \langle J'^{P'}\lambda'_J\lambda_c|T(s,t)|\lambda_a\lambda_b\rangle^* \qquad (A.1)$$

From M. E. Rose, Elementary Theory of Angular Momentum, John Wiley & Sons, 1957, equations (4.17) and (4.25) we have

$$e^{i(\lambda_J-\lambda'_J)\phi} d^J_{\lambda_J,\lambda_\alpha-\lambda_\beta} d^J_{\lambda'_J,\lambda_\alpha-\lambda_\beta} = (-1)^{\lambda'_J-(\lambda_\alpha-\lambda_\beta)} \qquad (A.2)$$

$$\times \sum_\ell C(J,J',\ell;\lambda_J,-\lambda'_J) C(J,J',\ell;\lambda_\alpha-\lambda_\beta,-\lambda_\alpha+\lambda_\beta) \sqrt{\frac{4\pi}{2\ell+1}}\, Y_\ell^{\lambda_J-\lambda'_J}(\psi,\phi)$$

Using parity conservation, we obtain

$$\sum_{\lambda_a,\lambda_b,\lambda_c} \langle J^P\lambda_J\lambda_c|T(s,t)|\lambda_a\lambda_b\rangle \langle J'^{P'}\lambda'_J\,\lambda_c|T(s,t)|\lambda_a\,\lambda_b\rangle^*$$

$$= \sum_{\lambda_b>0,\lambda_a,\lambda_c} \langle J^P\lambda_J\lambda_c|T(s,t)|\lambda_a\lambda_b\rangle \langle J'^{P'}\lambda'_J\,\lambda_c|T(s,t)|\lambda_a\lambda_b\rangle^* +$$

XUM

Reproduced with permission of the copyright owner. Further reproduction prohibited without permission.

$$+ \sum_{\lambda_b>0,\lambda_a,\lambda_c} (-1)^{J+J'} PP' (-1)^{\lambda_J+\lambda'_J} \langle J^P -\lambda_J \lambda_c | T(s,t) | \lambda_a \lambda_b \rangle$$

$$\times \langle J'^{P'} - \lambda'_J \lambda_c | T(s,t) | \lambda_a \lambda_b \rangle^* \qquad (A.3)$$

Combine equations (A.1), (A.2), and (A.3). Then in the sums over λ_J and λ'_J corresponding to the second term in (A.3), make the transformation $\lambda_J \to -\lambda_J$ and $\lambda'_J \to -\lambda'_J$. Using Rose (3.16a) which states

$$C(J,J',\ell;\lambda_J,-\lambda'_J) = (-1)^{J+J'-\ell} C(J,J',\ell;-\lambda_J,\lambda'_J) \qquad (A.4)$$

we derive (18) and (19). Analogous considerations apply to three particle decays.

From the general expressions (18), (19) and (25), (26), one may derive angular distributions for the analysis of specific experiments by using tables of Clebsch-Gordan coefficients such as M. Rotenberg, R. Burns, M. Metropolis, and J. Wooten, The 3-J and 6-J Symbols, The Technology Press (1959).

As an example of the type of expressions that result, we give the angular distributions for $\pi N \to \pi(\pi N)$ in the case of helicity conservation. We identify from (15) and (16)

$$g^{JP}_{+1/2} \langle J^P + 1/2 | T | +1/2 \rangle = S^J_P$$

Using (17) it is found that (19) simplifies to

$$A_{\ell m} = (-2) \sqrt{\frac{4\pi}{2\ell+1}} \sum_{J,P} \sum_{J',P'} C(J,J',\ell;1/2,-1/2)\, C(J,J',\ell;-1/2,1/2)$$

$$\times \frac{(1+PP'(-1)^{\ell})^2}{4} S^J_P\, S^{*J'}_{P'}$$

XUM

Reproduced with permission of the copyright owner. Further reproduction prohibited without permission.

Then for $J \leq 5/2$

$$A_{00} = \sqrt{4\pi}\,[|S_+^{1/2}|^2 + |S_-^{1/2}|^2 + \tfrac{1}{2}|S_+^{3/2}|^2 + \tfrac{1}{2}|S_-^{3/2}|^2 + \tfrac{1}{3}|S_+^{5/2}|^2 + \tfrac{1}{3}|S_-^{5/2}|^2 + \cdots]$$

$$A_{10} = \sqrt{\frac{4\pi}{3}}\,[2\,\mathrm{Re}\,S_+^{*1/2}S_-^{1/2} + \tfrac{1}{5}\,\mathrm{Re}\,S_+^{*3/2}S_-^{3/2} + \tfrac{2}{35}\,\mathrm{Re}\,S_+^{*5/2}S_-^{5/2} + 2\,\mathrm{Re}(S_+^{*1/2}S_-^{3/2} + S_-^{*1/2}S_+^{3/2}) + \tfrac{6}{5}\,\mathrm{Re}(S_+^{*3/2}S_-^{5/2} + S_-^{*3/2}S_+^{5/2}) + \cdots]$$

$$A_{20} = \sqrt{\frac{4\pi}{5}}\,[\tfrac{1}{2}|S_+^{3/2}|^2 + \tfrac{1}{2}|S_-^{3/2}|^2 + \tfrac{8}{21}|S_+^{5/2}|^2 + \tfrac{8}{21}|S_-^{5/2}|^2 + 2\,\mathrm{Re}(S_+^{*1/2}S_+^{3/2} + S_-^{*1/2}S_-^{3/2}) + 2\,\mathrm{Re}(S_+^{*1/2}S_+^{5/2} + S_-^{*1/2}S_-^{5/2}) + \tfrac{2}{7}\,\mathrm{Re}(S_+^{*3/2}S_+^{5/2} + S_-^{*3/2}S_-^{5/2}) + \cdots]$$

$$A_{30} = \sqrt{\frac{4\pi}{7}}\,[\tfrac{9}{5}\,\mathrm{Re}\,S_+^{*3/2}S_-^{3/2} + \tfrac{16}{45}\,\mathrm{Re}\,S_+^{*5/2}S_-^{5/2} + 2\,\mathrm{Re}(S_+^{*1/2}S_-^{5/2} + S_-^{*1/2}S_+^{5/2}) + \tfrac{4}{5}\,\mathrm{Re}(S_+^{*3/2}S_-^{5/2} + S_-^{*3/2}S_+^{5/2}) + \cdots]$$

$$A_{40} = \sqrt{\frac{4\pi}{9}}\,[\tfrac{2}{7}|S_+^{5/2}|^2 + \tfrac{2}{7}|S_-^{5/2}|^2 + \tfrac{12}{7}\,\mathrm{Re}(S_+^{*3/2}S_+^{5/2} + S_-^{*3/2}S_-^{5/2}) + \cdots]$$

$$A_{50} = \sqrt{\frac{4\pi}{11}}\,[\tfrac{100}{63}\,\mathrm{Re}\,S_+^{*5/2}S_-^{5/2} + \cdots]$$

$A_{\ell m} = 0$ for $m \neq 0$.

Although this particular distribution is true only if helicity is conserved, it exhibits features which were mentioned in Sections II and IV to characterize angular distributions in general: e.g., (1) the

XUM

Reproduced with permission of the copyright owner. Further reproduction prohibited without permission.

$A_{\ell m}$ for ℓ odd involve only terms mixed in parity; (2) the 5/2 - 1/2 interference term appears only in A_{2m} and A_{3m} while the 3/2 - 1/2 term appears only in A_{1m} and A_{2m}; and (3) a given term such as $3/2^+ - 5/2^+$ contributes to the various $A_{\ell m}$ such as A_{20} and A_{40} in proportion to numbers calculable from C-G coefficients (in this case $A_{20}(3/2^+ - 5/2^+)/A_{40}(3/2^+ - 5/2^+) = \frac{1}{2\sqrt{5}}$) .

XUM

Reproduced with permission of the copyright owner. Further reproduction prohibited without permission.

References

1. R. T. Deck, Phys. Rev. Letters 13, 169 (1964). The diagrams responsible for these kinematic enhancements were considered earlier by S. D. Drell, K. Hiida, Phys. Rev. Letters 7, 199 (1961).

2. J. Ballam et al, Phys. Rev. Letters 24, 960 (1970); H. Harari and Y. Zarmi, Phys. Letters 32B, 291 (1970).

3. That s-channel helicity conservation is present in πN scattering and may be a property of all reactions with asymptotically constant cross sections has been suggested by F. J. Gilman, J. Pumplin, A. Schwimmer, and L. Stodolsky, Phys. Letters 31B, 307 (1970).

4. D. R. O. Morrison, Phys. Rev. 165, 1699 (1968).

5. T. T. Chou and C. N. Yang, Phys. Rev. 175, 1832 (1968).

6. R. Carlitz, S. Frautschi, and G. Zweig, Phys. Rev. Letters 23, 1134 (1964). This paper contains a thorough review of the experimental distinctions between the various selection rules.

7. For tests for helicity conservation using polarized photons in $\gamma p \to \rho^o p$, see K. Schilling, P. Seyboth, and G. Wolf, Nucl. Phys. B15, 397 (1970).

8. K. Gottfried and J. D. Jackson, Nuovo Cimento 33, 309 (1964).

9. R. K. Adair,

10. We have absorbed some common factors into the invariant amplitudes. For the full formalism see M. Jacob and G. C. Wick, Annals of Phys. 7, 404 (1959).

11. After the completion of this work, the author learned that this test has been suggested previously in several places including: G. Cohen-Tannoudji, J. M. Drouffe, P. Moussa, and R. Peschanski, Phys. Letters 33B, 183 (1970); A. Bialas, J. Dabkouski, L. Van Hove, TPJU-23/70. However, these authors did not consider the question of pion exchange.

XUM

Reproduced with permission of the copyright owner. Further reproduction prohibited without permission.

12. S. M. Berman and M. Jacob, Phys. Rev. 139, 1023 (1965).

13. See also L. Stodolsky, Phys. Rev. Letters 18, 973 (1967).

14. Strictly speaking, of course, the helicities of c and a as defined in $a+b \to c+\alpha+\beta$ are not the same as the s-channel helicities for $\alpha+a \to \alpha+c$. We denote this by placing a bar over the helicities $\lambda_c \to \bar{\lambda}_c$. However, these helicities play no role in the present considerations.

15. J. Bartsch, et al, Phys. Letters 27B, 336 (1968);
W. D. Walker, University of Wisconsin preprint (1968).

16. We used data from an 80-in bubble chamber exposure at the Brookhaven National Laboratory by the Walker-Erwin group of the University of Wisconsin.

17. That OPE could account for the variation of momentum transfer dependence with invariant mass was first published by B. Y. Oh and W. D. Walker, Phys. Letters 28B, 564 (1969).

18. A spin-parity analysis of a multi-regge model for the A_1 has been presented by C. D. Froggatt, G. Ranft, Phys. Rev. Letters 23, 943 (1969).

19. A spin-parity analysis of an elementary OPE model for N* production has been presented by J. G. Rushbrooke, Phys. Rev. 177, 2357 (1969).

20. The exact model we employ is

$$\langle \psi\phi\lambda_\alpha\lambda_\beta\lambda_c | S(s,t) | \lambda_b\lambda_a \rangle \propto \frac{is_{c\alpha}\, e^{Bt/2}\, e^*(\lambda_\beta)\cdot p_b}{[t_{\beta b}-\alpha^2][(t_{\beta b}-(\beta+b)^2)(t_{\beta b}-(\beta-b)^2)]^{1/2}}$$

Although this model reproduces the Deck enhancement and variation of momentum transfer with invariant mass unlike the elementary OPE model of Ref. 19, it is not a prescription that is consistent with the available data of other pion exchange reactions such as pion photoproduction. Similar objections apply

XUM

Reproduced with permission of the copyright owner. Further reproduction prohibited without permission.

to the model of Ref. 18. Therefore, we feel that the quantitative predictions of these models are not to be taken seriously. The general considerations we present in this paper we believe to be independent of the questionable details of these models.

21. J. V. Beaupre, et al, ABBCCHLV collaboration, CERN/D.Ph.II/Phys. 70-65.

22. David J. Crennell, et al, Phys. Rev. Letters 24, 781 (1970).

23. J. Ballam, et al, Phys. Rev. D1, 94 (1969).

24. That elementary OPE must contribute strongly both to $J^P = 1/2^+$ and $J^P = 1/2^-$ was also found by J. G. Rushbrook, Ref. 19.

25. P. Söding, Phys. Letters 19, 702 (1965); H. Bingham, et al, Phys. Rev. Letters 24, 955 (1970).

26. G. F. Chew and A. Pignotti, Phys. Rev. Letters 20, 1078 (1968).

27. A resonance interpretation has been provided by E. W. Colglazier, J. L. Rosner, Nucl. Phys. B27, 349 (1971).

28. K. Boesebeck et al, ABBCCHW collaboration, CERN/D.Ph.II/Phys. 70-49.

XUM

Reproduced with permission of the copyright owner. Further reproduction prohibited without permission.

PART II

INDEPENDENT PRODUCTION OF PIONS

XUM

Reproduced with permission of the copyright owner. Further reproduction prohibited without permission.

I. Introduction

The phenomenology of inelastic reactions at high energies is unavoidably more complicated than that of two-body scattering. There are typically a bewildering variety of variables upon which the scattering amplitudes may depend. It is unclear which variables, if any, are of particular significance. The absence of a theory of strong interactions precludes a priori knowledge of which features should be expected to dominate the data. Our present understanding of two-body scattering suggests the existence of a number of competing effects in inelastic reactions, but, so far, few have been unambiguously identified.

Despite these practical difficulties, it is clear that inelastic reactions are important to an overall view of the strong interactions, if only because they are related by unitarity to two-body scattering. In fact, this connection provides some insight. The s and u channel reactions have differing degrees of resonance formation and yet there is an apparent asymptotic equality between s and u channel inelastic cross sections. This suggests that direct channel resonance formation accounts for only a small portion of the inelastic cross sections at high energies. It is also apparent from the sizes of diffraction dissociation cross sections that they, as well, constitute only a small fraction of inelastic reactions.

For the remaining majority of inelastic reactions a variety of widely divergent models have been proposed, each attempting to describe some aspects of the data but with little predictive power. It

XUM

Reproduced with permission of the copyright owner. Further reproduction prohibited without permission.

is preferable to discuss the model independent statements that appear to characterize inelastic reactions. In this introduction we shall review the salient features of the data and the experimental situation that motivates the work of this thesis. These points shall be illustrated primarily with the published and unpublished data of the ABBCCHW collaboration[1,2].

We begin by examining the distributions of final particles in momentum space. These are commonly expressed in terms of the momenta along and transverse to the direction of the incident particles in the center of mass of the collision. In Fig. 1 we exhibit the average longitudinal and transverse momenta for various configurations of final particles resulting from $\pi^- p$ collisions at 16 Gev/c. This figure illustrates behavior common to most multiparticle reactions.

Instead of occupying uniformly the available phase space, the outgoing particles have low transverse momenta whose average is roughly 300 Mev/c. This average may be estimated from the observed total and elastic cross sections as follows. From the assumptions that the elastic amplitudes are purely imaginary and vary exponentially with t, which we showed in Part I to be a good approximation at high energies, one can derive that the inelasticities are given by

$$1 - \eta_\ell = 4 \frac{\sigma_{el}}{\sigma_{tot}} \exp\left(- \frac{\ell^2 8\pi \sigma_{el}}{k^2 \sigma_{tot}^2}\right) \qquad (1)$$

The inelastic cross section for a given partial wave is

$$\sigma_{inel}^{\ell} = \frac{(2\ell+1)\pi}{k^2} (1 - \eta_\ell^2) \qquad (2)$$

XUM

Reproduced with permission of the copyright owner. Further reproduction prohibited without permission.

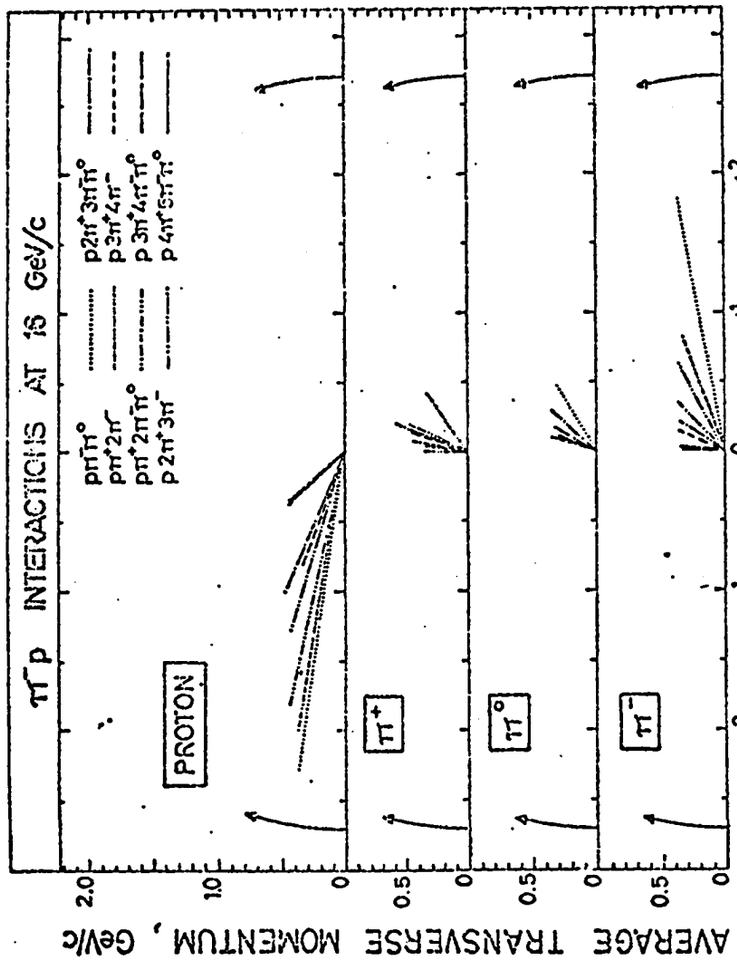

Fig. 1. Vectors of the average momenta of various particles in different modes observed in the $\pi^- p$ experiment. Taken from Ref. 2

XUM

Reproduced with permission of the copyright owner. Further reproduction prohibited without permission.

Thus the radius of interaction for inelastic reactions is given approximately by $R^2 = \sigma_{tot}^2/8\pi\sigma_{el}$. The uncertainty in transverse momentum is related to the uncertainty in position by

$$\Delta p_T = \frac{1}{\Delta x} = \frac{1}{R} = \sqrt{\frac{8\pi\,\sigma_{el}}{\sigma_{tot}^2}} \qquad (3)$$

Using $\sigma_{tot}(\pi^- p) = 23.5$ mb and $\sigma_{el}/\sigma_{tot} = .17$, we obtain $\Delta p_T \simeq 250$ Mev/c . Despite the crudeness of this calculation, one sees that the approximate magnitude of the cutoff in transverse momenta may only be as fundamental as the asymptotic values of strong interaction cross sections.

Without making any assumptions, the statement that the transverse momenta should be limited by the sizes of observed cross sections can be justified quite simply. Note that in (2) unitarity limits the contribution of a given angular momentum. To achieve σ_{inel} of the size seen experimentally, the number of partial waves which contribute strongly should increase with increasing energy. By angular momentum conservation the distribution of final particles becomes less and less isotropic for fixed σ_{inel} as the energy increases, a phenomenon which can be approximately described by fixing the average value of p_T .

Figure 1 also illustrates that outgoing particles with the same quantum numbers as the incident particles tend to have longitudinal momenta comparable to those of the incident particles, while the other produced particles have longitudinal momenta which average around zero in the center of mass. This is further demonstrated in

XUM

Reproduced with permission of the copyright owner. Further reproduction prohibited without permission.

Fig. 2 which is a scatter plot of the momenta in 16 Gev/c $\pi^- p \to p\pi^+\pi^-\pi^-\pi^0$. One says that the two "leading particles" have momenta near the limit set by energy momentum conservation, while the "nonleading particles" have low longitudinal momenta. The π^- distribution includes nonleading as well as leading pions.

It is possible that, except for the low transverse momenta, the distributions of nonleading particles may be largely understood in terms of phase space. The main products of high energy collisions are pions, which is certainly the mode favored by phase space. The peaking at low longitudinal momenta may arise from the relativistic phase space d^3P/E enhancing the distribution of low momentum pions in whatever frame we choose to view them. A more meaningful statement is that the distributions are the most symmetrical when viewed in the center of mass of the collision. If one assumes that the prime effect of the dynamics is to restrict the transverse momenta, then the cross section for producing a particle may be crudely approximated by

$$\sigma \propto \int \frac{d^2p_T\, dp_L}{\sqrt{m^2 + p_T^2 + p_L^2}} \exp(-p_T^2/\Delta p_T^2) \qquad (4)$$

Since the longitudinal momenta are limited by energy conservation to values less than $\sqrt{s}/2$, this integral looks like $\int^{\sqrt{s}/2} \frac{dp_L}{p_L}$ at large s. We thus calculate that the average multiplicities of produced particles should be proportional to $\ln s$, as is observed empirically.

Leading particles may also be resonances that are emitted with low momentum transfers from the incident particles. An interesting question is whether one can distinguish between nonleading pions

XUM

Reproduced with permission of the copyright owner. Further reproduction prohibited without permission.

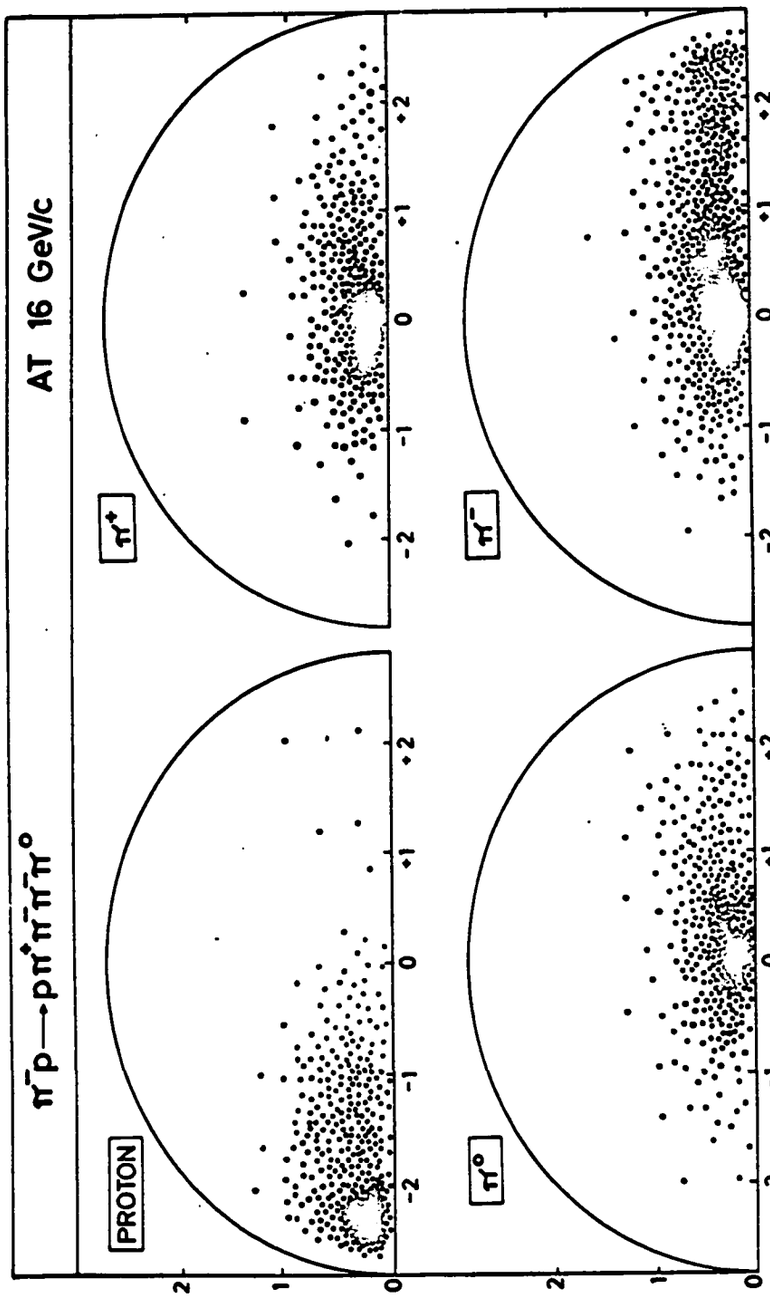

Fig. 2. Peyrou Plot of $\pi^- p \rightarrow p\pi^+\pi^-\pi^0$. Data of Ref. 2.

XUM

Reproduced with permission of the copyright owner. Further reproduction prohibited without permission.

and pions which result from the decay of leading resonances. Consider the production of a leading N* which subsequently decays into a pion and a nucleon. The velocity of the N* is given by

$$M_{N^*} \frac{V}{\sqrt{1 - V^2/c^2}} \simeq p_{inc}^{c.m.} = \frac{\sqrt{s}}{2} \quad \text{at large } s \tag{5}$$

Then, the average longitudinal momentum for the pion is

$$\langle p_L \rangle_\pi = \frac{m_\pi V}{\sqrt{1 - V^2/c^2}} \simeq \frac{\sqrt{s}\, m_\pi}{2 m_{N^*}} \tag{6}$$

For 16 Gev/c πp collisions, a pion from N*(1236) decay would have $\langle p_L \rangle_\pi \tilde{=} 300$ Mev/c which is the same order of magnitude as the longitudinal momenta of nonleading pions. These pions should on the average, of course, move in the direction of the incident N . A pion from a leading ρ should have $\langle p_L \rangle_\pi \tilde{=} 500$ Mev/c and should on the average move in the direction of the incident π . Higher mass resonances would yield even smaller average longitudinal momenta for their decay products. Hence, resonances could also produce distributions of pions with predominantly low longitudinal momenta as are observed experimentally.

The model in which all inelastic reactions proceed via the formation of leading resonances is termed the "two-fireball model". The model in which the nonleading pions are considered to be the debris left over from the collision of the two incident hadrons is termed "pionization". Various other models range themselves in a rather smooth spectrum between these two extremes. Clearly, experiments at

XUM

Reproduced with permission of the copyright owner. Further reproduction prohibited without permission.

higher energies would aid greatly in establishing which, if any, of these qualitative descriptions is correct.

Correlations may be observed in "inclusive" hadronic reactions by measuring the n-particle probability distributions. Inclusive reactions are those in which a few of the final particles are measured and the rest are ignored. They are to be contrasted with "exclusive" reactions wherein all of the final particles are measured. If $P(k_1)$ is the single particle distribution and $P(k_1,\cdots,k_n)$ [7] the n-particle distribution, the quantity of interest is

$$G^{(n)}(k_1,\cdots,k_n) = P(k_1,\cdots,k_n) - P(k_1)\cdots P(k_n)$$

which in the quantum theory of optics is called the n^{th} order correlation function. A state of produced particles in which the correlation functions through order n are zero is called "n^{th} order uncorrelated" or "n^{th} order coherent".

Since inclusive n-particle distributions have not as yet been measured, we will examine the evidence for correlations among particles in exclusive reactions. Figure 3 gives the distribution[3] in $\pi^+\pi^-$ invariant mass for $\pi^-p \to 3\pi^-,2\pi^+,p$. Clearly, it is difficult to discern appreciable ρ or f . Uncorrelated pions would naturally have the qualitative behavior indicated, but it may be that the various resonant effects among the final particles are difficult to resolve. To test further the absence of second order correlations, we should ideally look at a six-dimensional plot of two pions. Instead we restrict ourselves to a check of the correlation between longitudinal momenta. Figure 4 shows the longitudinal center of mass distribution[1]

XUM

Reproduced with permission of the copyright owner. Further reproduction prohibited without permission.

XUM

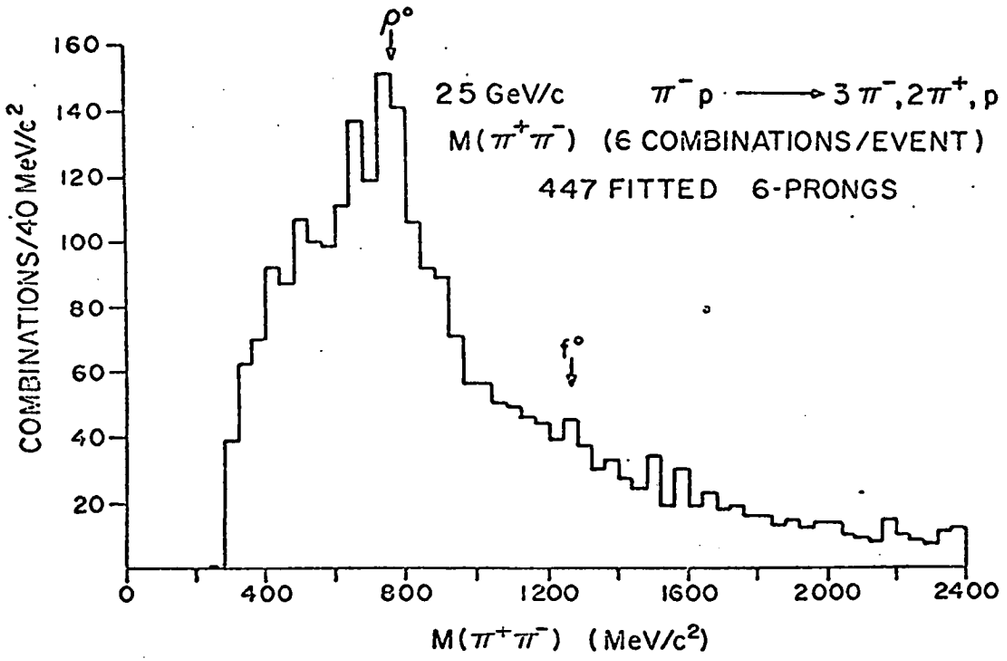

Fig. 3. Search for ρ and f mesons in all neutral combinations of six prong events. Taken from Ref. 3.

Reproduced with permission of the copyright owner. Further reproduction prohibited without permission.

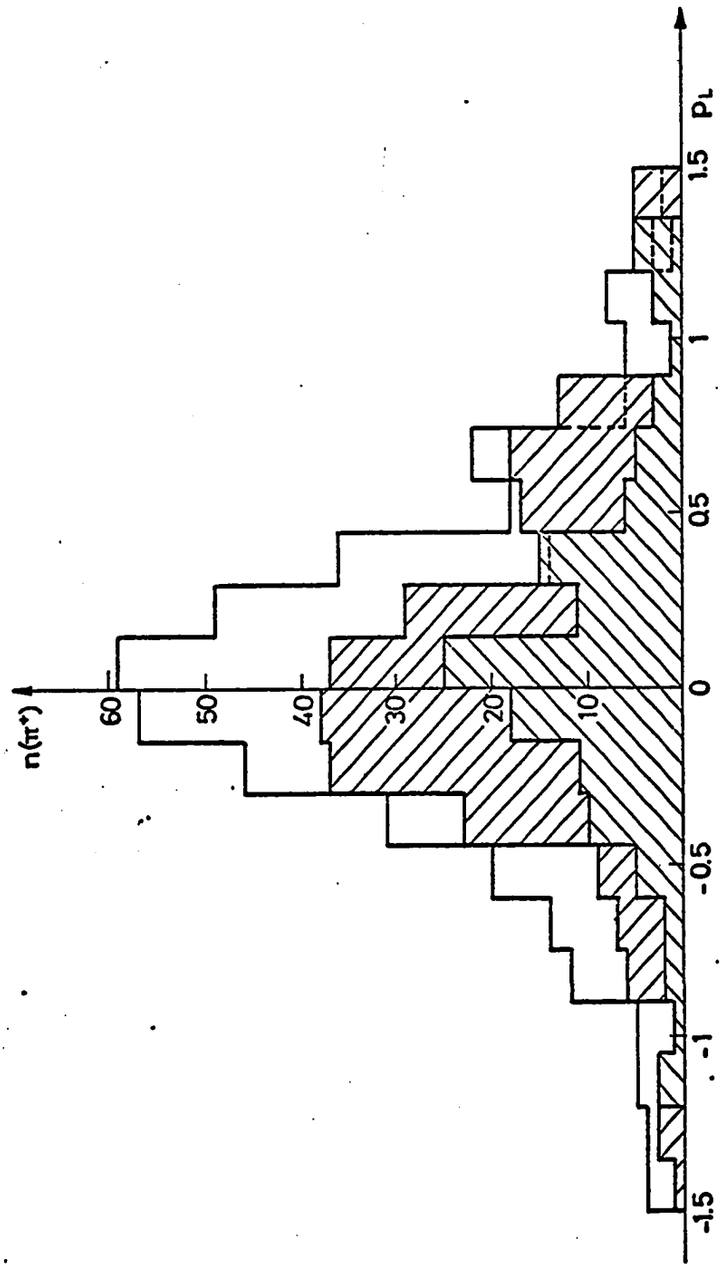

Fig. 4. Distribution of π^+ events vs. their longitudinal center-of-mass momentum as a function of the other π^+'s longitudinal momentum in $\pi^- p \to \pi^+\pi^+\pi^-\pi^-\pi^0$. See explanation in text. Unpublished data of Ref. 1.

XUM

Reproduced with permission of the copyright owner. Further reproduction prohibited without permission.

of one π^+ in $\pi^- p \to \pi^- p \pi^+ \pi^+ \pi^- \pi^-$ for several choices of the longitudinal momenta of the other π^+ (these choices are (0,-0.1 Gev/c), (-0.2,-0.3), (-0.4,-0.5) for the three shown distributions). The general trend is a uniform decrease in agreement with uncorrelated production. One may argue that since $\pi^+\pi^+$ is an exotic channel it should not exhibit strong correlations whereas the $\pi^+\pi^o$ channel should. A similar check of $\pi^+\pi^o$ shows a far less regular behavior than Fig. 4. Nevertheless, it is still true that the bulk of the events are concentrated around low longitudinal momenta in the center of mass. We may conclude that uncorrelated production may be a crude approximation to the data.

We define the emission of pions as <u>independent</u> if the same $P(\vec{k})$ can be used in all configurations of outgoing particles. In addition we take independence to mean that if the cross section for producing n pions in a certain fraction of phase space is proportional to

$$\frac{d^3k_1}{2\omega_1} fP(k_1) \cdots \frac{d^3k_n}{2\omega_n} fP(k_n) \tag{7}$$

the cross section for producing $n+1$ pions is proportional to

$$\frac{d^3k_1}{2\omega_1} fP(k_1) \cdots \frac{d^3k_n}{2\omega_n} fP(k_n) \frac{d^3k_{n+1}}{2\omega_{n+1}} fP(k_{n+1})$$

$fP(\vec{k})$ may in principle depend on the charge of the pion, but is supposed to be fixed for any given momentum of the incident particles.

If the emission is independent one expects to find distributions of many particle events similar to Poisson distributions. The

XUM

Reproduced with permission of the copyright owner. Further reproduction prohibited without permission.

distributions[1] for charged particle production are given in Fig. 5, and are well described by Poisson-like distributions. Of course, independent emission is not the only explanation for these distributions, but it is suggested. Figure 6 shows the center of mass longitudinal momentum distributions[1] of the π^+ in two different configurations. The similarity between the dominant features of these two curves would also be implied by independent production of π^+. We may also expect independence to imply that the energy dissipated into the pion cloud is proportional to the number of produced pions. Consequently the energy of the leading particles will decrease with increasing pion multiplicity. Figure 1 demonstrates that the average momenta of the proton and leading π^- indeed follow this behavior. The other pions' behavior does not change nearly as drastically.

We are thus led to consider as a possibility that an approximate phenomenological description of multipion production at high energies may be that pions are produced independently and are essentially uncorrelated. Such descriptions have in fact played a significant historical role in the development of our current ideas concerning the relation between elastic and inelastic reactions. Beginning with the pioneer work of Van Hove[4], attempts have been made to calculate via unitarity observed properties of elastic scattering from assumed models for inelastic scattering. In specific uncorrelated models the experimental linearity of $\ell n \frac{d\sigma_{el}}{dt}$ in t has been "derived". It has also been possible to connect constancy of the average transverse momenta to the asymptotic constancy of total and elastic cross sections, as we have in the intuitive

XUM

Reproduced with permission of the copyright owner. Further reproduction prohibited without permission.

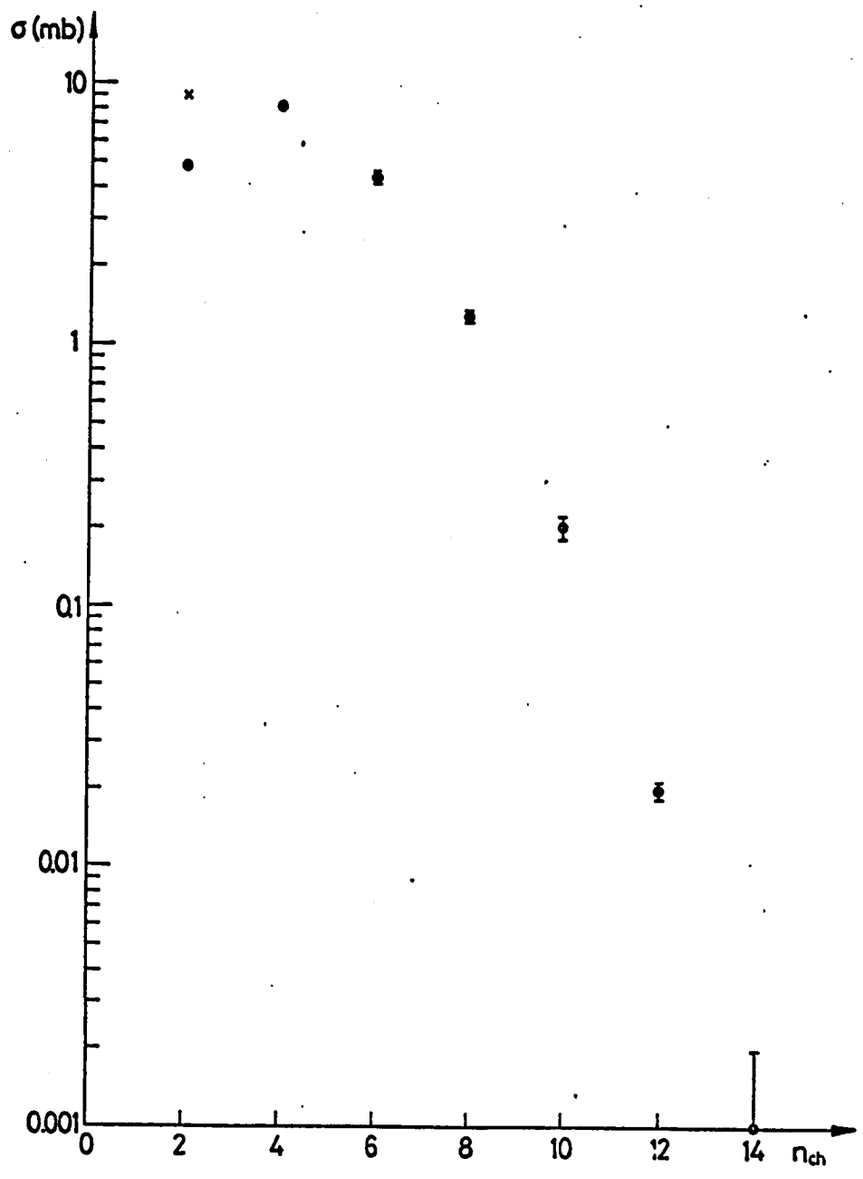

Fig. 5. Distributions of cross sections for non-strange particle production in the $\pi^- p$ experiment. Data of Ref. 1. The cross represents the value obtained for $n_{ch} = 2$ if the elastic reaction is included.

XUM

Reproduced with permission of the copyright owner. Further reproduction prohibited without permission.

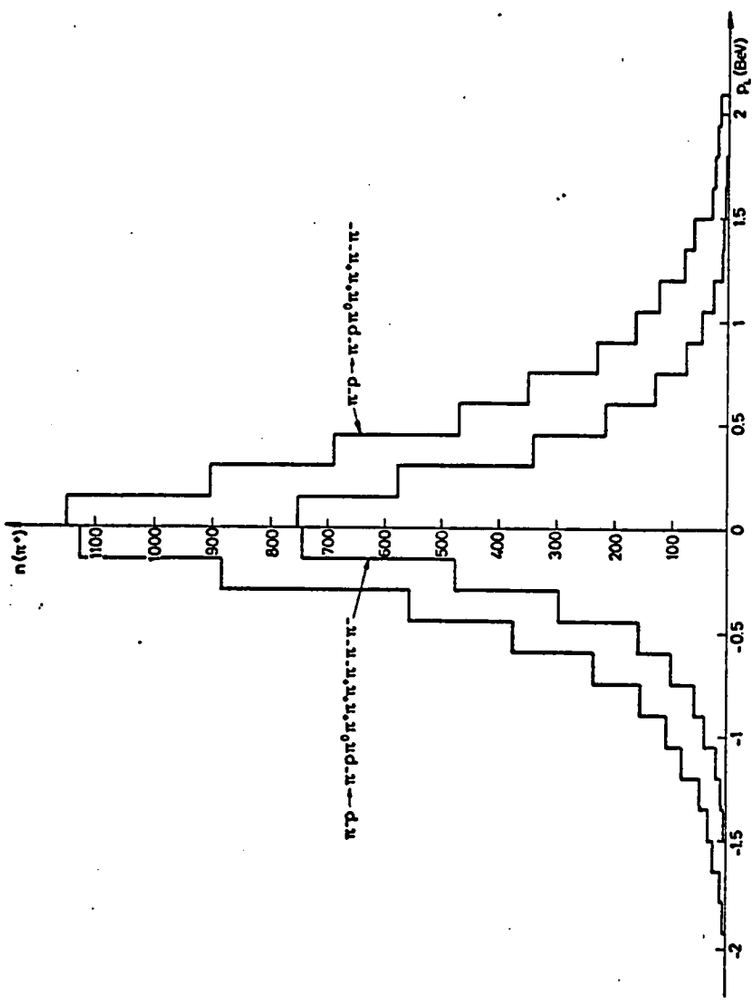

Fig. 6. Distributions of π^+ events vs. their longitudinal center of mass momentum for two different final configurations. Unpublished data of Ref. 1.

XUM

Reproduced with permission of the copyright owner. Further reproduction prohibited without permission.

arguments presented above. Many models with approximate independence, known as "factorable" models, achieve Poisson-like distributions for the n-particle cross sections.

The question we address in Part II of this thesis is an obvious one. To what degree can independent emission of uncorrelated pions be true when there are some obvious constraints which must be obeyed, i.e., four-momentum conservation, charge conservation, parity and charge conjugation invariance, and isospin conservation?

A state of pions uncorrelated to all orders, emitted independently, and in which also the phase of the pion wave function (whose norm is $fP(k)$) is fixed as a "coherent state". This phase is obviously unmeasurable, since measuring cross sections involves looking at the square of the pion wave function. This phase will be important when we discuss the isospin question. As an example of independent production of uncorrelated pions, we will discuss in the next section how a coherent state may be employed in a scattering matrix description of many pion production[5]. Since we apply the method to the description of pions emitted with low energies in the center of mass of the collision, it can be called "coherent pionization".

In the following sections we will systematically discuss the effects of strong interaction symmetries on independent emission, and we will examine briefly independent emission of two-pion resonances. Several results will be achieved for which we will give model-independent justifications.

A word about the relation of our work to other models for multipion production; currently fashionable proposals such as the

XUM

Reproduced with permission of the copyright owner. Further reproduction prohibited without permission.

multiperipheral model and scaling in inclusive hadronic reactions concern the distribution in momentum space of the produced particles. Inasmuch as we focus on the effects of symmetries and conservation laws, our work is complementary rather than orthogonal to the other approaches. The single particle distribution will be irrelevant to our considerations, and we will make no proposal concerning its behavior.

Sections II and III discuss the emission of a coherent state. Section IV concerns the distribution of pions resulting from charge conservation; Section V, parity and charge conjugation; Sections VI and VII, implications of isospin conservation; Section VIII, two-pion correlations such as resonances; and Section IX, conclusion.

XUM

Reproduced with permission of the copyright owner. Further reproduction prohibited without permission.

II. The Coherent State

A coherent state of bosons is quite unique in its physical interpretation and mathematical structure. It is the quantum mechanical state that is closest to a classical system in its dynamical properties[6]. Thus, a coherent state of particles is the quantized description of classical radiation of the corresponding field. It is used in describing electromagnetic radiation in quantum optics as well as in the analyses of bremstrahlung and the related infrared catastrophe[7]. In the present section we apply this concept to pions. For the moment we will disregard their quantum numbers and use only the fact that they are bosons. Modifications introduced in the following sections can be simply implemented within the formalism of Sections II and III.

We start with creation and annihilation operators satisfying

$$[a(\vec{k}),a^{\dagger}(\vec{k}')] = 2k_o(2\pi)^3\,\delta^{(3)}(\vec{k}-\vec{k}) \tag{8}$$

Then a coherent state of bosons is defined by

$$a(\vec{k})|f> = f(\vec{k})|f> \tag{9}$$

where $f(\vec{k})$ is the momentum space wave function for each boson, k is the four-momentum and $k_o = \omega = \sqrt{\vec{k}^2+\mu^2}$. $f(\vec{k})$ is a relativistic invariant function of k. The solution to (9) is given by

$$\begin{aligned}|f> &= \exp\{\int d\mu(\vec{k})\,[f(\vec{k})a^{\dagger}(\vec{k}) - \tfrac{1}{2}|f(\vec{k})|^2]\}\,|0> \\ &= \exp\{\int d\mu(\vec{k})\,[f(\vec{k})a^{\dagger}(\vec{k}) - f^*(\vec{k})a(k)]\}|0>\end{aligned} \tag{10}$$

XUM

Reproduced with permission of the copyright owner. Further reproduction prohibited without permission.

where $d\mu(k) = d^2k/2\omega(2\pi)^3$, and we have normalized $|f>$ so that $<f|f> = 1$. The basic equation (9) gives the clue to the classical behavior: the expectation value of a second quantized boson field within the state $|f>$ will be given by a classical field with momentum distribution $f(k)$.

The expectation value of the four-momentum operator P_μ is

$$<f|P_\mu|f> = <f|\int d\mu(\vec{k})k_\mu a^\dagger(\vec{k})a(\vec{k})|f> = \int d\mu(\vec{k})k_\mu|f(\vec{k})|^2 \qquad (11)$$

Obviously $|f>$ is a combination of all n-particle states, i.e., if $\bar{n} = \int d\mu(\vec{k})|f(\vec{k})|^2$

$$\frac{1}{n!}\int d\mu(\vec{k}_1)\cdots d\mu(\vec{k}_n)|<\vec{k}_1\cdots\vec{k}_n|f>|^2 = \frac{(\bar{n})^n}{n!}\bar{e}^{\bar{n}} \qquad (12)$$

a Poisson distribution in n .

In dealing with the production of a coherent state we have to project out of it the piece that corresponds to a definite four-momentum K . We will denote this new state by $|f,K>$. It is given by

$$|f,K> = \frac{1}{(2\pi)^4}\int d^4x\, e^{-iK\cdot x}\exp\{-\frac{\bar{n}}{2}+\int d\mu(\vec{k})f(\vec{k})a^\dagger(\vec{k})e^{ik\cdot x}\}|0> \qquad (13)$$

and obeys

$$\int d^4K\,|f,K> = |f> \qquad (14)$$

$$<f|f,K> \equiv \rho_f(K) = \frac{1}{(2\pi)^4}\int d^4x\, e^{-iK\cdot x}\exp\{\int d\mu(\vec{k})|f(\vec{k})|^2(e^{ik\cdot x}-1)\} \qquad (15)$$

XUM

Reproduced with permission of the copyright owner. Further reproduction prohibited without permission.

$$<f,K'|f,K> = \delta^{(4)}(K'-K)\rho_f(K) \tag{16}$$

The quantity $\rho_f(K)$ corresponds to the distribution of the coherent state in momentum space. To see this we decompose $\rho_f(K)$ in a series of n-particle contributions

$$\rho_f(K) = \sum_{n=0}^{\infty} \rho_f^n(K) = \overline{e^n}\{\delta^{(4)}(K) + \frac{1}{(2\pi)^3}|f(K)|^2\delta(K^2-\mu^2)\theta(K_o)$$

$$+ \frac{1}{2!}\int d^4k|f(k)|^2|f(K-k)|^2\delta(k^2-\mu^2)\delta[(K-k)^2-\mu^2]\theta(k_o)\theta(K_o-k_o)+\cdots\} \tag{17}$$

Equation (17) reveals the momentum spectrum one would expect: a contribution at $K = 0$ from the vacuum component, one at $K^2 = \mu^2$ from the one-particle state, and a continuum that starts from the threshold of two particles.

For the sake of further use we also list some properties of scalar products of two different coherent states:

$$<g|f> = \exp\{-\frac{1}{2}\int d\mu(\vec{k})(|f|^2 + |g|^2 - 2g^*f)\} \tag{18}$$

Equation (18) shows that two different coherent states are not orthogonal to each other (they are not eigenstates of Hermitian operators). Nevertheless, they do form an over-complete set[6]. The analogue of (15) is

$$<g|f,K> = \rho_{g,f}(K) = \frac{1}{(2\pi)^4}\int d^4x\, e^{-iK\cdot x}\exp\{-\frac{1}{2}\int d\mu(k)(|f|^2+|g|^2 - 2g^*f\, e^{ikx})\} \tag{19}$$

XUM

Reproduced with permission of the copyright owner. Further reproduction prohibited without permission.

The calculation of quantities like $\rho_f(K)$ or $\rho_f^n(K)$ is not an easy matter. Thus $\rho_f^n(K)$ can be rewritten as

$$\rho_f^n(K) = \frac{\bar{n}^n}{n!} \int d\mu(\vec{k}_1)\cdots d\mu(\vec{k}_n) |f(\vec{k}_1)|^2 \cdots |f(k_n)|^2 \delta^{(4)}(k_1+\cdots+k_n-K) \tag{20}$$

To simplify matters we can define normalized distributions $\tilde{\rho}_f^n(K)$ such that

$$\rho_f^n(K) = \bar{n}^n \frac{(\bar{n})^n}{n!} \tilde{\rho}_f^n(K) \int d^4K\, \tilde{\rho}_f^n(K) = 1 \tag{21}$$

One can then use the central limit theorem to find that

$$\hat{\rho}_f^n(K) \simeq \frac{1}{n^2} \frac{\sqrt{\det \eta}}{4\pi^2} \exp\{-\frac{1}{2n} \eta_{\mu\nu}(K^\mu - n\bar{k}^\mu)(K^\nu - n\bar{k}^\nu)\} \tag{22}$$

where

$$\bar{k}^\mu = \frac{1}{\bar{n}} \int d\mu(\vec{k}) k^\mu |f(\vec{k})|^2$$

$$\frac{\eta_{\mu\nu}}{\bar{n}} \int (k^\nu - \bar{k}^\nu)(k^\sigma - \bar{k}^\sigma) |f(\vec{k})|^2 d\mu(\vec{k}) = \delta_\mu^\sigma \tag{23}$$

This result was given by Van Hove[4] and the corrections to the approximation (22) were analyzed in detail by Lurcat and Mazur[8]. Let us discuss here briefly the expected form for $\tilde{\rho}_f^n$ if $f(k)$ has the characteristics of the distribution functions described in the introduction. A reasonable guess would be $\bar{k} = (\bar{\omega}, 0)$ with $\eta_{\mu\nu}$ a diagonal matrix with elements $(\sigma_E^{-2}, \sigma_T^{-2}, \sigma_L^{-2})$ where T and L designate transverse and longitudinal directions respectively. There is obviously a connection given by $\sigma_E^2 = 2\sigma_T^2 + \sigma_L^2 + \mu^2 - \bar{\omega}^2$. It then follows from (22) that

XUM

Reproduced with permission of the copyright owner. Further reproduction prohibited without permission.

$$\tilde{\rho}_f^n(K) \simeq \frac{1}{n^2} \frac{1}{4\pi^2 \sigma_T^2 \sigma_E \sigma_L} \exp\left\{ -\frac{1}{n}\left[\frac{(K_o - n\bar{\omega})^2}{2\sigma_E^2} + \frac{K_T^2}{2\sigma_T^2} + \frac{K_L^2}{2\sigma_L^2} \right] \right\} \qquad (24)$$

Equation (24) tells us that the overall distribution of pions is peaked around a linearly increasing energy with an increasing width as expected from a typical random walk problem.

XUM

Reproduced with permission of the copyright owner. Further reproduction prohibited without permission.

III. Emission of a Coherent State

In this section we discuss a formalism that describes a process in which the two incoming particles (with momenta q_1 and q_2) produce two outgoing leading particles (with momenta p_1 and p_2) and n mesons of momenta $k_1,\cdots,k_n$ which are part of a coherent state.

For the moment we continue to ignore the quantum numbers of the pions. We propose now, in analogy to the bremstrahlung case, the following S-matrix structure.

$$<p_1p_2k_1\cdots k_n|S|q_1q_2> = i\int d^4x\, e^{ix\cdot(p_1+p_2-q_1-q_2)} <p_1p_2k_1\cdots k_n|S(fe^{ikx})\tilde{T}|q_1q_2> \qquad (25)$$

To the extent that the incoming particles are not mesons of the kind appearing in the coherent cloud (or, if they are such mesons, they have momenta outside the range of f(k)) independent emission means that the S-matrix can be brought into the factored form

$$<p_1p_2k_1\cdots k_n|S|q_1q_2> = i\int d^4K(2\pi)^4\delta^{(4)}(K+p_1+p_2-q_1-q_2) <k_1\cdots k_n|f,K><p_1p_2|\tilde{T}|q_1q_2> \qquad (26)$$

$\tilde{T}$ acts only on the leading particles $q_1q_2p_1p_2$ that form what we call the "skeleton" of the process. It can thus depend on the invariant variables:

$$s=(q_1+q_2)^2,\ \bar{s}=(p_1+p_2)^2,\ t=(q_1-p_1)^2,\ \bar{t}=(q_2-p_2)^2,$$
$$u=(q_1-p_2)^2,\ \bar{u}=(q_2-p_1)^2 \qquad (27)$$

XUM

Reproduced with permission of the copyright owner. Further reproduction prohibited without permission.

$$s + t + u + \bar{s} + \bar{t} + \bar{u} = K^2 + 2\Sigma \tag{28}$$

where

$$K = q_1 + q_2 - p_1 - p_2 \qquad \Sigma = q_1^2 + q_2^2 + p_1^2 + p_2^2$$

Note that $f(\vec{k})$ is an invariant function of k and depends therefore on the four momenta of the skeleton. We refer to this fact by using the notation $f_{pq}(\vec{k})$.

The form (26) leads to the following result for the cross section of n meson production

$$\sigma_{2+n} = \int (dp)\, \rho^n_{f_{pq}}(q_1+q_2-p_1-p_2)\,|\langle p|\tilde{T}|q\rangle|^2 \tag{29}$$

where (dp) stands for the invariant phase space element of the outgoing leading particles and the relevant flux factor. Equation (29) is formally similar to the two-particle production cross section

$$\sigma_2 = \int (dp)\delta^{(4)}(q_1+q_2-p_1-p_2)\,|\langle p|T|q\rangle|^2 \tag{30}$$

with the ρ^n replacing the δ-function. Thus again we see that ρ^n describes the distribution of four momenta absorbed in the mesonic cloud. We will discuss later whether the recipe (29) can be smoothly continued to $n = 0$ to give $\sigma_2 = \tilde{\sigma}$ where

$$\begin{aligned}\tilde{\sigma} &= \int (dp)\, \rho^o_{f_{pq}}(q_1+q_2-p_1-p_2)\,|\langle p|\tilde{T}|q\rangle|^2 \\ &= \int (dp)\delta^{(4)}(p_1+p_2-q_1-q_2)\, e^{-\bar{n}_{pq}}\,|\langle p|\tilde{T}|q\rangle|^2\end{aligned} \tag{31}$$

Equation (24) told us that we may expect $\rho^n(K)$ to be concentrated

XUM

Reproduced with permission of the copyright owner. Further reproduction prohibited without permission.

around $K_o = n\bar{\omega}$, $\vec{K} = 0$. If we assume $<p|\tilde{T}|q>$ is independent of K^2 then, at least until the end of phase space is reached, we can approximate (29) by

$$\sigma_{2+n} = \int (dp)\, d^4K\, \rho^n_{f_{pq}}(K)\delta^{(4)}(K+p_1+p_2-q_1-q_2)\,|<p|\tilde{T}|q>|^2$$

$$\simeq \int (dp)\delta^{(4)}(p+\bar{K}-q)\,|<p|\tilde{T}|q>|^2 \int d^4K\, \rho^n_{f_{pq}}(K)$$

$$\simeq \int (dp)\delta^{(4)}(p-q)\,|<p|\tilde{T}|q>|^2\, \frac{e^{-\bar{n}_{pq}}\,(\bar{n}_{pq})^n}{n!} \qquad (32)$$

which means a Poisson distribution for the differential cross section If, further, $\bar{n}$ depends only on q we have

$$\sigma_{2+n} \overset{\sim}{=} \frac{(\bar{n})^n\,\tilde{\sigma}}{n!} \qquad (33)$$

This calculation makes sense only provided phase space restrictions can be avoided; in other words, if the number of pions is smaller than the maximum allowed by energy conservation $n\bar{\omega} < \sqrt{s} - m_1 - m_2$. This works best for an $f(\vec{k})$ concentrated around the c.m. with a narrow width. For high n that violate this inequality, we have to expect distortions of (33).

By "elastic skeleton" we mean that the outgoing particles are the same as the incoming one. This does not imply $\sigma_2 = \tilde{\sigma}$. An "inelastic skeleton" can have resonances among its outgoing particles. For elastic skeletons Fig. 7 gives experimental evidence[3] that (33) cannot be extended to $n = 0$. In all other multiplicities the reactions without a π^o form a small minority of the events. We have therefore to rely on unitarity to give us the elastic amplitude in terms

XUM

Reproduced with permission of the copyright owner. Further reproduction prohibited without permission.

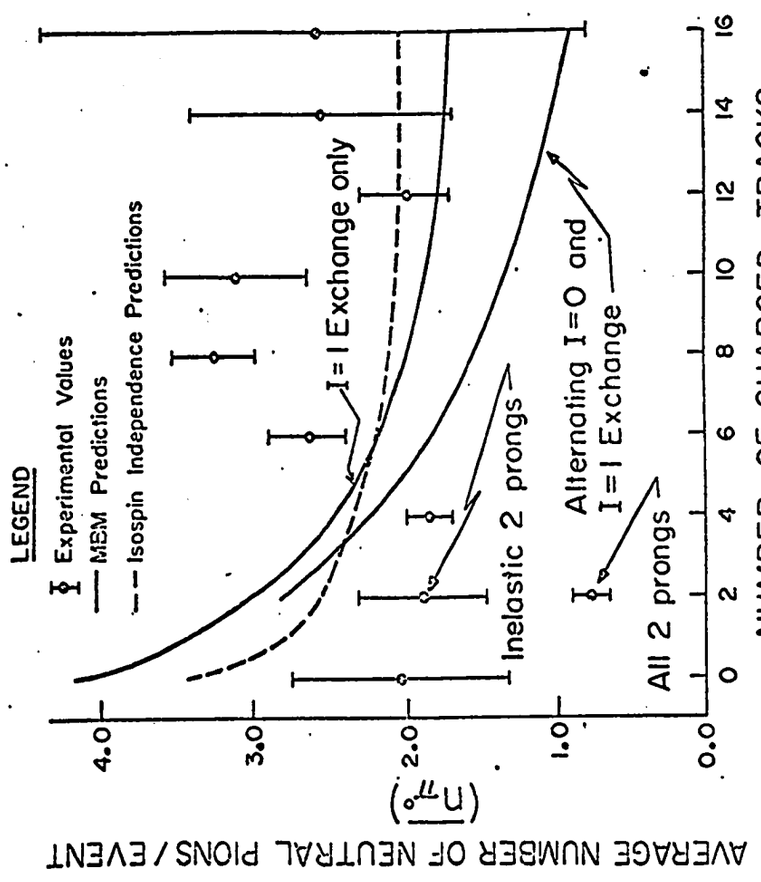

Fig. 7. The average number of π^0's produced in $\pi^- p$ at 25 Gev/c vs. the number of charged particles. Taken from Ref. 3. The solid curves are the predictions of various multiperipheral models.

XUM

Reproduced with permission of the copyright owner. Further reproduction prohibited without permission.

of the inelastic reactions. As a crude approximation one may consider a model in which all inelastic reactions are described by (26) with an elastic skeleton. Unitarity then leads to

$$i[\langle p_1p_2|T^\dagger|q_1q_2\rangle - \langle p_1p_2|T|q_1q_2\rangle] - \int d\mu(\vec{p}_1')d\mu(\vec{p}_2')(2\pi)^4 \times \delta^{(4)}(p_1'+p_2'-q_1-q_2)\langle p_1p_2|T^\dagger|p_1'p_2'\rangle\langle p_1'p_2'|T|q_1q_2\rangle \qquad (34)$$

$$= \sum_{n=1}^{\infty} \int d\mu(\vec{p}_1')d\mu(\vec{p}_2')(2\pi)^4 \rho^n_{f_{pp'},f_{p'q}}(q_1+q_2-p_1'-p_2') \times \langle p_1p_2|\tilde{T}^\dagger|p_1'p_2'\rangle\langle p_1'p_2'|\tilde{T}|q_1q_2\rangle$$

where $\rho^n_{f_{pp'},f_{p'q}}$ is the object of the type defined in equation (19). The right hand side of (34) is analogous to Van Hove's "overlap integral" that determines the t structure of the elastic amplitude. In fact, Van Hove[4] used a formalism similar to the one presented here to show how the properties of elastic scattering are correlated with the properties of inelastic scattering.

At this point it is interesting to see how the bremstrahlung theory solves the unitarity problem[7]. The function f_{pq} is given in this case by

$$(2\pi)^{3/2} f_{pq}(\vec{k}) = e_1' \frac{\varepsilon\cdot p_1}{k\cdot p_1} + e_2' \frac{\varepsilon\cdot p_2}{k\cdot p_2} - e_1 \frac{\varepsilon\cdot q_1}{k\cdot q_1} - e_2 \frac{\varepsilon\cdot q_2}{k\cdot q_2} \qquad (35)$$

where e_i's are the various charges and ε the photon's polarization vector. Clearly f is peaked around $k=0$ and the whole treatment is valid in QED only in the limit $k \to 0$. Then it turns out that

XUM

Reproduced with permission of the copyright owner. Further reproduction prohibited without permission.

indeed

$$\langle p|T|q\rangle = \langle p|\tilde{T}|q\rangle \; e^{-\bar{n}_{pq}/2} \tag{36}$$

and unitarity is satisfied provided $\tilde{T}$ satisfies elastic unitarity. To see this we rewrite (34) as

$$i[\langle p|T^\dagger|q\rangle - \langle p|T|q\rangle] = \int d\mu(\vec{p}_1')d\mu(\vec{p}_2')\langle p|\tilde{T}^\dagger|p'\rangle \langle p'|\tilde{T}|q\rangle$$

$$\times (2\pi)^4 \int d^4x \exp\{-\frac{1}{2}\int \frac{d^3\vec{k}}{2\omega}(|f_{p'p}|^2 + |f_{p'q}|^2$$

$$- 2f^*_{p'p} e^{ik\cdot x} f_{p'q}\} e^{ix(p_1'+p_2'-q_1-q_2)}$$

Replacing the $e^{ik\cdot x}$ in the integrand by 1 (the limit $k \to 0$!) we find

$$i[\langle p|T^\dagger|q\rangle - \langle p|T|q\rangle] = e^{-\bar{n}_{pq}/2} \int d\mu(\vec{p}_1')d\mu(\vec{p}_2')\langle p|\tilde{T}^\dagger|p'\rangle$$

$$\times \langle p'|\tilde{T}|q\rangle (2\pi)^4\delta^{(4)}(p_1'+p_2'-q_1-q_2) \tag{37}$$

which shows the ansatz (36) works provided $\langle p|\tilde{T}|q\rangle$ obeys by itself a unitarity equation.

There are clearly several important differences between the formalism of bremstrahlung and the emission of the mesons in high energy collisions. The first is that experimentally the identification (36) is invalid. Another is that the limit $k \to 0$ is not justifiable and cannot be obtained with massive (and energetic) mesons. This can be circumvented by having a skeleton matrix element that does not vary significantly with K. A very important third difference is that

XUM

Reproduced with permission of the copyright owner. Further reproduction prohibited without permission.

we may choose f to depend on q only. In the introduction we show characteristic distributions that depend on k_T and k_L. These variables can be given an invariant definition in terms of $k \cdot q_1$, $k \cdot q_2$, $q_1 \cdot q_2$ and the masses involved. Thus, present experiments can be described approximately without a p dependence. This makes it possible to go from (32) to (33) and get simple relations for integrated cross sections.

The explicit construction of an example of coherent production shows that independent uncorrelated emission can take place. Coherence is also a statement about the phases that are not directly measurable. They will, however, be important when we discuss the isospin question. The easiest things to measure are of course the cross sections. Their distributions, suggested by equation (28), will get modified in consideration of the quantum numbers of the pions to which we turn in the next sections.

XUM

Reproduced with permission of the copyright owner. Further reproduction prohibited without permission.

IV. Distributions of Charged Pions

The second constraint we will consider is that of charge conservation. In the model discussed in the previous sections, the coherent state must have a fixed electric charge that matches the charge of the skeleton. This is not true of simple charged coherent states

$$|f_i\rangle = \exp\left\{-\frac{1}{2}\int d\mu(\vec{k})|f_i|^2 + \int d\mu(\vec{k}) f_i(\vec{k}) a_i^\dagger(k)\right\}|0\rangle$$

$$\text{for } i = +,0,- \qquad (38)$$

One way to deal with the problem can be to start from the state

$$|F\rangle = |f_+\rangle\,|f_o\rangle\,|f_-\rangle \qquad (39)$$

and project out the required charge. An alternative is to define a state $|f_+f_-,Q\rangle$ obeying the equation

$$a_+(\vec{k})\,a_-(\vec{k})\,|f_+f_-Q\rangle = f_+(\vec{k})f_-(\vec{k})\,|f_+f_-,Q\rangle \qquad (40)$$

which has definite charge Q. This is analogue of equation (9) and can serve as a definition of a coherent state of charged particles. The solution to (40) is

$$|f_+f_-,Q\rangle = C^{-1/2}\sum_n \frac{1}{(n+Q)!\,n!}\left(\int d\mu(\vec{k}) f_+(\vec{k}) a_+^\dagger(\vec{k})\right)^{n+Q}$$

$$\left(\int d\mu(\vec{k}) f_-(\vec{k}) a_-^\dagger(\vec{k})\right)^n |0\rangle \qquad (41)$$

where the sum starts from $n = 0$ for positive Q and from $n = -Q$ for negative Q. The normalization constant C turns out to be

XUM

Reproduced with permission of the copyright owner. Further reproduction prohibited without permission.

$$C = (-i)^Q J_Q(2ix) \tag{42}$$

where

$$x^2 = \int d\mu(\vec{k}) |f_+(\vec{k})|^2 \int d\mu(\vec{k}) |f_-(\vec{k})|^2 \tag{43}$$

It is straightforward to show that the projection of $|F>$ onto a specific charge Q does indeed contain this state. It is

$$|f,Q> = |f_o> |f_+f_-,Q> \tag{44}$$

which we will regard as the right choice to take the place of $|f>$ in equation (26). The distribution of charged particles that results from this state is

$$P_n^{(Q)} = P_{n+Q}^{(-Q)} = \frac{i^Q x^{2n+Q}}{J_Q(2ix)n!(n+Q)!} \tag{45}$$

One can, however, give an argument for the validity of this distribution independent of the specific model that suggests it to us, as follows:

Most inelastic reactions at available accelerator energies involve primarily the emission of pions. One can argue that the gross features (multiplicities) of the events should be independent of the specific production mechanisms, which suggests that one should approach the problem on a statistical basis. There are several overall constraints that have to be obeyed by the system, namely, momentum, isospin, and charge conservation. Since experimentally the emitted pions occupy a small fraction of the available phase space, we expect momentum conservation to be a weak constraint. By summing over all neutral pions, we may expect the constraint of total isospin

XUM

Reproduced with permission of the copyright owner. Further reproduction prohibited without permission.

conservation to be weak also. We are thus left with the obvious constraint of charge conservation.

It is quite straightforward to arrive at the desired distribution. If the pions are emitted independently one would expect a Poisson distribution for each kind of pion. Because of the charge constraint we ask for the conditional probability of emitting n positive and n negative pions simultaneously. If the Poisson distributions for the positive and negative pions are given by

$$p_n^{(\pm)} = \frac{e^{-x_\pm}(x_\pm)^n}{n!} \tag{46}$$

the resulting distribution for n charged pairs is[9]

$$P_n = \frac{1}{J_o(2ix)} \frac{x^{2n}}{(n!)^2} \tag{47}$$

where $x^2 = x_+ x_-$. It follows that

$$\langle n \rangle = \sum_n n P_n = -ix \frac{J_1(2ix)}{J_o(2ix)} \tag{48}$$

which gives a one-to-one correspondence between $\langle n \rangle$ and x. We find also $\langle n^2 \rangle = x^2$

$$\sigma = \langle n^2 \rangle - \langle n \rangle^2 = x^2 \left(1 + \frac{J_1^2(2ix)}{J_o^2(2ix)}\right) \tag{49}$$

For high values of n, one can use Stirling's approximation to show that

$$P_n \to \frac{1}{J_o(2ix)} \frac{(2x)^{2n}}{(2n)!(2n)^{1/2}} \tag{50}$$

which differs slightly from a Poisson distribution in $2n$.

XUM

Reproduced with permission of the copyright owner. Further reproduction prohibited without permission.

In Fig. 8 we compare the predictions of equation (47) with the data compilation by Wang[10] of many $\pi^{\pm}p$,pp, and nn inelastic production experiments below 27 Bev. The number of charged pions (n_c) should be related to our n by $n_c = 2n+2$ (in the case of nn collisions $n_c = 2n$). The data are assembled in a way that tests just the character of the distribution, namely, it is a plot of the probability for a certain n_c to occur provided $\langle n_c \rangle$ is given. Hence there is no free parameter to be adjusted. Wang tried to fit the data with two of the distributions shown in Fig. 8: W^I is a Poisson distribution in $\frac{1}{2}(n_c-2)$ and W^{II} is built of the even terms in a Poisson distribution in n_c-2. The data points seem to follow a universal curve that is not very well reproduced by either W^I or W^{II}. Although W^I fits the low-n_c and low-$\langle n_c \rangle$ region, it fails at higher n_c and higher $\langle n_c \rangle$. We note that the curve of distribution (47) does depict correctly the experimental behavior.

In view of the success of distribution (47), we mention at this point that in plotting all the experiments together, we are closer to the case of a statistical ensemble. One may expect that some remnants of the momentum and isospin constraints are still left in any particular type of experiment. We anticipate that higher statistics experiments will show deviations from universal curves for individual reactions.

The agreement achieved in Fig. 8 raises the question of whether this can serve as proof that all the reactions are mainly of one type, namely, A+B → A+B+pions, where obviously the pion cloud is neutral. In order to answer that, we look for the probability $P_n^{(Q)}$ of finding

XUM

Reproduced with permission of the copyright owner. Further reproduction prohibited without permission.

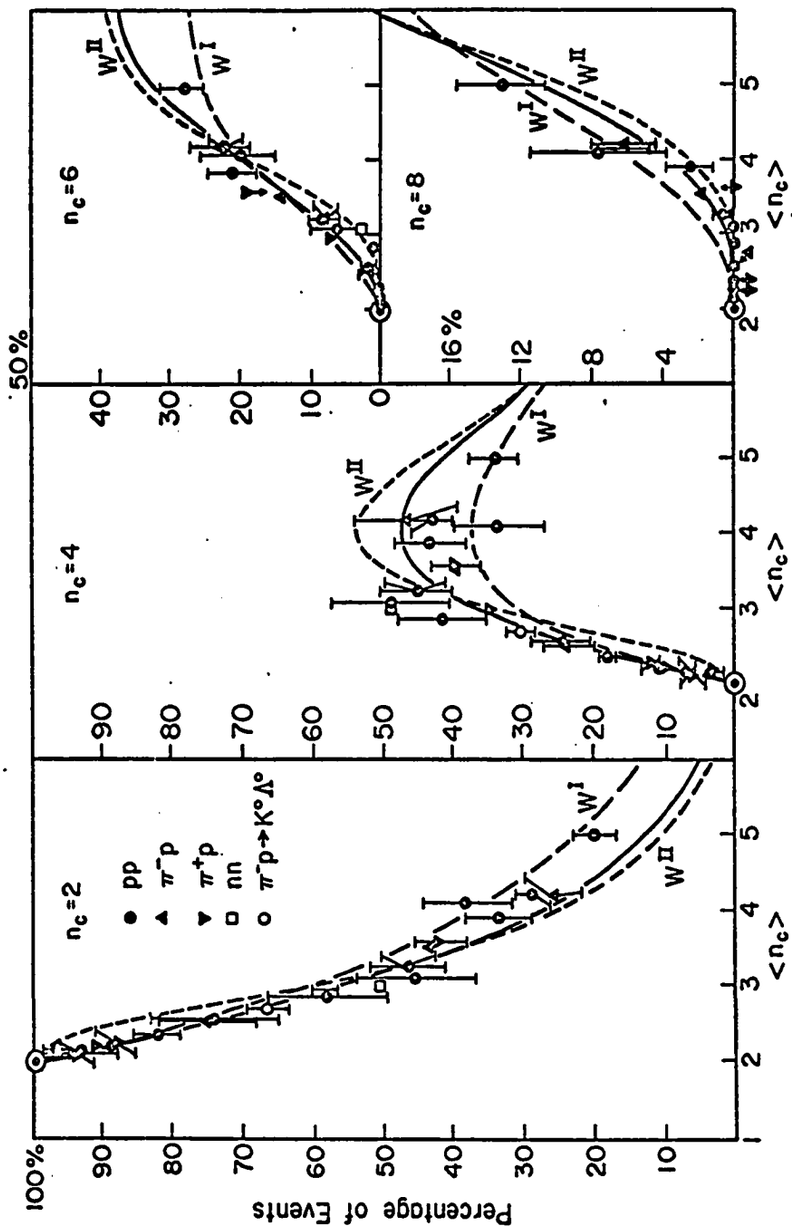

Fig. 8. Compilation of inelastic production data and its comparison with theoretical distributions. The data, as well as the fits W^I and W^{II} are taken from Wang's paper (Ref. 10). The solid curve is the distribution $P^{(0)}$.

XUM

Reproduced with permission of the copyright owner. Further reproduction prohibited without permission.

n+Q positive and n negative pions. This will then correspond to the expected behavior from a cloud of pions of overall charge Q . Following a similar line of reasoning to the one used above we find equation (45) where

$$\langle n_Q \rangle = -ix\, J_{Q+1}(2ix)/J_Q(2ix) \tag{51}$$

In Fig. 9 we plot the predictions of $P^{(0)}, P^{(1)}, P^{(2)}$ in the same way as in Fig. 8. It turns out that they all coincide in the region where most data points are available. This may even be the reason for the universal character of the experimental data. For example, in $\pi^- p$ reactions, one finds outgoing "leading" particles π^- and p following the initial momenta of the incoming ones, and a cloud of pions with relatively low momenta in the center of mass system. This cloud of pions should fit the $P^{(0)}$ description. However, as the multiplicity increases the leading π^- loses momentum and eventually will be indistinguishable from the π^- particles in the cloud. Thus one should perhaps expect a smooth transition from $P^{(0)}$ to $P^{(1)}$. We will discuss this question further with respect to the implications of isospin conservation.

Reproduced with permission of the copyright owner. Further reproduction prohibited without permission.

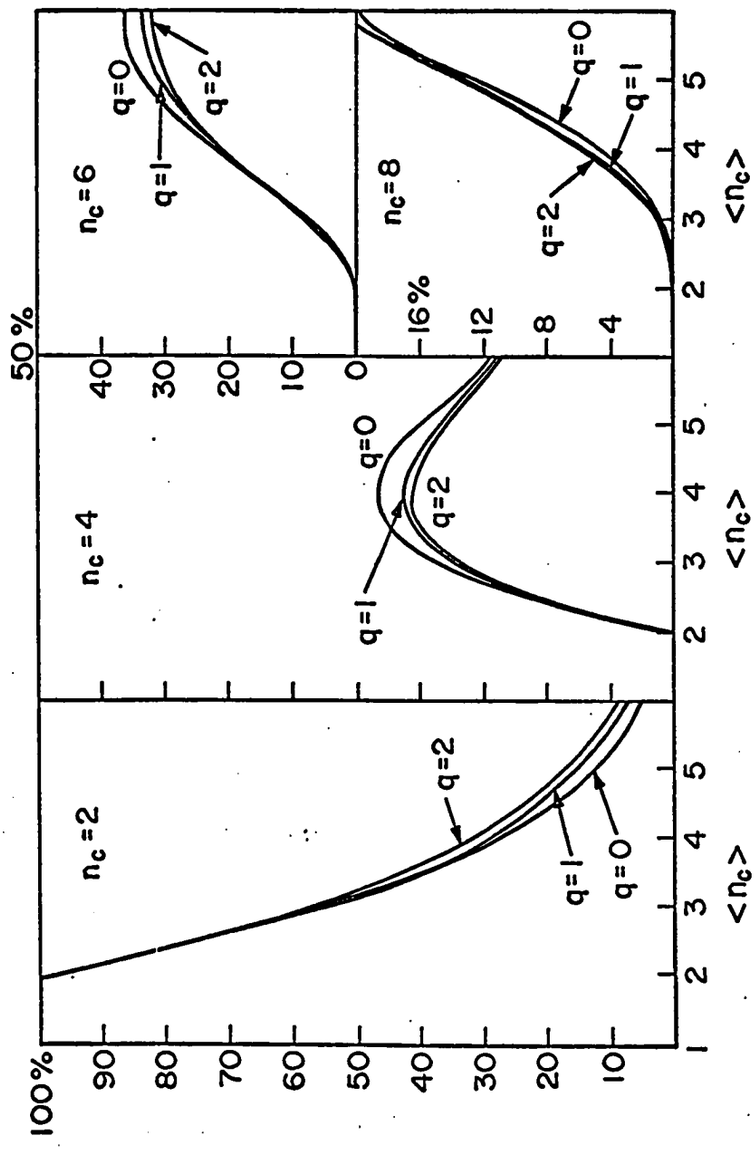

Fig. 9. Comparison of various $P^{(Q)}$ distributions

V. Parity and Charge Conjugation

Questions of parity conservation are invariably intertwined with the distribution in momentum space of produced pions, which we do not care to speculate on here. However, given a specific distribution the effect of parity conservation can be established. For example, consider the extreme case of isotropic pionic distribution $f(\vec{k}) = f(k)$. Then clearly the transitions in the skeleton conserve j. However, in the case of an even number of pions we have even (odd) $\ell \to$ even (odd) ℓ, whereas if the number of pions is odd we find even(odd) $\ell \to$ odd(even) ℓ. Hence, in the emission of an odd number of pions in this limit a spin transition must be involved. One expects that the more spins there are in the skeleton the easier it is to emit pions independently. It is interesting to note in this connection that the direction of the inequalities in $\sigma_{inel}(\pi\pi) < \sigma_{inel}(\pi p) < \sigma_{inel}(pp)$ is also that of the number of spins involved.

Several selection rules arise from charge conjugation considerations. Thus a skeleton of four pions can be connected only to even numbers of pions, which is the same condition as that of parity conservation in the case of isotropic pions. A neutral system of uncorrelated pions with identical momentum distributions has positive charge conjugation. Thus it cannot couple, e.g., to e^+e^- (via a photon). Similarly $\bar{p}p$ annihilation at rest is restricted by charge conjugation. Both e^+e^- and $\bar{p}p$ annihilations are different from πp and pp collisions, because in annihilations it should not be meaningful to distinguish leading from nonleading particles. Our conclusion is that uncorrelated production is possible in systems

XUM

Reproduced with permission of the copyright owner. Further reproduction prohibited without permission.

such as elastic scattering where charge conjugation and four-momentum conservation are not severe constraints.

XUM

Reproduced with permission of the copyright owner. Further reproduction prohibited without permission.

VI. Isospin Analysis of Identical Pions

As a necessary preliminary to our discussion in the next section of the implications of isospin conservation, we develop here a formalism for the isospin analysis of pions with identical momentum distributions. We limit ourselves to identical pions, since this case may be treated in an elegant and simple manner, but a similar analysis is possible for non-identical pions.

We start by defining a normalized momentum space distribution $\phi(\vec{k})$ satisfying

$$\int d\mu(\vec{k}) \; |\phi(\vec{k})|^2 = 1 \tag{52}$$

The fact that the momentum distributions of the pions are identical is summarized in the assumption

$$f_i(\vec{k}) = f_i \phi(\vec{k}) \quad , \quad i = +,0,- \tag{53}$$

where the f_i are three constants. The magnitudes and phases of the f_i determine the isospin structure of a definite combination of identical pions.

Let us now define three operators

$$a_i^\dagger = \int d\mu(\vec{k}) \; \phi(\vec{k}) a_i^\dagger(\vec{k}) \tag{54}$$

which obey the commutation relations

$$[a_i, a_j^\dagger] = \delta_{ij} \tag{55}$$

The isospin generators for a system of identical pions can be simply expressed in terms of these operators

XUM

Reproduced with permission of the copyright owner. Further reproduction prohibited without permission.

$$\vec{I} = a_i^\dagger \vec{\tau}_{ij} a_j \tag{56}$$

where

$$\tau_x = \frac{1}{\sqrt{2}}\begin{pmatrix} 0 & 1 & 0 \\ 1 & 0 & 1 \\ 0 & 1 & 0 \end{pmatrix} \quad \tau_y = \frac{1}{\sqrt{2}}\begin{pmatrix} 0 & -i & 0 \\ i & 0 & -i \\ 0 & i & 0 \end{pmatrix} \quad \tau_z = \begin{pmatrix} 1 & 0 & 0 \\ 0 & 0 & 0 \\ 0 & 0 & -1 \end{pmatrix} \tag{57}$$

The number operators are

$$N_i = a_i^\dagger a_i \qquad N = N_+ + N_o + N_- \tag{58}$$

The bilinear isoscalar creation and annihilation operators are

$$A = a_o a_o + 2a_+ a_- \qquad [\vec{I},A] = [\vec{I},A^\dagger] = 0 \tag{59}$$

The three operators play a key role in the isospin analysis. They close on the algebra

$$[N,A] = -2A \qquad [N,A^\dagger] = 2A^\dagger \qquad [A,A^\dagger] = 4N+6 \tag{60}$$

Their importance stems from the fact that the operator $\vec{I}^2$ can be written in terms of them as

$$\vec{I}^2 = N(N+1) - A^\dagger A \tag{61}$$

It follows from (61) that a state of n identical pions will have isospin $I = n$ if and only if

$$A|I = n, n> = 0 \tag{62}$$

One may construct such a state by using

XUM

Reproduced with permission of the copyright owner. Further reproduction prohibited without permission.

$$T^{\dagger} = -a_{+}^{\dagger} + \sqrt{2}\, a_{o}^{\dagger} + a_{-}^{\dagger} \tag{63}$$

which obeys

$$\frac{1}{2}[A,T^{\dagger}] = a_{+} + \sqrt{2}\, a_{o} - a_{-} \equiv U \ , \ [U,T^{\dagger}] = 0 \tag{64}$$

Because of these properties it is evident that

$$A(T^{\dagger})^{n}|0> = 0 \tag{65}$$

Hence every I_z projection of the state $(T^{\dagger})^{n}|0>$ has an isospin of $I = n$. Actually this state contains all $2n+1$ I_z projections. From (65) we obtain

$$|I = n, I_z, n> = B^{-1/2} \sum_{p} \frac{n!}{(I_z+p)!\,p!\,(n-2p-I_z)!} (-a_{+}^{\dagger})^{I_z+p} \times (\sqrt{2}\, a_{o}^{\dagger})^{n-2p-I_z} (a_{-}^{\dagger})^{p} |0> \tag{66}$$

where the sum is over all integer p such that the factorials can be defined. B is a normalization constant equal to

$$B = \sum_{p} \frac{(n!)^2\, 2^{n-2p-I_z}}{(I_z+p)!\,p!\,(n-2p-I_z)!} \tag{67}$$

A system of identical pions can include in addition to $I = n$ also all isospins of $n-2$, $n-4$, $\cdots$ down to 0 or 1. All together these form $\frac{1}{2}(n+1)(n+2)$ states, characteristic of the completely symmetric combination. We can prove that this is the case by direct construction of the isospin states. We have already seen that $A^{\dagger}$ is a creation operator of an $I = 0$ system, indeed

XUM

Reproduced with permission of the copyright owner. Further reproduction prohibited without permission.

$$|I = 0,\ n = 2m\rangle = \frac{1}{\sqrt{(2m+1)!}} (A^{\dagger})^m \ |0\rangle \tag{68}$$

The general state is then

$$|I,I_z,n = 2m+I\rangle = D^{-1/2}(A^{\dagger})^m \ |I,I_z,n = I\rangle \tag{69}$$

D is a normalization constant equal to

$$D = \frac{4^m\, m!\ \Gamma(m+I+\frac{3}{2})}{\Gamma(I+\frac{3}{2})} \tag{70}$$

The states (69) form an orthonormal system as may be seen by using (64). Simple calculation of the number of states shows that we constructed in this way all possible isospin states of identical pions.

Let us apply this formalism to the coherent state $|F\rangle$ of equation (39) as an example of independent uncorrelated pions. We have

$$A|F\rangle = (f_o^2 + 2f_+f_-)|F\rangle \tag{71}$$

We see that if we choose $f_o^2 = -2f_+f_-$ we have a coherent state which contains only states with $I = n$, i.e., this choice of phase leads to maximal isospin content. In general

$$\langle\vec{I}^2\rangle = \langle F|\vec{I}^2|F\rangle = \bar{n}(\bar{n}+2) - |f_o^2+2f_+f_-|^2 \tag{72}$$

where

$$\bar{n} = \langle F|N|F\rangle = |f_+|^2 + |f_o|^2 + |f_-|^2 \tag{73}$$

It follows from (67) that $\langle\vec{I}^2\rangle$ is minimal if

$$\arg(f_o^2) = \arg(f_+f_-) \quad \text{and} \quad |f_+| = |f_-| \tag{74}$$

XUM

Reproduced with permission of the copyright owner. Further reproduction prohibited without permission.

These are also the conditions that ensure that the state $|F>$ has no preferred direction in isospace $<F|\vec{I}|F> = 0$. Thus the minimal value is achieved by random walk in isospace

$$<\vec{I}^2>_{min} = 2\bar{n} \tag{75}$$

We believe that in general a cloud of independently produced pions will have no preferred direction on isospace and so will have distributions in isospin whose average is given by (75).

Consideration of non-identical pions cannot give a lower value of $<I^2>$. In this case, direct computation leads to

$$<\vec{I}^2> = 2\bar{n} + [\int d\mu(\vec{k})(|f_+(\vec{k})|^2 - |f_-(\vec{k})|^2)]^2 + 2\left|\int d\mu(\vec{k})[f_+^*(\vec{k})f_o(\vec{k}) - f_o^*(\vec{k})f_-(\vec{k})]\right|^2 \tag{76}$$

The minimal value is again achieved by (74) which is equivalent to saying that all the f_i in (53) are relatively real.

XUM

Reproduced with permission of the copyright owner. Further reproduction prohibited without permission.

VII. Implications of Isospin Conservation

Isospin conservation has two major consequences: 1) the isospins of the pion cloud must match the isospins of the skeleton, i.e. πp can emit up to $I = 3$ and pp up to $I = 2$ for elastic skeletons; and 2) the amplitude for the emission of a charged pion cloud is related by the Wigner-Eckart theorem to the amplitude for the emission of a net neutral cloud of pions.

Obviously a coherent state of identical pions contains all isospins and cannot exactly satisfy condition (1). The question of the severity of the isospin constraint concerns the degree to which a coherent state can approximately match the isospins of the skeleton. The result of equation (75) looks quite pessimistic in this regard. However, we should remember that $|F>$ contains all possible I_z projections. By limiting ourselves to $|f,Q = 0>$ the situation improves considerably. The calculation in this case is more difficult because $|f,Q = 0>$ is no longer an eigenstate of a_+ and a_- separately. It is, however, an eigenstate of A

$$A|f,Q> = (f_o^2 + 2f_+f_-)|f,Q> \ , \ a_o|f,Q> = f_o|f,Q> \qquad (77)$$

Again we have limited ourselves to identical pions and retain the freedom to play with the phases and magnitudes of the f_i. The parameter of interest is

$$\xi = - f_o^2/f_+f_- \qquad (78)$$

By choosing $\xi = 2$ we reach the maximal isospin state. In Section VI we learned that minimal growth of $<I^2>$ with $\bar{n}$ is achieved for

XUM

Reproduced with permission of the copyright owner. Further reproduction prohibited without permission.

negative ξ. Before turning to the numerical evaluation we would like to point out that suitable choices of ξ can eliminate a particular isospin altogether from any combination of identical pions. To see this, note

$$<I = n,\ I_z = 0,\ n|f> = B^{-1/2} <0|f> (\sqrt{2}\ f_o)^n \sum_p \frac{n!}{p!p!(n-2p)!} (2\xi)^{-p} \tag{79}$$

Hence a suitable choice of ξ leads to $<I = n,\ I_z = 0,\ n|f> = 0$. Once this is achieved it follows from (65) that all $<I, I_z = 0,\ n+2m|f> = 0$. The choice $\xi = -1$ eliminates $I = 2$ and the choice $\xi = -3$ eliminates $I = 3$.

Let us now turn to the question of minimal isospin content. We choose $f_+ f_-$ as real and denote it by $x = f_+ f_-$. We then find

$$<\vec{I}^2> = \frac{4xJ_1(2ix)}{iJ_o(2ix)} (1 + |f_o|^2) - \frac{2x^2 J_2(2ix)}{J_o(2ix)} - 2x^2 + 2|f_o|^2 + 4\ \mathrm{Re}(f_o^2 x) \tag{80}$$

$$<n> = <f|N|f> = \frac{2xJ_1(2ix)}{iJ_o(2ix)} + |f_o|^2 = 2<n_{\pi^+}> + <n_{\pi^o}>$$

The results for $<I>$ vs. $<n>$, where $<I><I+1> = <\vec{I}^2>$ are plotted in Fig. 10 for several values of ξ. We see that for negative ξ they all lie close to each other obeying

$$<\vec{I}^2> \simeq <n> \tag{81}$$

Thus by going from the state $|F>$ to $|f, Q = 0>$ we gained a factor of two in the minimal value of $<\vec{I}^2>$. This is of course essential in order for independent uncorrelated emission subject to charge constraints to remain a good approximation to the experimental situation,

XUM

Reproduced with permission of the copyright owner. Further reproduction prohibited without permission.

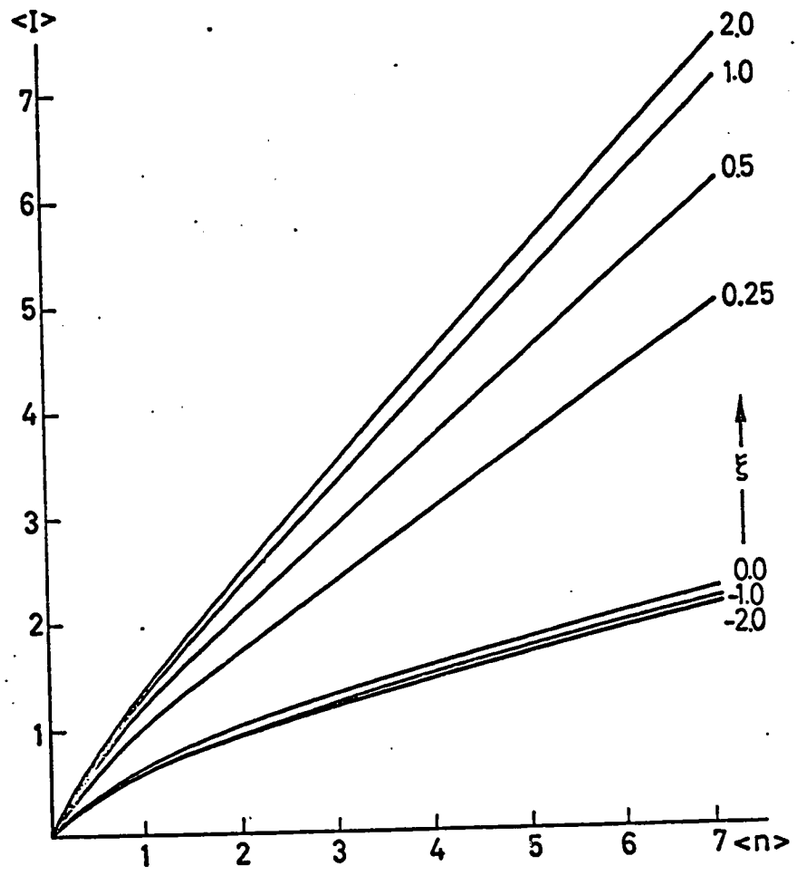

Fig. 10. Plots of <I> vs. <n> for various choices of the parameter ξ in the coherent state $|f,Q = 0\rangle$

XUM

Reproduced with permission of the copyright owner. Further reproduction prohibited without permission.

and we see the importance of the phase of the pion wave function in minimizing the restrictions isospin conservation places on independent emission.

The absolute value of ξ is the asymptotic (i.e., for large $\langle n \rangle$) ratio of the number of π^0 to the number of π^+. Therefore we do not consider values that are too far from unity. In Figs. 11-13 we show the distribution of $\langle I \rangle$ for various choices of ξ. Figure 11 shows that for $\xi = -0.5$ all isospins higher than three are strongly quenched. Figure 12 has the choice $\xi = -1$ that eliminates $I = 2$, and Fig. 13 is drawn with $\xi = -3$ that eliminates $I = 3$. In all figures we see the important roles of low isospins for the presently observed ranges of $\langle n \rangle$.

A similar calculation leads to the distributions of specific isospin values in the n-pion configurations. Figure 14 shows these distributions for $\xi = -2$ where $I = 0$ and 1 are important values. The relative amounts of the low isospins change slowly with ξ. We see from Fig. 15 that although the leading terms have low I spin values, one still encounters sizable contributions from forbidden isospins.

We conclude that insofar as a cloud of identical uncorrelated pions is produced with no preferred direction in isospace, isospin conservation is a weak constraint compared to charge conservation. However, the approximation of independent production becomes less accurate with increasing n and increasing $\langle n \rangle$. With regard to the second consequence, the exact manner of satisfying this depends on the details of the isospin recoupling coefficients which is a model dependent problem we do not give a prescription for solving here.

XUM

Reproduced with permission of the copyright owner. Further reproduction prohibited without permission.

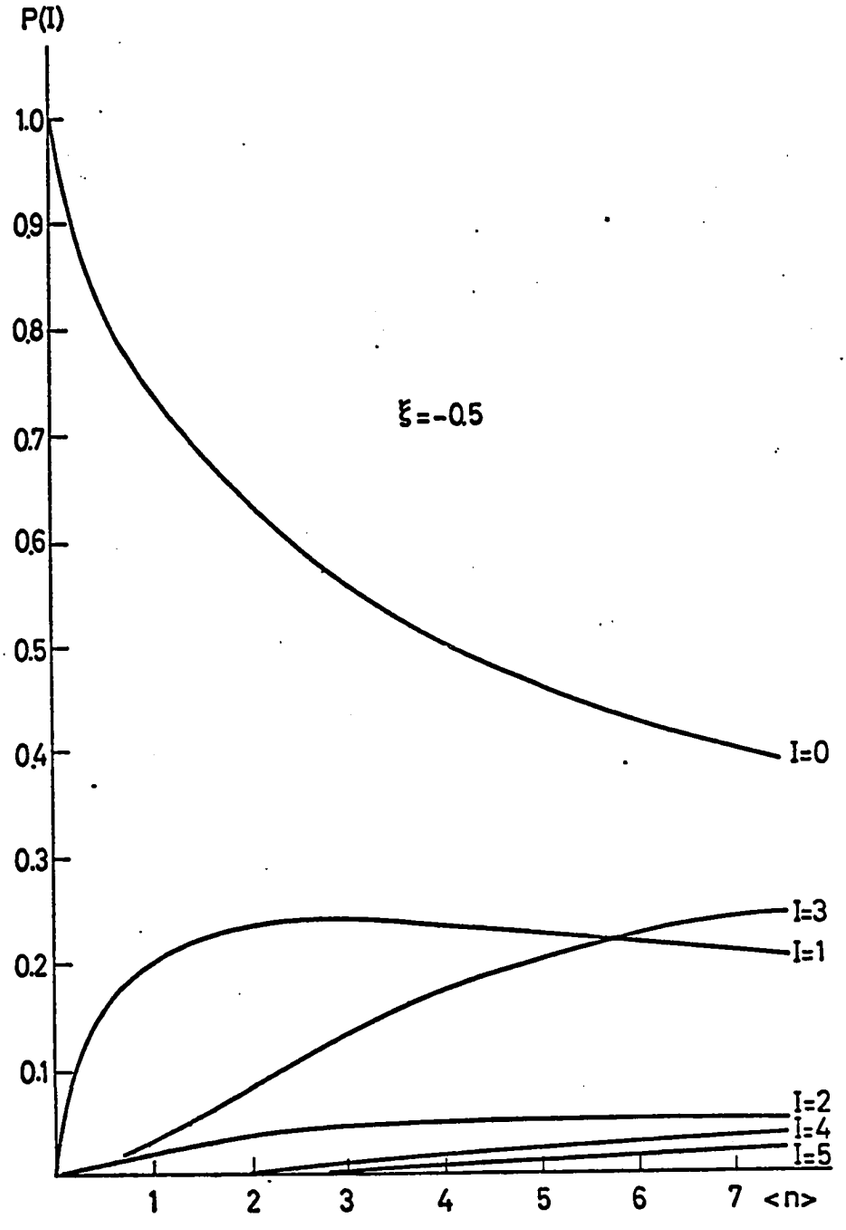

Fig. 11. The percentages of the contents of different isospins in the coherent state $|f,Q = 0>$ plotted vs. $<n>$ for the choice $\xi = -0.5$.

XUM

Reproduced with permission of the copyright owner. Further reproduction prohibited without permission.

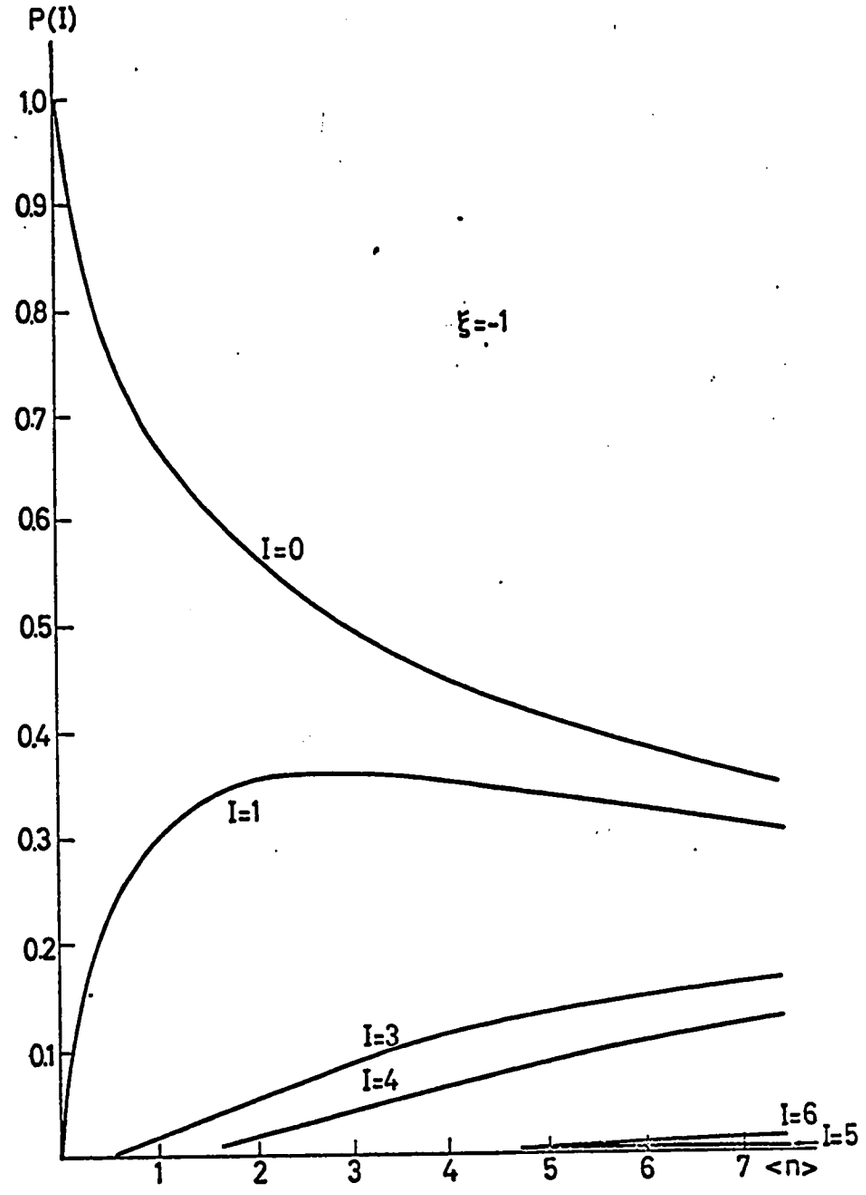

Fig. 12. Same as Fig. 11 for $\xi = -1$

XUM

Reproduced with permission of the copyright owner. Further reproduction prohibited without permission.

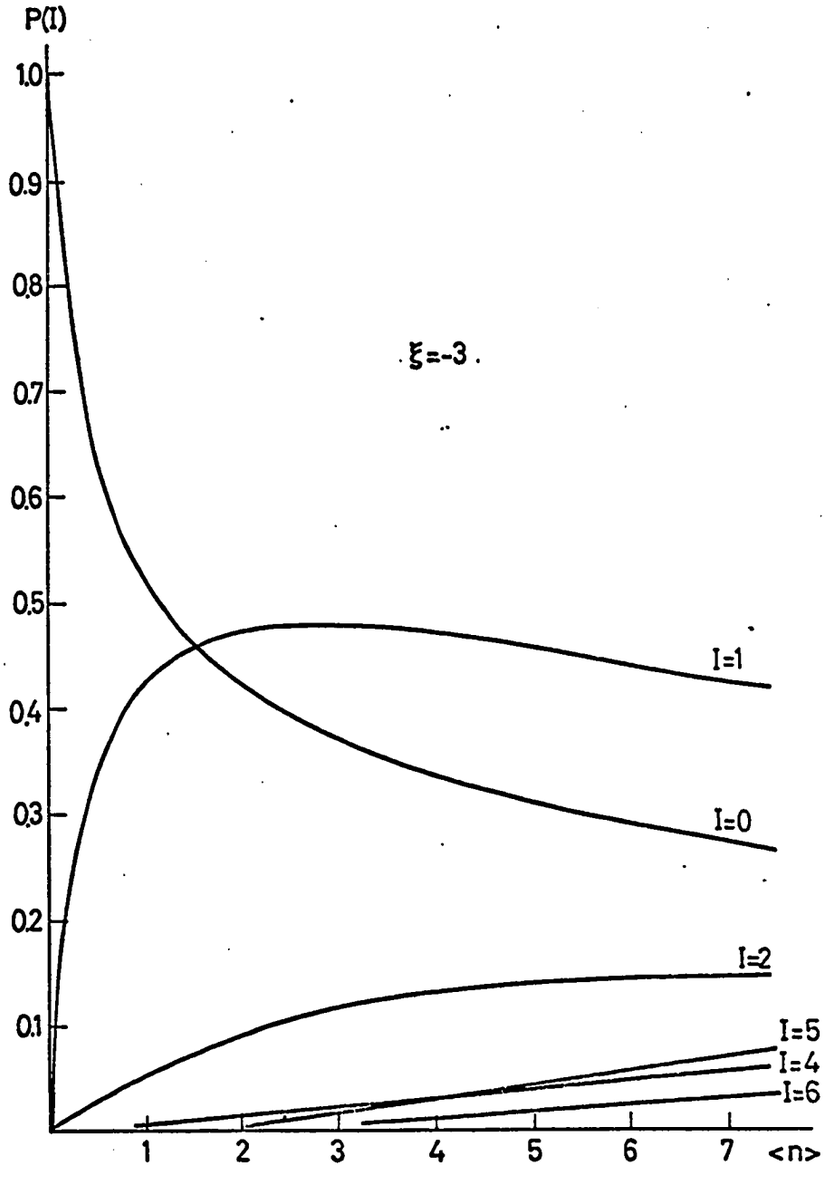

Fig. 13. Same as Fig. 11 for $\xi = -3$

XUM

Reproduced with permission of the copyright owner. Further reproduction prohibited without permission.

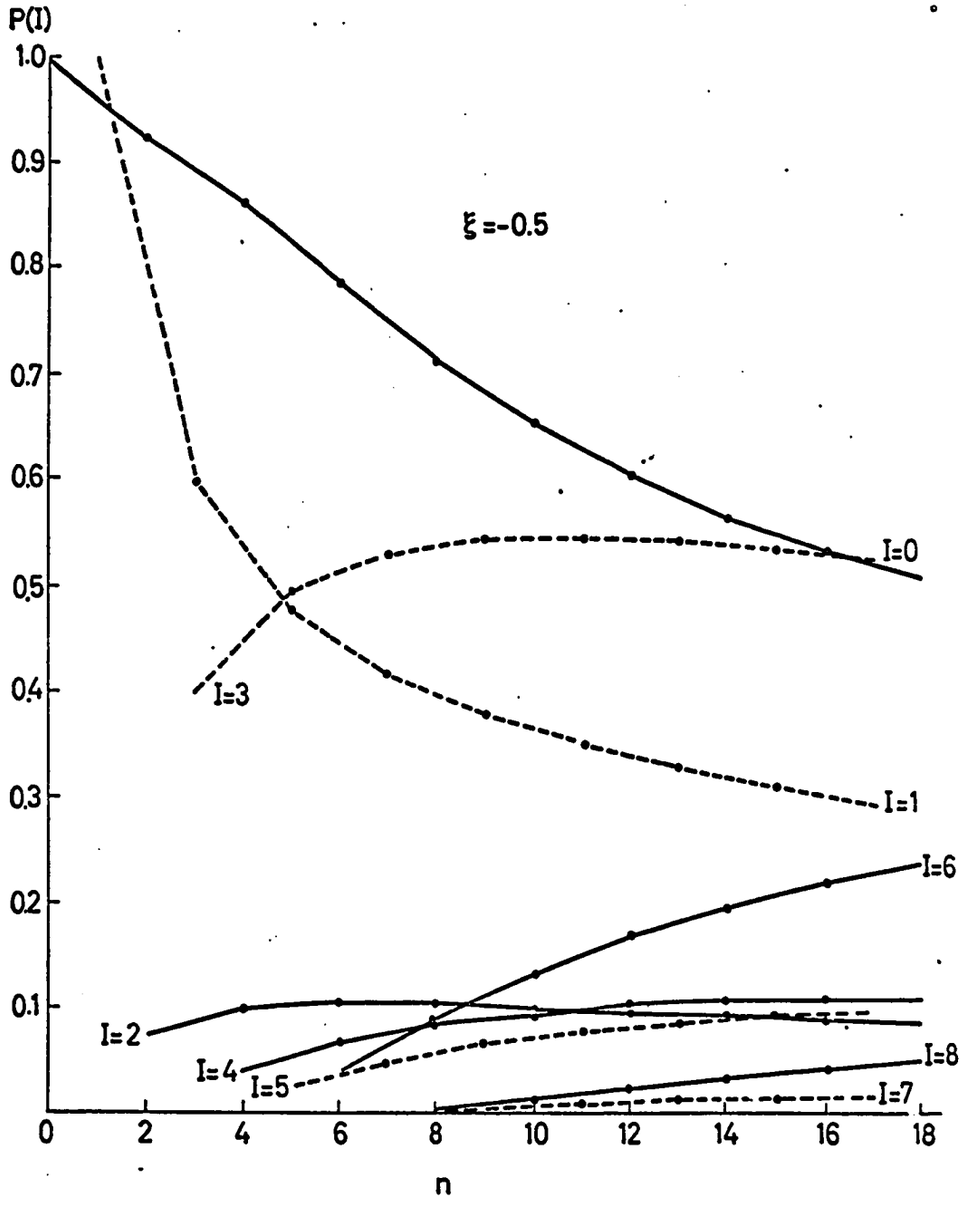

Fig. 14. The percentages of the different isospins in the various n particle states included in $|f,Q = 0\rangle$ plotted vs. n for the choice $\xi = -0.5$. Note the two types of curves that describe even and odd isospins for even and odd n respectively.

XUM

Reproduced with permission of the copyright owner. Further reproduction prohibited without permission.

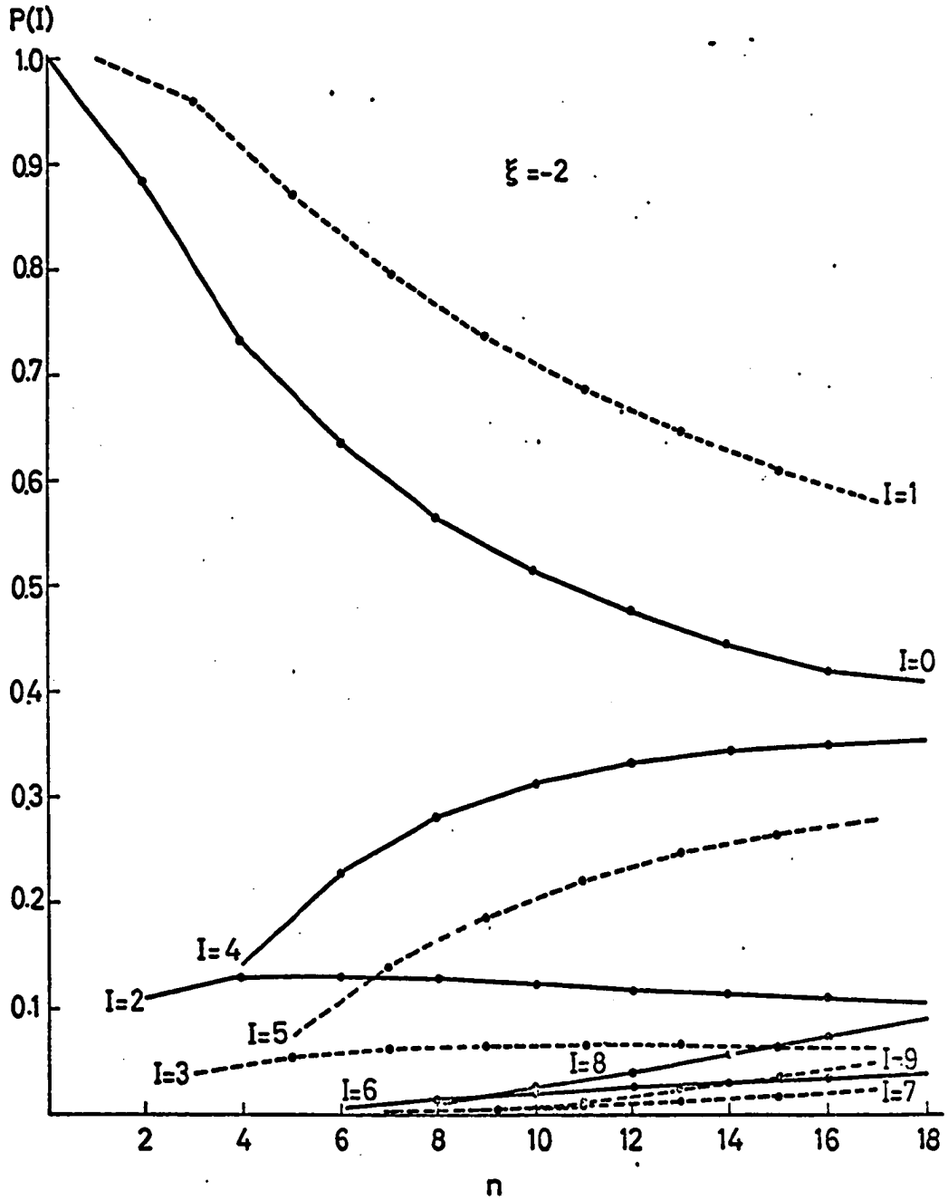

Fig. 15. Same as Fig. 14 for $\xi = -2$

XUM

Reproduced with permission of the copyright owner. Further reproduction prohibited without permission.

VIII. Two-Pion Correlations

One possibility for eliminating the isospin problem altogether is the production of pions in scalar isoscalar pairs. This of course requires different skeletons for even and odd pionic reactions. As an example of independent production of isoscalar pairs, we will examine the distributions that result from a coherent state of isoscalar pairs satisfying

$$A|g> = g|g> \tag{82}$$

The purely $I = 0$ solution is

$$|g> = \sqrt{\frac{g}{\sinh g}} \sum_m \frac{g^m}{(2m+1)!} (A^\dagger)^m |0> =$$

$$= \sqrt{\frac{g}{\sinh g}} \sum_m \frac{g^m}{\sqrt{(2m+1)!}} |I = 0,\ n = 2m> \tag{83}$$

The n pion distribution is given by

$$P(n=2m) = \frac{1}{\sinh g} \frac{g^{2m+1}}{(2m+1)!} \tag{84}$$

One important property of (83) is that the isoscalar state has the same multiplicities of all different charges

$$<n_{\pi^+}> = <n_{\pi^-}> = <n_{\pi^o}> = \frac{1}{3}<n> \tag{85}$$

The probability of finding r charged pairs in a state $|I = 0,\ n = 2m>$ is

$$P(r,m) = \frac{m!\ m!}{(2m+1)!} \binom{2m - 2r}{m - r} 4^r \tag{86}$$

XUM

Reproduced with permission of the copyright owner. Further reproduction prohibited without permission.

From (86) and (84) we find the probability for r charged pairs in the coherent state $|g>$. It is

$$P_r^{(g)} = \frac{(2g)^{2r}}{\sinh g} \sum_{p=0}^{\infty} g^{2p+1} \left(\frac{(p+r)!}{p!(2p+2r+1)!}\right)^2 (2p)! \qquad (87)$$

Since $|g>$ describes the production of neutral pion pairs, we may expect it to be similar to W^I of Wang[10]. The distributions $P^{(g)}$, $P^{(0)}$ and W^I are compared in Fig. 16 where we see that indeed $P^{(g)}$ resembles W^I and both differ somewhat from the more successful distribution $P^{(0)}$.

However, the major difference between isoscalar pair emissions and independent emission is that now the probability of finding neutral pions is correlated to that of charged pions. Using the fact that the average number of pions is

$$<n> = g \coth g - 1 \qquad (88)$$

we may calculate the expected correlation of $<n_{\pi^o}>$ vs. r for fixed $<n>$. These correlations are shown in Fig. 17 where $<n_{\pi^o}>$ is plotted versus $n_{ch} = 2+r$ in a way to be compared with Fig. 7. They clearly do not correspond to the trend of the data.

Note the resemblance between our curve and that achieved with alternating $I = 0$ and $I = 1$ exchanges in a multiperipheral model. Since such a model corresponds to emission of isoscalar pairs of pions, this resemblance is to be expected. Caneschi and Schwimmer[11] have presented other schemes involving the inclusion of ρ^+ and ρ^- production within a multiperipheral model that achieve better fits to the

XUM

Reproduced with permission of the copyright owner. Further reproduction prohibited without permission.

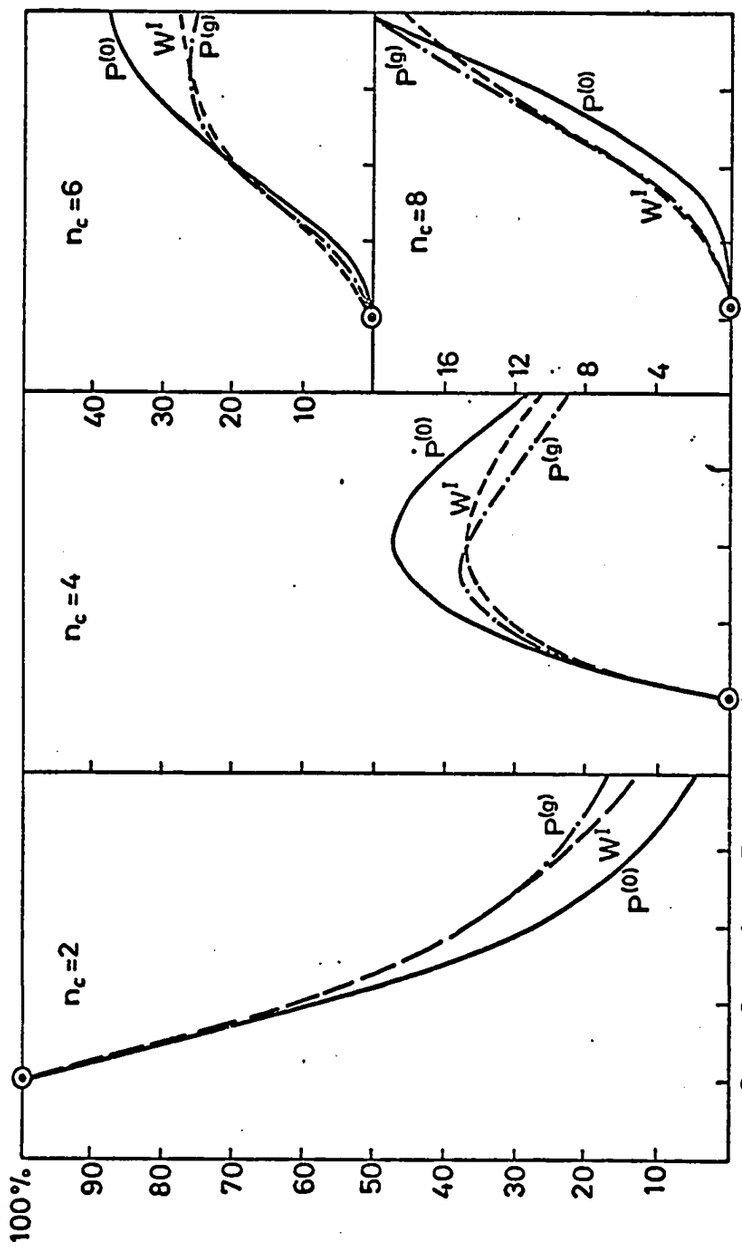

Fig. 16. Comparison of W^I, $P^{(0)}$, and $P^{(g)}$ distributions displayed as in Fig. 8.

XUM

Reproduced with permission of the copyright owner. Further reproduction prohibited without permission.

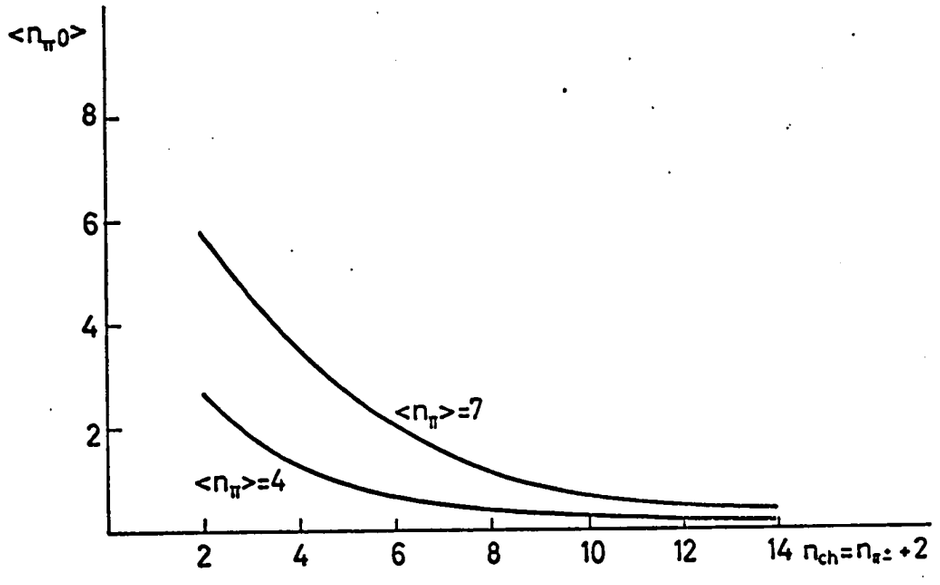

Fig. 17. The dependence of $\langle n_{\pi^o} \rangle$ on n_{π^+} is shown for two different values of $\langle n_\pi \rangle = 3 \langle n_{\pi^o} \rangle$ in the coherent state $|g\rangle$ to be compared with Fig. 7.

XUM

Reproduced with permission of the copyright owner. Further reproduction prohibited without permission.

data. That this should be an improvement should be obvious from the fact that it introduces a positive correlation between neutral and charged pions. As we may treat ρ production in an analogous manner to the way we treated isoscalar production above, the success of Caneschi and Schwimmer does not constitute evidence for the multiperipheral model. Since the general trend of the data is at best only slightly rising, we conclude that either (1) there is little correlation in pion production, or (2) the various correlations are difficult to resolve.

XUM

Reproduced with permission of the copyright owner. Further reproduction prohibited without permission.

IX. Conclusions

Our purpose was to study the degree to which pions emitted in multiparticle production experiments can be independent and uncorrelated. As an example of independent uncorrelated emission we developed, in analogy to the bremstrahlung formalism, a model for pion production in coherent states. We showed that, insofar as the pion momentum distributions occupy only a small fraction of the available phase space, four-momentum conservation need not affect independence except at high multiplicities. Independence implies that the particle production cross sections are approximately Poisson distributed in the number of particles. Unlike bremstrahlung, such distributions cannot be continued to $n = 0$ to describe elastic scattering. Charge conservation as the most obvious quantum number constraint leads to modifications of the distributions for charged pions that agree well with experiment. The effects of parity are sensitive to the assumed distributions in momentum space of produced pions, about which we make no conjecture here. Charge conjugation implies a number of constraints on neutral systems such as $e^+e^- \rightarrow$ pions or $\pi\pi \rightarrow$ pions. One of the consequences of isospin conservation is that the isospins of the pion cloud must match the isospins of the skeleton. We developed a formalism for the isospin analysis of pions with identical momentum distribution and applied it to coherent states. The fixed phase of the pion wave function is important for minimizing the increase of $\langle I^2 \rangle$ with $\langle n \rangle$. The minimum that can be achieved with independent uncorrelated pions is a random walk in isospace. In this case the dominant contributions at

XUM

Reproduced with permission of the copyright owner. Further reproduction prohibited without permission.

present multiplicities come from the lowest isospins. Thus independent and coherent pions can be an approximation to experiment. Finally, we studied the role of two pion correlations. Independent emission of scalar isoscalar pairs of pions solves the isospin and parity problems and gives reasonable distributions for charged pions, but leads to negative correlations between charged and neutral pions that seriously disagree with experiment. Emission of isovector pions as well, as in recent multiperipheral models, improves the agreement with the observed slightly positive correlations.

As we mentioned in the introduction, there are a number of essentially model-independent statements that characterize inelastic reactions. We have shown that the possibility of independent production of uncorrelated pions can be compatible with basic principles at the most only as an approximate statement. It is certainly not the only way of achieving the experimental results which suggest it. The distributions of charged pions, or topological cross sections are relatively insensitive to the presence of correlations. Much more sensitive are the distributions of neutral versus charged pions. The present experimental status is compatible either with independent emission, or with the possibility that there are various correlations whose effects are cancelling against one another. Similar considerations apply to the interpretation of mass distributions and longitudinal momentum distributions. Hopefully, measurements of the correlation functions will help to resolve the present ambiguities.

We would suggest that whenever there are a large number of competing effects a statistical approach is often a good approximation.

XUM

Reproduced with permission of the copyright owner. Further reproduction prohibited without permission.

It is in this sense that multipion production at high energies may resemble the independent production of uncorrelated pions. Whether in such a statistical approach the general quantum number considerations presented here will continue to apply is an open question.

XUM

Reproduced with permission of the copyright owner. Further reproduction prohibited without permission.

References

1. M. Deutschmann et al, ABBCCHW Collaboration; submitted to the Kiev Conference on Elementary Particles, 1970, and unpublished information. We would like to thank Dr. D. R. O. Morrison and this collaboration for making their unpublished data available to us.

2. R. Honecker et al, ABBCCHW Collaboration, Nuclear Physics B13, 571 (1969).

3. J. W. Elbert et al, Nuclear Physics B19, 85 (1970), and A. R. Erwin, Report to the Conference on Expectations for Particle Reactions at the New Accelerators, Madison, Wisconsin (1970).

4. L. Van Hove, Nuovo Cimento 28, 798 (1963); Rev. Modern Physics 36, 655 (1964).

5. The possibility that pions are produced in coherent states or as classical radiation has been suggested in several places. As examples of different models based on this central idea we give the following references:
H. W. Lewis, J. R. Oppenheimer, and S. A. Wouthuysen , Phys. Rev. 73, 127 (1948);
H. A. Kastrup, Phys. Rev. 147, 1130 (1966); Nuclear Physics B1, 309 (1967);
M. G. Gundzik, Phys. Rev. 184, 1537 (1969);
P. E. Heckman, Phys. Rev. D1, 934 (1970);
C. G. Zipfel, Jr., Phys. Rev. Letters 24, 756 (1970).

6. R. J. Glauber, Phys. Rev. 130, 2529 (1963); 131, 2766 (1963).
For a general review and extensive list of references, see:
T. W. B. Kibble, Cargèse Lectures in Physics, Vol. 2, edited by M. Lèvy (Gordan and Breach, 1968), p. 299.

7. T. W. B. Kibble, Lectures at Boulder Conference (1968), appeared in Mathematical Methods in Theoretical Physics (Gordan and Breach, 1969), Vol. XID, p. 387.

8. F. Lurcat and P. Mazur, Nuovo Cimento 31, 140 (1964).

XUM

Reproduced with permission of the copyright owner. Further reproduction prohibited without permission.

9. See also H. A. Kastrup, Nuclear Physics B1, 309 (1967).

10. C. P. Wang, Phys. Rev. 180, 1463 (1968).

11. L. Caneschi, A. Schwimmer, SLAC-PUB-829 (1970), and SLAC-PUB-839 (1970).

XUM

Reproduced with permission of the copyright owner. Further reproduction prohibited without permission.